Doctoral Dissertation (Shinshu University)

Study on analysis of puncture resistance mechanism and influencing factors of aramid composite materials

March 2023

LUO CHAO

Contents

List of Figures

List of Tables

Chapter 1

Introduction

Chapter 1: Introduction

1.1 Introduction of Stab-Resistant Materials

Harvard University professor Steven Pinker has said that we are living in the most peaceful era in human history. Of course, most of us live in an era of peace and have never experienced the turmoil brought about by war, let alone any threat to life. However, in the context of peace, there are always various dangerous factors lurking. With the process of global economic integration, various exchange activities are becoming more and more frequent. In peacetime, the greatest impact on social security is today's terrorism and various violent activities. After experiencing tragic terrorist attacks and various violent cases, people's awareness of self-protection has gradually increased. [1-2]

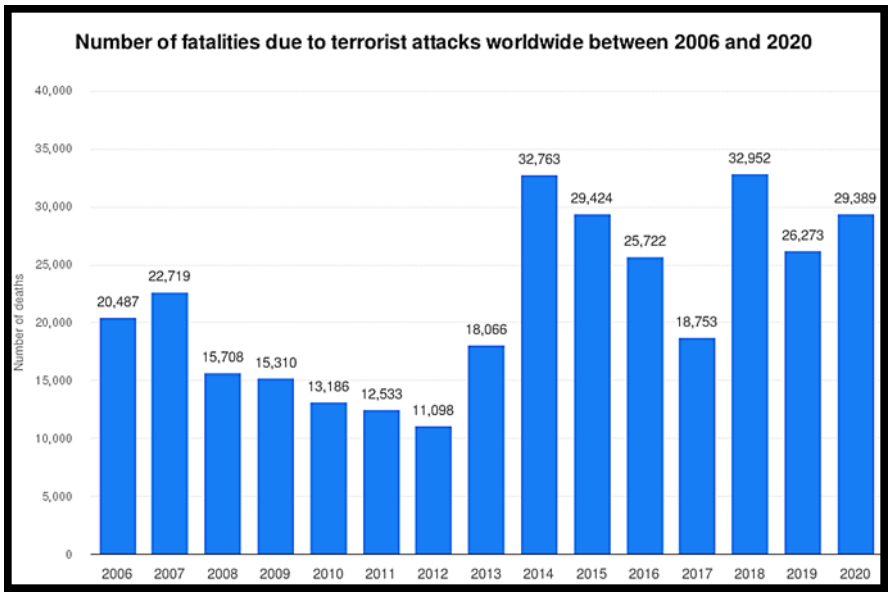

Figure 1-1. The number of fatalities due to terrorist attacks worldwide [3]

Among them, anti-terrorism has become an event that has attracted much attention in the international community, especially in developed countries. Figure 1-1 shows the number of fatalities due to terrorist attacks worldwide. In response to this, personal

protective products have developed rapidly. In some countries such as Japan, firearms and ammunition are strictly controlled, so the injury of sharp objects such as daggers and ice picks has become a major threat to people's lives. Under this background, the research and development of stab-resistant materials in the field of personal protection has become a hot spot. [4-5]

Stab-resistant materials are protective equipment used to protect vital organs of the human body from sharp weapons such as sharp knives and daggers. It has been widely used in some security departments and police agencies. As the most dangerous occupation in peacetime, stab-resistant materials can effectively protect their lives. Not only that, with the continuous development of stab-resistant materials, it also has good application prospects in the civilian field. For example, it is used in the construction industry for the safety protection of construction workers and decoration workers, and in the sports industry for the safety protection of fencers. [6-7]

The development of stab-resistant materials is very rapid, benefiting mankind in a unique way. But in fact, stab-resistant materials are not modern products. In ancient times, due to various reasons such as hunting, war, etc., the idea of people protecting their own safety with external materials has always existed. Therefore, stab-resistant materials with distinctive characteristics have appeared in each era. These different materials constitute a splendid history of the development of stab-resistant materials.

1.1.1 Development History

The most important factor affecting puncture resistance is the type of material. The stronger the material performance, the better its stab-proof effect. At the same time, due to a certain quantity to be produced, the selected materials cannot be too rare or too

expensive. In this context, each era has produced its own unique stab-proof equipment.

In the Neolithic period, as shown in Figure 1-2, the first stab-resistant material to appear is leather armor. [8] The greatest talent of human beings is learning. In the distant ancient times, the earliest leather armors begin to imitate animals. Under the laws of nature, many animals have evolved hard shells, and thick armors have successfully protected their lives. So, the ancient ancestors also begin to equip themselves with similar materials, and leather armor begin to develop slowly. The formation of the protection concept has accelerated the development of stab-resistant materials. Gradually, people are no longer bound by leather, and materials such as rattan armor, wood armor, and bone armor are born. [9-10] These are the most readily available materials and at the same time are very protective for the people of the day. While providing protection performance, comfort performance is also an important reference index. Among these materials, leather armor can not only provide a certain degree of protection, but also have a certain degree of thermal insulation and comfort. [11] Therefore, leather armor has become the most comprehensive and longest-used stab-resistant material.

Copper, as the earliest metal used, successfully helps mankind enter the Bronze Age. To survive and benefit, war is inevitable, and various offensive weapons also appear. While possessing weapons, the desire for their own safety also increases.[12] The appearance of bronze swords make traditional leather armor insufficient to deal with threats, so metal armor made of bronze was born.

Then entered the Iron Age, and the excellent stab resistance of iron armor gradually replaces bronze armor and becomes the mainstream of the times. In order to protect your own safety, you only need to wear iron armor all over your body. But with thick armor comes high cost and poor comfort. The weight of dozens of kilograms makes it difficult

to perform the most basic movements, let alone use them on the battlefield. Before there are more powerful materials, people begin to design the structure of the armor. A very typical armor - chain mail appeared in the Middle Ages in Europe.[13] Chain mail is a clothing-like armor composed of small iron rings. This kind of armor can effectively protect the attack of sharp weapons, and at the same time has the characteristics of softness, which greatly improves the combat effectiveness of soldiers. The disadvantage is that its preparation process is very complicated, so the production time is long, and the cost is high. Another typical armor is called plate armor.[14] Plate armor is armor made of large plastic plate-like metal armor pieces. In order to facilitate movement, the surface of the armor has many grooves and folds, and the convex arc area can effectively resist external attacks.

Figure 1-2. The pictures of leather armor, chain mail and plate armor [6-7]

The pace of human development of offensive weapons will never stop. With the advent of the age of gunpowder, ordinary armor can no longer withstand such powerful firepower. In the first and second world wars, the steel armor is damaged, and the ancient metal armor finally completes its mission and withdrew from the stage of history.

1.1.2 Modern Stab-Resistant Materials

After such a long period of development, people's requirements for stab-resistant materials have been basically clear: excellent protection performance, reasonable comfort, and mature preparation technology. Obviously, traditional metal materials are difficult to meet all the above requirements, and at this time some people begin to turn their attention to the field of textiles. The appearance of glass fiber has made everyone realize that it is not irreplaceable to be a metal material. Glass fiber composite material has the characteristics of light weight and high strength, and can completely replace metal in many occasions. These areas of course include stab protection, and as a result, the development of even stronger yarns has become the goal of research.

Figure 1-3. EOD suit (left) and stab proof vest (right) [15]

In the 1960s, the DuPont company successfully developed aramid fiber and took the lead in industrialization. The characteristics of light weight, high strength and high modulus make it widely used in various fields as a representative of high-performance yarns.[16] The emergence of high-performance yarns has also brought new vitality to the traditional textile industry. For example, the most protective armor, such as the Explosive Ordnance Disposal (EOD) suit and stab proof vest shown in Figure 1-3. As an ancient

industry, textiles have been meeting our most basic life guarantees. Warmth, comfort and aesthetics are our most demanding requirements. And due to the limitation of the strength of traditional yarn materials, we never think that clothing could take on such a big responsibility to protect our lives.

Until the emergence of high-performance yarns, combined with textile technology, high-performance textile materials have become the most dazzling new star in the material field. The stab-resistant materials made of aramid fiber, ultra-high molecular weight polyethylene, etc. by woven, knitted and non-woven methods have attracted much attention due to their softness and stab-resistant properties. The emergence of soft stab-resistant materials has simultaneously met people's three needs for stab-resistant materials, so it has developed very rapidly and has become the symbol of current stab-resistant materials.

I believe that with human wisdom, the development of stab-resistant materials will never stop here. With the development of science and technology, there will be materials with better performance to replace them and become new hot spots.

1.1.3 Threat from Ice Pick

From leather armor to bronze armor, from iron armor to soft stab-resistant materials, the replacement and elimination of stab-resistant materials from generation to generation are the results of historical tests. The conditions for judging its replacement are also very simple and clear, whether this material can resist the attack of weapons. Sometimes people may wonder why this material can work and other materials can't. With the development of science, a more rigorous judgment condition that can be recognized by everyone has appeared, which is the standard. The research on the mechanism of puncture

behavior is also a good solution to the above doubts. Essentially, the act of stabbing prevention is the act of keeping puncture energy out of our body as much as possible. The faster the energy is consumed and absorbed, the less the puncturing tool will move forward, and the less damage will be done to the human body. From this point of view, those materials that were once used as stab protection were eventually eliminated because of their insufficient ability to withstand piercing energy.

Although the result is consumption and absorption of puncture energy, the stab-proof mechanism of different stab-resistant materials is quite different when dealing with different sharps. Next, I will take the soft stab-proof material as an example to analyze the damage to the material by the knife and the ice pick respectively.

The first is the analysis of the damage mechanism of the knife to the material. Here, the angle of penetration of the knife is straight down. After analysis, it is found that the puncturing process can be divided into the following three stages [17-18]. The fabric deformation during penetration of the knife is shown in Figure 1-4.

(1) The yarn is squeezed and slipped. After the blade tip is in contact with the yarn, the puncture force is low due to the small contact surface, so the yarn around the blade tip slips around. Among them, due to the shape of the blade tip, the amount of yarn slip around is not uniform. Yarns in the direction parallel to the tip of the knife slip less to both sides, while yarns perpendicular to the tip of the knife slip more to both sides. Due to the slippage of the yarn, the frontmost part of the knife tip penetrates the fabric more easily.

(2) The yarn is subjected to two different damages. In the fabric, the spacing between the yarns is limited, so the range of free movement when squeezed by an external force is limited. When the yarn slips beyond the free range of motion, under the action of the

extrusion friction force between the cutter and the yarn, the yarn begins to bend and deform under the action of the tensile force. At this time, the yarn parallel to the blade tip is stretched, while the yarn perpendicular to the blade tip is stretched and also cut due to the frontal contact with the blade.

(3) The yarn is cut and broken. As the knife continues to penetrate, the yarn is pulled more and more tightly, and the cutting action of the yarn perpendicular to the tip of the knife is also increased. Finally, the yarn here is cut and broken. The knife continues to puncture forward, and the next yarn repeats the above process. The knife penetrates the material until the cut portion of the fabric becomes larger.

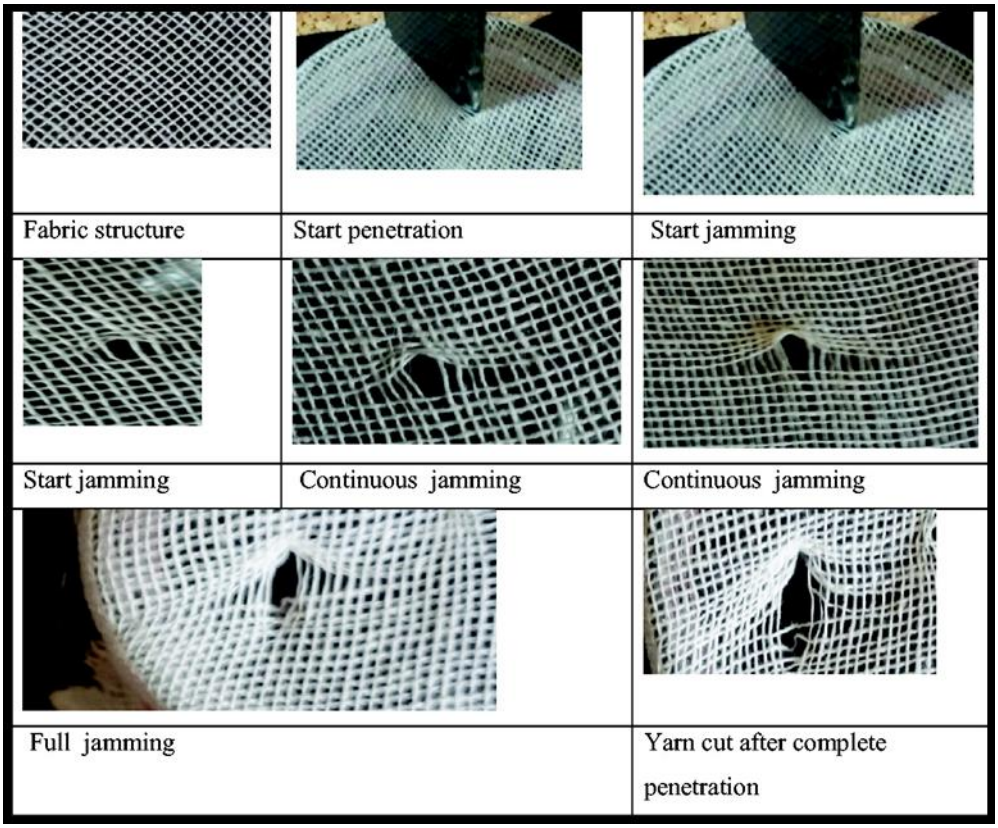

Figure 1-4. The fabric deformation during penetration of the knife [17]

From the above three stages, it can be found that the damage mechanism of knife puncture mainly includes slippage between yarns, axial tensile damage and radial cutting

damage. The puncture energy is absorbed and consumed through frictional heating between fibers, yarn deformation and yarn breakage. Among them, the most important part is the cutting damage of the yarn.

Then it is the analysis of the damage mechanism of the ice pick to the material. Here, the penetration angle of the ice pick is also considered to be 0°. The puncture process of the ice pick can also be divided into the following three stages [19-20]. The fabric deformation during penetration of the ice pick is shown in Figure 1-5.

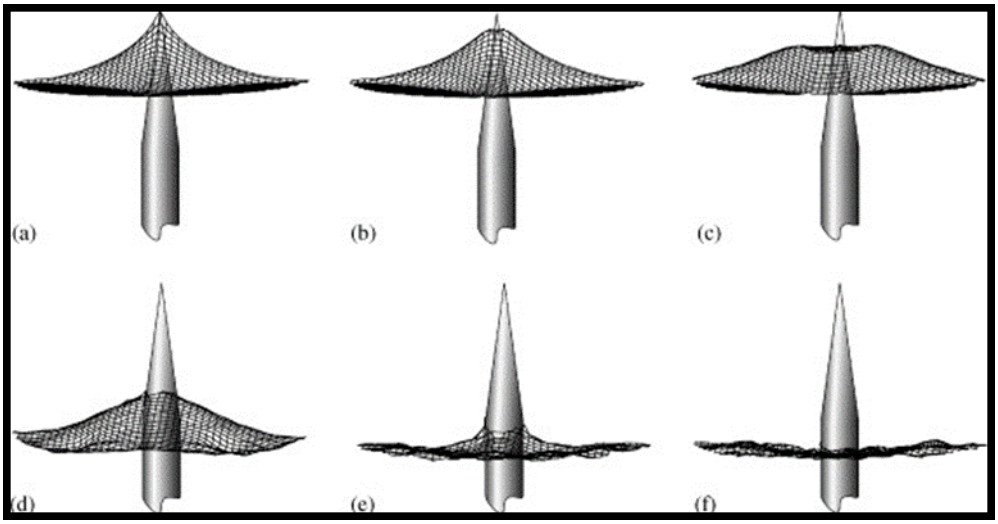

Figure 1-5. The fabric deformation during penetration of the ice pick [19]

(1) The yarn is squeezed and slipped. Similar to the above knife piercing, when the ice pick contacts the fabric, the yarn is subjected to a small piercing force and slides around the piercing point. The ice pick head is a four-sided symmetrical structure, so the slippage of the warp and weft yarns is the same here. Also due to the slippage of the yarn, the taper easily penetrates the fabric.

(2) Yarns are rubbed against each other. Because the vertical cross-section of the ice pick is triangular, the tip of the ice pick is very small in contact with the fabric, so the amount of yarn slippage is not large. With the piercing of the ice pick, the contact part

between the ice pick and the fabric gradually increases. The puncture begins to spread outward in a shape like water ripples. At this time, the slippage of the yarn has exceeded the range of free movement, so it begins to stretch and deform under the dual action of the ice pick's extrusion and the friction between the yarns.

(3) The fabric is penetrated. The continuous penetration of the ice pick makes the yarn squeezed tighter and tighter, and the frictional force generated by it increases. Finally, after the cone of the ice pick completely penetrates the fabric, the ice pick no longer causes the fabric to be compressed, and the fabric is damaged by the puncture.

From the above three stages, it can be found that the failure mechanism of ice pick puncture mainly includes slippage between yarns, axial tensile failure and yarn friction. The puncture energy is absorbed and consumed through the frictional heating between fibers, the deformation of the yarn and the friction between the yarn and the ice pick. Among them, the most important part is the friction between the yarn and the ice pick.

Among them, the main mechanism is the friction self-locking mechanism. [21] With the penetration of the thorn, the yarn will be pulled and slipped, and the expansion of the yarn will cause the adjacent yarn to be pulled, slipped and tightened. The force required for yarn drawing is the sum of the frictional force on the drawn thread during the drawing process. During the piercing process, when the yarn reaches the point where the yarn cannot continue to expand, the blade will stop going deep. At this time, the friction force of the yarn required for expansion is of a large magnitude. As long as the coil wire can continue to slide, the blade will continue to go deep. If the strength of the yarn is strong enough, when the coil thread reaches the point where it cannot slip, the state reached by the deformation of the fabric is called the "locked" state. [22]

Through a detailed analysis of the damage mechanism of the above two sharp

weapons, it is found that ice picks are more difficult to protect than knives. There are two reasons. The first is that the main damage of the cutter is the cutting damage of the yarn, and the ice pick is the extrusion friction of the yarn. Comparing the two, it is obvious that more energy is consumed to break the yarn, so the piercing energy of the knife is consumed more. The second is the duration of the puncture. In general, the blade portion of the knife is longer than the cone portion of the ice pick. This results in the knife having to advance a longer distance to penetrate the material. Under the same energy, the knife needs to destroy a larger area of fabric, so it needs to consume more piercing energy. It can be found that ice picks are more difficult to protect.

In order to develop more lightweight and high-performance stab-resistant materials, many scientists at home and abroad have conducted serious research. Next, this paper will summarize the current research on stab-resistant materials.

1.2 Current Research on Stab-Resistant Materials

In recent years, there have been more and more threats from sharp objects such as knives and ice picks, so the importance of stab-proof materials has become more and more important, and it has been a research hotspot in the field of protection in recent years. People's requirements for stab-resistant materials are not limited to protective performance, but also have certain requirements for comfort performance. Therefore, the development of fabric-based flexible stab-resistant materials based on high-performance yarns is favored. Here we sort out the research status of stab-resistant materials from two aspects: experimental research and simulation research.

1.2.1 Experimental Study of Performance

In the experimental study, the main research directions of the researchers include

two parts, the improvement of stab-resistant materials and the design of stab-resistant structures.

(1) The research on material improvement of stab-resistant materials.

From the above analysis of the puncturing process, it can be found that the slippage of the yarn always exists along with the puncturing process. In response to this phenomenon, the researchers use the power of shear thickening fluid (STF) to study the effect of interlayer interfacial sliding between yarns on enhanced impact resistance and energy absorption. Through rheological test and yarn pullout test, the relationship between STF state and interfacial slip between yarns is analyzed. The effects of impact velocity and restraint conditions on interfacial sliding are investigated by drop weight and ballistic tests. [23] Experiments prove that STF is effective, and on this basis, quasi-static/dynamic tensile tests and shear tests are carried out on multiphase STF / Kevlar fabrics. Its quasi-static stretching behavior is manifested in four distinct stages, the curling stage, the linear pre-peak stage, the linear post-peak stage, and the nonlinear post-peak stage. Among them, the mechanical parameters such as peak load, elongation at break and elastic modulus of Kevlar fabric are improved after STF treatment. [24] The shear thickening liquid has a certain fluidity, and it is very weak when it is coated on the surface of the fabric. To solve this problem, stab-resistant materials are prepared by coating TPU/SiO2/STF on aramid fabrics. It is found that the puncture resistance and yarn drawing performance of TPU coated fabrics are greatly improved.[25] In addition to aramid, UHMWPE can also be prepared into STF/UHMWPE composite fabrics. The puncture resistance of UHMWPE fabrics is greatly improved after impregnation with STF. [26]

Most studies focus on selecting a single yarn as a raw material to prepare stab-

resistant materials. After the technology of covered yarn is introduced to the field of high-performance yarns, it is found that the effects of different combinations are very different. The schematic diagram of covered yarn structure material is shown in Figure 1-6. Kevlar fibers and ultra-high molecular weight polyethylene fibers are prepared into covered yarns with different structures. The test finds that the cut resistance of the covered yarn fabric is better than that of pure Kevlar or UHMWPE fabric.[27] During the preparation of different covered yarns, the density of the yarn is changed virtually, and the effect of different fabric densities on the puncture resistance is also strongly related. The optimum level of fabric density will exhibit the most effective stab protection. [28] The appearance of covered yarn also solves a problem, which is to improve the comfort properties of the material. Using high-performance yarn as the core yarn and yarn with comfortable wearing performance as the covering yarn can improve the comfort of the material while ensuring the puncture performance. [29]

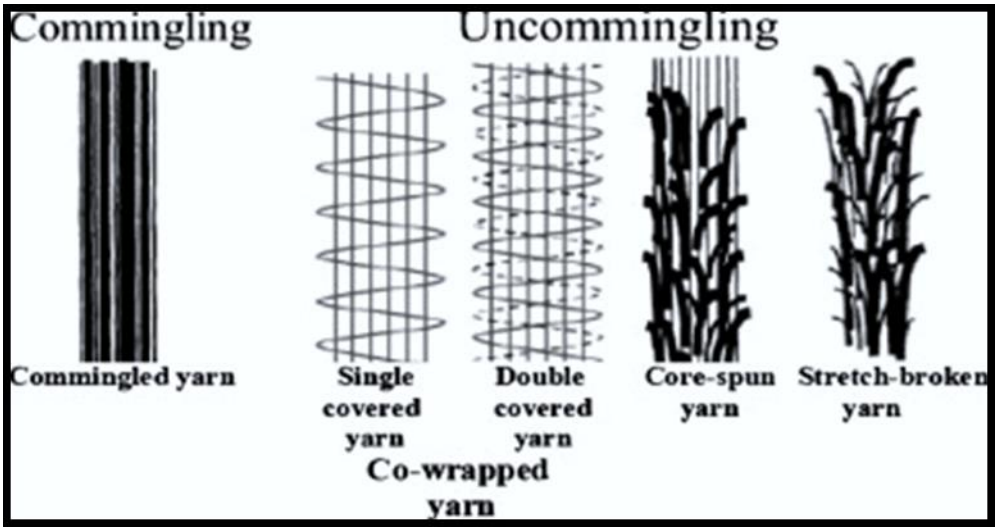

Figure 1-6. Schematic diagram of covered yarn structure material [30]

High-performance yarns make up a large portion of protective materials, while metallic materials are still developing. The emergence of metallic yarns has also led to its

rapid use in stab-resistant materials. Reinforced woven fabric prepared with metal wire as weft yarn, the fabric has enhanced resistance to bending and penetration of sharp objects. However, it leads to an increase in the stiffness of the fabric, sacrificing a certain degree of comfort. [31] Nanoscale metal stab-resistant materials are also being researched and developed. Development and testing of nanocrystalline copper metallized and non-metallized laser sintered nylon materials confirming their stab resistance properties. With the addition of nanocrystalline copper, the thickness of the material to achieve the same stab resistance is significantly reduced. [32]

(2) The research on the structural improvement of stab-resistant materials.

Based on the structure of traditional textile materials, the general idea is to use high-performance yarns for the preparation of textile structural materials. In terms of structure, it is mainly divided into 2-dimensional fabric structure and 3-dimensional fabric structure. The most widely used 2D structural material is plain weave. Rigid stab-resistant materials are developed by using fiber-reinforced composite materials made of different types of high-performance yarns such as carbon fiber, glass fiber and aramid, which are arranged and stacked according to the stab-resistant effect of different materials at different stages. [33] This is the structure of the most common stab resistant material, a stacked combination of a single layer of plain weave material. In addition to woven fabrics, knitted fabrics are used for stab-resistant materials due to their structural flexibility and ability to bring more yarn through shearing during the cutting process. [34-35]

2D structural materials need to be stacked to achieve a strong stab-proof effect, but the strength between layers will be relatively weak, so 3D structural materials are gradually developed and utilized. The difference between the two-dimensional structure and the three-dimensional structure material is shown in the Figure 1-7. The 3D plane

fully interwoven fabric structure has three yarn groups of warp yarn, weft yarn and z yarn. To form this structure, the warp and weft yarns are interwoven with the warp yarns in each layer based on the weave pattern in the in-plane main direction, and the z yarns are interwoven with the warp yarns in each layer based on the weave pattern in the out-of-plane main direction. [36] In a puncture study on 3D warp interlocking structured fabrics based on UHMWPE yarns, it is found that the fabric structure has a significant effect on the puncture impact performance, and the orthogonal fabrics have good puncture impact resistance. [37] In addition to high-performance yarns, metal filaments are also attracting attention due to their unique properties. The three-layer fabric structure reinforced by metal wires plays an important role in preventing penetration by sharp objects. The metal reinforcement layer is woven by a specific weaving system, which bears the highest penetration force and penetration energy in the three-layer structure. The multi-layer fabric structure thus designed excels in absorbing the penetrating energy of sharp objects[38].

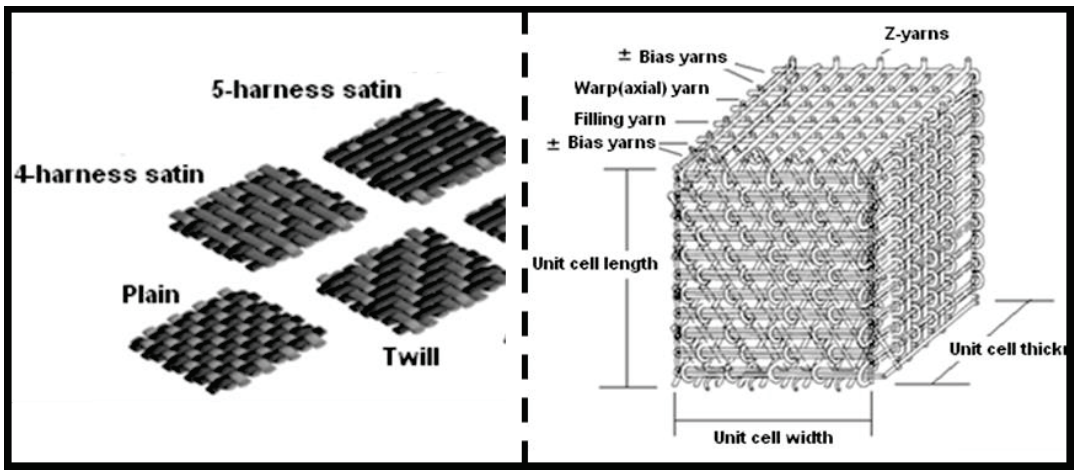

Figure 1-7. The 2D fabric structure and 3D fabric structure [39]

In 3D materials, in addition to the above structures, there is also a special structure, sandwich structure. Generally, it consists of multiple layers of woven fabrics and various

fibers. The upper and lower layers are composed of high-strength fabrics, while the middle layer is composed of thermoplastic resin materials. Due to the high melting point of aramid, when the intermediate material is heated and melted, the upper and lower layers of the material will connect the molten inner material to form a stab-resistant fabric as a whole. [40] Through a series of structural designs, the direct preparation of the overall stab-resistant material can be achieved.

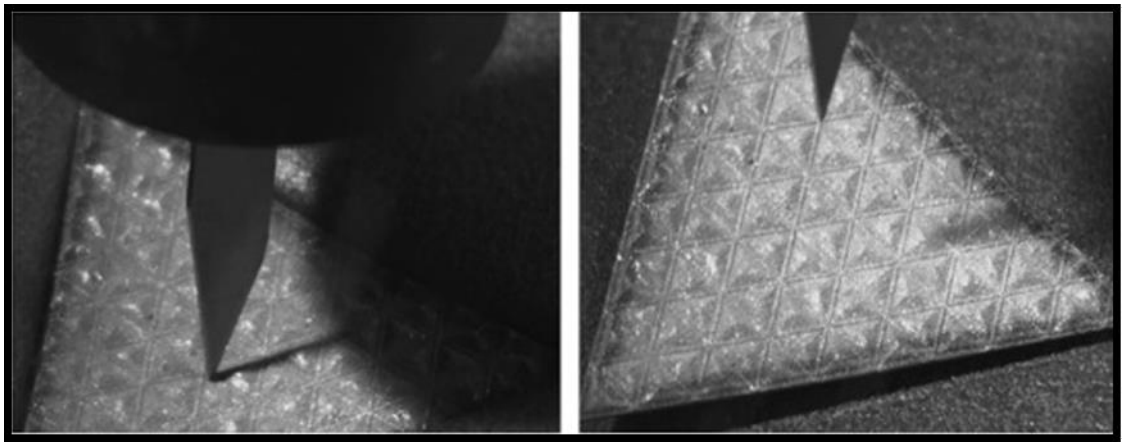

Figure 1-8. Pictures of knife impacts on the bionic structure [45]

In addition to various fabric structures, the evolution of nature has also enabled many organisms to have various strategies to protect themselves. The biological structure of plants and animals is a rich source of inspiration, both of which have structures with outstanding mechanical properties. Therefore, biomimetic engineering structures have also become a hot research topic. [41-44] Natural armor based on keratin exists in terrestrial animals, and its defense performance is very outstanding. Crocodiles [45], alligators [46] and turtles [47] have sturdy and protective armor shells that help them survive longer in often violent environments. Inspired by it, the researchers design and realize a stab-resistant substrate with a triangular pyramid structure. Due to the dispersion effect of the structure, the triangular pyramid structure produces twice the in-knife energy

than the planar substrate. Forces parallel to the inclination cause significant scratches on the substrate surface, while forces perpendicular to the substrate result in significant deformation of the substrate. [45], From large animals to small insects, they can be a source of inspiration. Bombyx mori cocoon is a natural non-woven material with excellent puncture resistance and unique structure. Based on this structure, a biomimetic composite is designed to improve its puncture performance through polyurethane impregnation treatment. [48]

With the development of science and technology, environmental protection issues have become increasingly prominent. Traditional manufacturing methods are often wasteful and environmentally damaging. And a new generation of green high-end manufacturing, 3D printing technology is developing and growing with its unique production method. With the help of 3D printing technology, scaly protective armor produced from aramid fibers has become a new type of stab-resistant material. [49] For the puncture soft composite materials that have been produced, recycling is also challenging. Therefore, a new strategy of puncture-resistant composites with self-healing and synergistic toughening effects has emerged for secondary utilization after puncture injury. To realize this idea, puncture-resistant soft composites are prepared using hydrogels and aramid fabrics. This material with certain self-healing capabilities serves as an important guide for the design of recyclable puncture-resistant composites in the future. [50]

1.2.2 Simulation Study of the Mechanism

The stab-proof process is a transient process, and it is difficult to analyze the internal force of the material through simple experimental research. Therefore, it is very difficult

to study the stab-proof mechanism. With the development of finite element software, the simulation study can analyze the specific force of each part of the material at each stage of puncture under the condition that the simulation results are correct. With the help of finite element software, researchers have carried out many related studies.

Numerical simulation studies on the impact properties of STF / Kevlar fabrics are carried out. The study finds that the main factor in energy absorption is the friction between the impact head, the fabric and the yarns within the fabric during impact. The experimentally obtained static and dynamic coefficients of friction yield analytical results that visually agree well with the experimental results. [51-52] Yarn extraction plays a vital role in stab-resistant materials. The simulation study finds that the more protective stitched samples allowed the fabric to absorb more strain and kinetic energy. [53] To prevent the movement of the yarn, coated fabrics are developed. After simulation, it is found that the puncture resistance of the coated fabric is closely related to the size of the penetrator shape. The finite element model provides reasonable predictions for the puncture resistance of the coated fabrics. [54] In addition to woven fabrics, much research on stab-resistant simulation of knitted fabrics have also been carried out. [52]

In order to improve the accuracy of the stab-resistant simulation, many methods are also used. A yarn-level finite element model including failure criteria and progressive damage laws is established to compare structural deformation and damage behavior. [55] A mesoscale yarn-scale 3DAWF model is constructed using membrane elements to improve computational efficiency and accuracy. A simplified Johnson-Cook (SJC) material model is also used to simulate the dynamic behavior of the yarn under high-speed shock loading. This method can accurately simulate the mechanism of material failure. [56] L. Wang et al. [57] establishes a detailed model of plain weave fabrics, and

simulated knife piercing through plain weave fabrics by finite element method to understand the penetration process and fiber fracture mechanism.

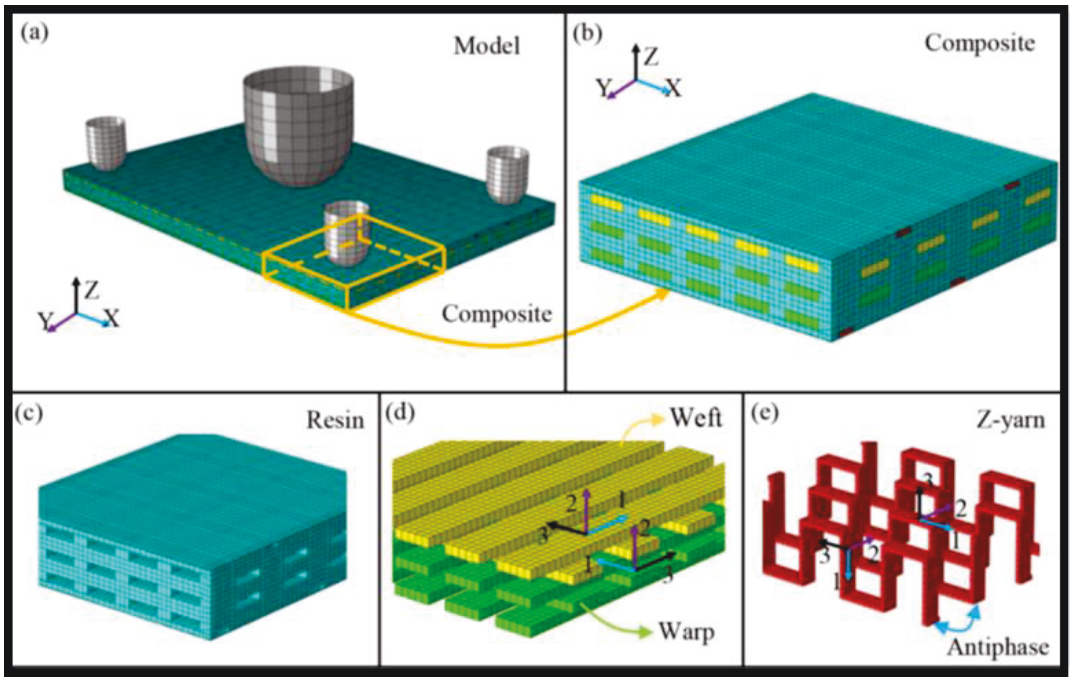

Figure 1-9. Finite element model of the hybrid composite.[55]

The last supplementary part is that in the puncture simulation, people rarely refine the model. However, Yuan et al. [58] establishes a micro-scale three-dimensional (3D) numerical model of plain weave fabrics. Although the puncture performance has not been studied, such refined modeling is already very rare. Similarly, Zhou et al. [59] develops a numerical simulation method at the yarn level in the process of studying tear damage. The tear properties of pre-cut samples in different directions are predicted and the results of finite element analysis are verified experimentally.

1.2.3 Research Summary

In summary, the research on stab-resistant materials mainly includes two aspects. The first aspect is experimental research. The second area is simulation research. From the above introduction, it can be found that predecessors have invested a lot of effort in

the research of stab-resistant materials. According to different materials, different structures and different preparation methods, a lot of research on stab-resistant materials has been carried out, which has promoted the development and industrialization of materials. In the process of research, for the blind spots that cannot be studied, with the help of finite element analysis software, people have a deeper understanding of the damage of materials in the process of stab prevention.

Therefore, the method of combining finite element simulation with actual experiment is a very effective research method. However, compared with the two aspects, the anti-stab simulation experiment part is not perfect. First of all, most studies are still in the experimental stage, and simulation studies are still lacking. At the same time, many simulation studies are carried out under very ideal conditions, and the simulation results may not be consistent with the actual situation. The results obtained from these simulation experiments do not provide a good guide for actual experiments.

To gain a deeper understanding of this issue, we will talk in detail about finite element simulations and issues that may be overlooked during stab prevention simulations.

1.3 Issues in Puncture Simulation Study

In order to better analyze the existing problems, in this section, we first introduce the finite element method, and then introduce the finite element software. Finally, the problems that may occur in the puncture simulation based on the finite element software are analyzed.

1.3.1 Introduction to Finite Element Method

The FEM is a modern computing method developed rapidly with the development

of computers. It is a method of discretizing the continuum into a finite number of grid elements, and then simplifying the solution of complex problems. It regards the solution domain as consisting of many small interconnected sub-domains, assumes a suitable approximate solution for each unit, and then derives and solves the total satisfying conditions of this domain to obtain the solution of the problem. This solution is not an exact solution, but an approximate solution because the actual problem is replaced by a simpler problem. Because most practical problems are difficult to obtain accurate solutions, finite element not only has high calculation accuracy, but also can adapt to various complex shapes. So it has become an effective engineering analysis method. [60]

Around the 1950s, the FEM was first applied in the field of continuum mechanics, that is, in the analysis of static and dynamic characteristics of aircraft structures. However, the huge amount of computation has restricted the development of the FEM all the time. With the development of computer science, the performance of computers has risen rapidly. The finite element technology has also rapidly expanded from structural engineering strength analysis to various disciplines and is widely used to solve continuity problems such as heat conduction, electromagnetic fields, and fluid mechanics. [61] The FEM provides a more efficient and faster platform to design and evaluate structures. On many occasions, people will use the FEM to replace part of the experiment to achieve the goals of advanced exploration, performance prediction, and influencing factor research, which allows designers to accurately predict the technical performance of products in the early stage of product design. Through this method, the cycle of product development can be greatly reduced, and the reliability of the product can be increased.

Similarly, in the field of scientific research, the FEM can be used to simulate the performance of materials under different parameters more efficiently, reducing the

experimental time and cost. When it is impossible to accurately observe the experimental process, the failure process and mechanism of the material can be clearly analyzed by means of FEM simulation.

1.3.2 Introduction to Simulation Software

Software based on finite element analysis algorithm is called finite element analysis software. Generally, according to the scope of application of the software, it can be divided into professional finite element software and large-scale general finite element software. After years of development and improvement, various finite element software has transformed the FEM into social productivity. Common general finite element software includes Ansys, Abaqus, MSC.Nastran, LUSAS, LMS-Samtech, Algor, Hypermesh, FEPG and so on.

According to the software advantages and areas of expertise, Ansys software is selected for simulation in this experiment. So here is an introduction to Ansys. Ansys is a large-scale general-purpose finite element analysis software that integrates structure, fluid, electric field, magnetic field, and sound field analysis. The software mainly includes three parts: preprocessing module, analysis calculation module and postprocessing module. The preprocessing module provides a powerful tool for solid modeling and meshing, and users can easily construct finite element models. Analysis and calculation modules include structural analysis, fluid dynamics analysis, electromagnetic field analysis, sound field analysis, piezoelectric analysis, and multi-physics coupling analysis. It can simulate the interaction of various physical media and has the ability of sensitivity analysis and optimization analysis. The post-processing module can display the calculation results in graphical ways such as color contour display, gradient display, vector display, particle

flow trace display, stereo slice display, transparent and semi-transparent display. The calculation results can also be displayed or output in the form of graphs and curves.

1.3.3 Current Issues

(1) Issues in structural models

The first step in the simulation experiment is the establishment of the material structure model. Simple structures can be easily drawn. However, most of the stab-resistant materials are fabric structures, and the fabrics are composed of yarns, which are composed of thousands of filaments. Obviously, it is an impossible task to build the model according to the real material structure. In this case, it is inevitable to simplify the model, and how to simplify the material becomes an important factor for the accuracy of the simulation results. Common simplifications include idealizing the yarn as a monolithic material and then drawing the fabric model, but it is unknown whether the simulation results will deviate significantly if the inner filaments of the yarn are ignored.

(2) Issues in material parameters

In the finite element simulation, the most important thing is the drawing of the material model and the setting of its engineering parameters. The most ideal simulation is the same as the actual experiment, but due to constraints such as the difficulty of model establishment and the computing power of the computer, people often idealize the model for analysis. The most common method is to idealize a piece of fabric as a monolithic material and simulate it as an isotropic material. This method will virtually change the engineering parameters of the material, and the anisotropic material will directly become an isotropic material. It can be seen from the above 1.1.3 that when the yarn is punctured, it will be squeezed, and the yarn with weak radial performance will bend and slip. The

setting of the isotropic material will cause the yarn to be compressed and fractured, which will cause great errors in the simulation results.

(3) Issues in interface contact

The next problem is the contact between the yarn materials. Taking a plain weave fabric as an example, the contact portion includes the inter-yarn interior and the yarn-to-yarn contact. Usually, when people conduct simulation calculations, they will be processed in the following three ways. The first and most comprehensive approach is to ignore the contact problem. In many simulation experiments, in order to reduce the calculation time, the complex contact problems such as fabrics are idealized. However, ignoring the contact problem directly makes the simulation results less accurate. The second approach is to set up frictional contact. Because of the large error of ignoring the contact directly, setting the frictional contact between the contact surfaces can improve the accuracy of the simulation. However, setting a friction coefficient directly also makes the simulation inconsistent with the actual situation, and there is still a large error in the simulation results. The third way is to set bonded contacts. The method used in many simulation experiments is to directly default to the bonded contact between the yarns. Therefore, whether there is a better way to optimize the contact part is also a very urgent issue.

Three problems are raised here in this paper: the simplification of the fabric model, the anisotropy of the yarns, and the contact between the yarns. In the process of stab prevention simulation, the changes of these three problems will affect the simulation results. However, what kind of errors will occur, and how the changes of these parameters will affect the stab resistance of the material are always overlooked due to the difficulty of research.

1.4 Constitution of the Dissertation

It can be seen from the above that there are three problems in the current stab-proof simulation experiments, including the simplification of the fabric model, the anisotropy of the yarns, and the contact between the yarns. It is obvious that these three issues will have a certain impact on the stab-resistant simulation results. At the same time, these problems have been ignored by idealization as the difficulties in simulation. In order to solve these problems, we prepare this research.

In this paper, we focus on the effect of considering yarn anisotropy and yarn-to-yarn contact on the accuracy of stab-resistance simulation results. On this basis, the influencing factors of material stab resistance are predicted. The study finds that in the stab-proof simulation, the addition of the radial properties of the yarn and the optimization of the contact part of the yarn will greatly improve the accuracy of the simulation results. After obtaining accurate simulations, we conduct an in-depth analysis of the real stab-proof mechanism and the factors affecting the performance. The experimental results can provide reference for the design of similar products. At the same time, the experimental approach can be extended to different domains for analysis and prediction.

In Chapter 2, we mainly carry out the material structure design. At present, flexible stab-resistant research mainly uses fabric structures as well as non-woven structures. There are many variables in these two structures, and it is difficult to judge the influence of the yarn anisotropy and the contact between the yarns on the accuracy of the results in the stab-proof simulation. In this context, we design a composite with a mesh structure for puncture analysis, using Kevlar/epoxy to prepare mesh composites with a mesh spacing of 1 mm. The puncture resistance of the material is tested by the puncture machine developed by our laboratory. The puncture failure morphology is analyzed with the help

of a high-speed camera, and the puncture energy is analyzed using the force-displacement curve. The results of this analysis will serve as a benchmark against which to simulate the experimental results.

In Chapter 3, we focus on yarn anisotropy. On the basis of the above experiments, we conduct stab-proof simulation experiments. Firstly, a 1:1 simulation model of mesh composite material is established by CAD software. Then, a simulated puncture experiment is carried out according to the actual experimental conditions and material parameters. When setting the material parameters, the problem of yarn anisotropy is mainly considered. The tensile properties of the yarn in the axial direction are tested, and then the compressive properties of the yarn in the radial direction are tested by the method developed by Professor KAWAMURA after optimization. The test finds that the radial modulus of the yarn is much smaller than the axial modulus of the yarn. Using the measured data, the model parameters are set according to the material anisotropy.

In Chapter 4, we focus on the issue of yarn-to-yarn contact. On the basis of the above model, the yarn-to-yarn interface is continued to be optimized to ensure that the simulation results match the actual experimental results as closely as possible. In this study, we use aramid yarn and epoxy resin for the preparation of composites. In order to ensure the accuracy of the interface optimization in the model, we have carried out a detailed analysis of the real object. The interface is then observed by electron microscope, and the damage morphology of the interface failure is analyzed by SEM. Comparing the types of subsequent destruction of the classic interface, the most accurate optimization solution is finally confirmed. In the model, a resin layer is added to the part where the yarn is in contact with the yarn, and the contact between the yarns is optimized by setting the contact surface of the resin layer and the setting of the failure criterion.

In chapters 5, we compare the simulation and experimental results, and discuss the factors that affect the stab resistance. Comparing the simulation results with the experimental results, it is found that after considering the anisotropy of the yarn and the contact between the yarns, the accurate value of the simulation results is greatly improved, and it is closer to the actual experimental results. That is, it is meaningful to consider the yarn anisotropy and the yarn-to-yarn contact in the simulation experiments. The simulation results show that the main failure modes of the mesh material are resin fracture and flexural deformation of the yarns at the splices, while the surrounding area of the material is hardly affected. Using this model, by adjusting the parameters of the material, the influencing factors of the stab resistance of the material are studied. Variable parameters include the ratio of the axial and radial elastic moduli of the yarn (E_L/E_T), the ratio of the tensile strength of the yarn to the shear strength of the resin (σ_F/σ_R), and the diameter of the yarn (R). Experiments show that as the E_L/E_T ratio increases, the stab resistance of the material decreases. The stab resistance performance of the material improves with increasing E_L or yarn diameter but deteriorates with increasing σ_F/σ_R ratio.

References

[1] JOHNSON, Andrew; BINGHAM, Guy A.; WIMPENNY, David I. Additive manufactured textiles for high-performance stab resistant applications. Rapid Prototyping Journal, 2013.

[2] DEMPSEY, Paddy C.; HANDCOCK, Phil J.; REHRER, Nancy J. Impact of police body armour and equipment on mobility. Applied ergonomics, 2013, 44.6: 957-961.

[3] Terrorism - number of fatalities worldwide 2006-2020, Published by Statista Research Department, Aug 5, 2022

[4] WEI, Da; WANG, Rui; ZHANG, Shu Jie. The research progress of stab-resistant material. Advanced Materials Research, 2011, 332: 1896-1899.

[5] SITOTAW, Dereje Berihun, et al. A Review on the Performance and Comfort of Stab Protection Armor. Autex Research Journal, 2022, 22.1: 96-107.

[6] ASHDOWN, Charles Henry. British and foreign arms & armour. TC & EC Jack, 1909.

[7] BISHOP, Mike. Lorica Segmentata Volume I: A Handbook of Articulated Roman Plate Armour. The Armatura Press, 2002.

[8] SHARMA, Prakhar. A compresensive Review on Bioinspired Body Armor Materials. SPAST Abstracts, 2021, 1.01.

[9] CRESKO, William A. Armor development and fitness. Science, 2008, 322.5899: 204-206.

[10] JONES, David E. Native North American armor, shields, and fortifications. University of Texas Press, 2004.

[11] DIEN, Albert E. Armor in China before the Tang dynasty. Journal of East Asian Archaeology, 2000, 2.3-4: 25-59.

[12] LIAO, Ling-Min; PAN, Chun-Xu; YU, M. A. Manufacturing techniques of armor strips excavated from Emperor Qin Shi Huang's mausoleum, China. Transactions of Nonferrous Metals Society of China, 2010, 20.3: 395-399.

[13] STONE, George Cameron. Glossary of the Construction, Decoration and Use of Arms and Armor in all Countries and in all Times. Courier Corporation, 1999.

[14] JOHNSON, Andrew. Establishing design characteristics for the development of stab resistant Laser Sintered body armour. 2014. PhD Thesis. Loughborough University.

[15] Men’s Journal, “Record Book: The Explosive Miler,” Men’s Journal. Available: http://www.mensjournal.com/explosive-miler.

[16] CHATZI, E. G.; KOENIG, J. L. Morphology and structure of Kevlar fibers: a review. Polymer-Plastics Technology and Engineering, 1987, 26.3-4: 229-270.

[17] EL MESSIRY, Magdi; ELTAHAN, Eman. Analysis of woven fabric behavior under punching force. Journal of Industrial Textiles, 2022, 51.1_suppl: 880S-905S.

[18] EL MESSIRY, Magdi; ELTAHAN, Eman. Stab resistance of triaxial woven fabrics for soft body armor. Journal of Industrial Textiles, 2016, 45.5: 1062-1082.

[19] TERMONIA, Yves. Puncture resistance of fibrous structures. International Journal of Impact Engineering, 2006, 32.9: 1512-1520.

[20] TERMONIA, Yves. Impact resistance of woven fabrics. Textile Research Journal, 2004, 74.8: 723-729.

[21] XUHONG, Miao; XIANGYONG, Kong; GAOMING, Jiang. The experimental research on the stab resistance of warp-knitted spacer fabric. Journal of industrial textiles, 2013, 43.2: 281-301.

[22] SCHUBEL, Patrick M.; LUO, Jyi-Jiin; DANIEL, Isaac M. Impact and post impact behavior of composite sandwich panels. Composites Part A: applied science and manufacturing, 2007, 38.3: 1051-1057.

[23] ZHANG, Junshuo, et al. Intralayer interfacial sliding effect on the anti-impact performance of STF/Kevlar composite fabric. Composites Part A: Applied Science and Manufacturing, 2021, 145: 106401.

[24] LIU, Lulu, et al. Macroscopic numerical simulation method of multi-phases STF impregnated Kevlar fabrics. Part 1: Quasi-static and dynamic mechanical test. Composite Structures, 2021, 266: 113780.

[25] ZHANG, Xiayun, et al. Facile fabrication and mass production of TPU/Silica/STF coated aramid fabric with excellent flexibility and quasi-static stab resistance for versatile

protection. Progress in Organic Coatings, 2021, 151: 106088.

[26] SUN, Liang-Liang; XIONG, Dang-Sheng; XU, Cai-Yun. Application of shear thickening fluid in ultra high molecular weight polyethylene fabric. Journal of Applied Polymer Science, 2013, 129.4: 1922-1928.

[27] TIAN, Luxin, et al. Cut-resistant performance of Kevlar and UHMWPE covered yarn fabrics with different structures. The Journal of The Textile Institute, 2022, 113.7: 1457-1463.

[28] TIEN, Duong Tu; KIM, Jong S.; HUH, You. Stab-resistant property of the fabrics woven with the aramid/cotton core-spun yarns. Fibers and Polymers, 2010, 11.3: 500-506.

[29] PALANI RAJAN, T.; RAMAKRISHNAN, G.; KANDHAVADIVU, P. Permeability and impact properties of warp-knitted spacer fabrics for protective application. The Journal of The Textile Institute, 2016, 107.9: 1079-1088.

[30] SVENSSON, N.; SHISHOO, R.; GILCHRIST, M. Manufacturing of thermoplastic composites from commingled yarns-A review. Journal of Thermoplastic Composite Materials, 1998, 11.1: 22-56.

[31] AMIRSHIRZAD, Forough; MOUSAZADEGAN, Fatemeh; EZAZSHAHABI, Nazanin. Evaluating the resistance of metal reinforced multi-layer textile structure against penetration of sharp objects. International Journal of Protective Structures, 2021, 12.2: 245-262.

[32] JOHNSON, Andrew; BINGHAM, Guy A.; WIMPENNY, David I. Additive manufactured textiles for high-performance stab resistant applications. Rapid Prototyping Journal, 2013.

[33] CHEON, Jinsil; LEE, Minwook; KIM, Minkook. Study on the stab resistance mechanism and performance of the carbon, glass and aramid fiber reinforced polymer

and hybrid composites. Composite Structures, 2020, 234: 111690.

[34] ALPYILDIZ, Tuba, et al. Stab and cut resistance of knitted structures: a comparative study. Textile Research Journal, 2011, 81.2: 205-214.

[35] BILISIK, Kadir. Two-dimensional (2D) fabrics and three-dimensional (3D) preforms for ballistic and stabbing protection: A review. Textile Research Journal, 2017, 87.18: 2275-2304.

[36] Bilisik K, Karaduman NS, Bilisik NE and Bilisik HE. Three-dimensional circular various weave patterns in woven preform structures. Text Res J 2014; 84(6): 638–654.

[37] LI, Mengru, et al. Investigation of impact performance of 3-dimensional interlock polymer fabrics in double and multi-angle pass stabbing. Materials & Design, 2021, 206: 109775.

[38] A, Forough; M, Fatemeh; E, Nazanin. Evaluating the resistance of metal reinforced multi-layer textile structure against penetration of sharp objects. International Journal of Protective Structures, 2021, 12.2: 245-262.

[39] BILISIK, Kadir. Multiaxis three dimensional (3D) woven fabric. Advances in modern woven fabrics technology, 2011, 79-106.

[40] LU, Shiyan, et al. Design and development of three-dimensional woven fabrics with stab resistance. 2018.

[41] BALANI, Kantesh, et al. Multi-scale hierarchy of Chelydra serpentina: microstructure and mechanical properties of turtle shell. Journal of the Mechanical Behavior of Biomedical Materials, 2011, 4.7: 1440-1451.

[42] ACHRAI, Ben; BAR-ON, Benny; WAGNER, H. D. Biological armors under impact—effect of keratin coating, and synthetic bio-inspired analogues. Bioinspiration & biomimetics, 2015, 10.1: 016009.

[43] DAMIENS, R., et al. Compressive behavior of a turtle's shell: experiment, modeling, and simulation. Journal of the mechanical behavior of biomedical materials, 2012, 6: 106-112.

[44] ZHANG, Xu, et al. Understanding hydration effects on mechanical and impacting properties of turtle shell. Journal of the Mechanical Behavior of Biomedical Materials, 2018, 78: 116-123.

[45] GUO, Ya-xin; YUAN, Meng-qi; QIAN, Xin-ming. Bionic stab-resistant body armor based on triangular pyramid structure. Defence Technology, 2021, 17.3: 792-799.

[46] CHEN, Irene H.; YANG, Wen; MEYERS, Marc A. Alligator osteoderms: mechanical behavior and hierarchical structure. Materials Science and Engineering: C, 2014, 35: 441-448.

[47] WHITE, Zachary W.; VERNEREY, Franck J. Armours for soft bodies: how far can bioinspiration take us?. Bioinspiration & biomimetics, 2018, 13.4: 041004.

[48] HU, Jiayun, et al. The preparation and characteristics of high puncture resistant composites inspired by natural silk cocoon. Composites Part A: Applied Science and Manufacturing, 2021, 149: 106537.

[49] SITOTAW, Dereje Berihun, et al. Investigation of Stab Protection Properties of Aramid Fibre-Reinforced 3D Printed Elements. *Fibres & Textiles in Eastern Europe*, 2021.

[50] LI, Ting-Ting, et al. Construction of synergistic toughening, self-healing puncture-resistant soft composites by using fabric-reinforced pluronic/PMEA hydrogel. Composites Part A: Applied Science and Manufacturing, 2021, 145: 106388.

[51] PARK, Yurim, et al. Numerical simulation and empirical comparison of the high velocity impact of STF impregnated Kevlar fabric using friction effects. Composite Structures, 2015, 125: 520-529.

[52] LU, Zhenqian, et al. Numerical simulation of the impact behaviors of shear thickening fluid impregnated warp-knitted spacer fabric. Composites Part B: Engineering, 2015, 69: 191-200.

[53] ZHOU, Yi, et al. Ballistic response of stitched woven fabrics with superior energy absorption capacity: Experimental and numerical investigation. Composite Structures, 2021, 261: 113328.

[54] XU, Junhao, et al. Quasi-static puncture resistance behaviors of architectural coated fabric. Composite Structures, 2021, 273: 114307.

[55] WU, Zhenyu, et al. Low-velocity impact performance of hybrid 3D carbon/glass woven orthogonal composite: Experiment and simulation. Composites Part B: Engineering, 2020, 196: 108098.

[56] WEI, Qingsong; YANG, Dan; GAO, Bo. Ballistic penetration simulation of a 3D woven fabric using high strain-rate dependent yarn model. The Journal of The Textile Institute, 2022, 113.7: 1401-1410.

[57] WANG, Lijing, et al. FEM analysis of knife penetration through woven fabrics. Computer modeling in engineering and sciences, 2007, 20.1: 11-20.

[58] XIAO, Yuan, et al. Study on micro-scale 3D numerical modeling and droplet deposition of plain weave fabric. Journal of Mechanical Science and Technology, 2022, 36.4: 1739-1748.

[59] ZHOU, Hongtao, et al. Numerical simulation and experimental study of the bursting performance of triaxial woven fabric and its reinforced rubber composites. Textile Research Journal, 2020, 90.5-6: 561-571.

[60] REDDY, Junuthula Narasimha. Introduction to the finite element method. McGraw-Hill Education, 2019.

[61] STOLARSKI, Tadeusz; NAKASONE, Yuji; YOSHIMOTO, Shigeka. Engineering analysis with ANSYS software. Butterworth-Heinemann, 2018.

Chapter 2

Preparation of Material Structure and Research on Anti-stab Performance

Chapter 2: Preparation of Material Structure and Research on Anti-stab Performance

2.1 Introduction

With the globalization of the war on terror and increased awareness about the need for protection, personal safety has become an important issue. The use of firearms is severely restricted in many countries, but the threat from sharp objects used as weapons [1] is ubiquitous. Police and security guards in particular often encounter violent situations. Most existing anti-stab armor [2] is made from steel plates, which are very heavy. This greatly inconveniences the wearer and inhibits their ability to perform their tasks. Therefore, increasing attention has been paid to the development of new puncture-resistant materials.

In the field of lightweight protective materials, aramid fibers are essential. Due to their excellent performance, they have made great contributions in many fields. Zheng et al. [3] used the principle of bionics to develop and prepare three-dimensional Kevlar polyimide composite materials. Excellent three-dimensional structure makes it a composite with ultra-light, superior anti-compressive and flame-retardant properties. Zhou et al. [4] proposed to develop a high-performance multi-purpose composite material. Materials prepared using Kevlar fibers, shear-hardening gels, and MXene exhibit excellent thermal management and intelligent safeguarding.

Based on Kevlar fibers, many experts have carried out research on protective materials. Usman Javaid et al. [5] studied the effect of changes in the surface friction of the fabric and the knife penetration angle on quasi-static knife penetration resistance. Zhang et al. [6] put forward the relationship between the slippage of Intralayer interface

and the anti-impact performance. It is found that the impact velocity and constraint conditions are the two main influencing factors. Sy et al. [7] used flax fiber and Kevlar fiber as raw materials to prepare epoxy resin matrix composite materials. The impact resistance of materials under different layup methods has been studied. In order to improve the impact resistance of Kevlar composites, Eltaher et al. [8] prepared CFRP/Kevlar sandwich composites. The results show that the residual compressive properties of the sandwich composites are greatly improved. White et al. [9] considered that all armor depends on a combination of weight, flexibility, and protection. Guleria et al. [10] prepared Kevlar composites by improving the molding method of the material, that is, using microwave-assisted molding. The mechanical properties of the materials prepared by this method are improved. In terms of impact, different impact head shapes also have a big impact on performance. Karamooz et al. [11] found that among the hemispherical, conical, and flat shapes, the highest energy absorption and damage area are obtained with the conical impactor. As 3D printing technology matures, researchers also apply it to the field of stab prevention. Hetrick et al. [12] proposed the technology of continuous Kevlar fiber reinforced 3D printing composites. This material is used to study the effects of different fiber modes, stacking modes, and fiber orientations on the impact properties of the material.

At the same time, we have also carried out related experiments and have accumulated some experience. Bao et al. [13] developed a new high-density nonwoven structure to enhance the stab resistance of protective clothing. They found that material prepared by single-layer hot pressing guarantees puncture resistance and improves comfort. Bao et al. [14] tested the stab resistance of aramid fabrics comprising nanoparticles. They found that the puncture performance of the material increased as the

particle diameter decreased, and the friction of the intersecting parts of the plain weave fabric had the greatest impact on puncture resistance. Chuang et al. [15] studied the recycling of fiber materials and used nonwoven technology to prepare mixed fiber fiberboards. They reported that the material had higher puncture performance than traditional woven fabrics.

As can be seen from the research described above, many different structures and materials are used to make protective armor. Among these materials, high-performance fiber composites are currently the focus of intense research because they are lightweight and offer good protection. Puncture is a transient process, so it is difficult to study the mechanism by which it occurs in fabrics through practical experiments alone. To explore in depth the mechanism by which punctures occur, it is usually necessary to carry out auxiliary simulation experiments.

However, during simulation experiments it is easy to overlook the anisotropy of the inner yarn of the composite material, which is usually taken to be an isotropic material for finite element analysis. As is well known, yarn is an anisotropic material, and there is a big difference between its axial performance and its radial performance. If the yarn is regarded as an isotropic material, it may cause a large error in the calculation and analysis. At the same time, the definition of yarn-to-yarn contact is also an easily overlooked part. Therefore, exploring these two difficulties has become the focus of this experiment.

2.2 Experiments

2.2.1 Structural Design

In order to achieve the goal of this experiment perfectly, we need to design the material structure. It can be seen from the above that the establishment of the model is

very important in the implementation of the simulation experiment. Therefore, the structural design of the material here should not only meet the needs of the experiment, but also meet the constraints of the modeling conditions.

The first is the need for experimentation. As shown in Figure 2-1. The yarns inside ordinary fabrics are intertwined up and down, which will cause many uncertainties in the simulation analysis of this experiment. Especially the parameter setting of the yarns at the interlaces is very difficult. In view of this, in order to avoid experimental errors, this experiment specially designed the following structure. As shown in Figure 2-2, remove the upper and lower interwoven structure of the fabric and use a mesh structure. In this structure, the yarns are arranged in parallel, and their anisotropy parameters can be precisely defined in simulation experiments. At the same time, the yarn contact can also be set more precisely.

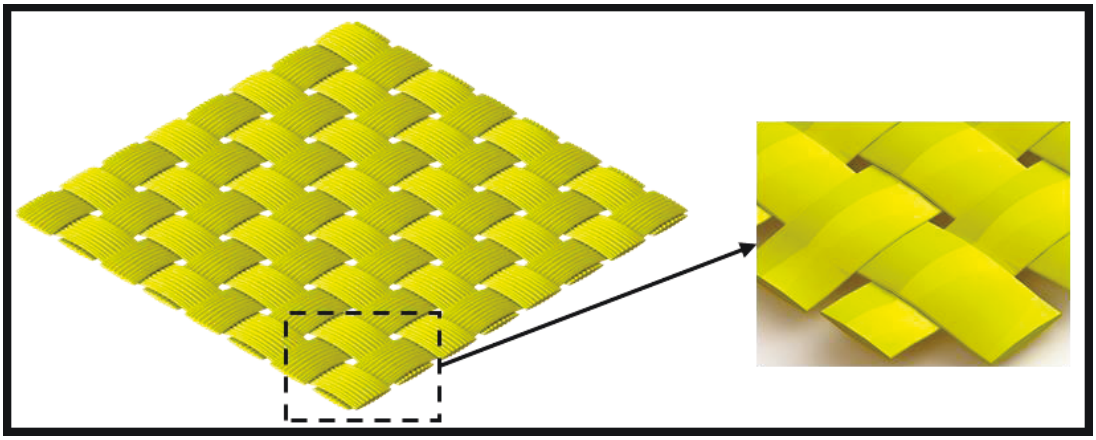

Figure 2-1 Structure of ordinary plain weave fabric

The second is the limitation of model establishment conditions. As we all know, yarn is made up of thousands of filaments. In the above discussion, we found that it is impossible to represent all the filaments in the yarn under the current simulation conditions. To solve this problem, we decided to use epoxy resin compounded with yarn to prepare yarn composites. On this basis, the simulation experiment can be carried out

with the yarn as a whole material, so that the accuracy of the simulation experiment can be controlled. The structure designed in this way is more conducive to the analysis of the experimental results.

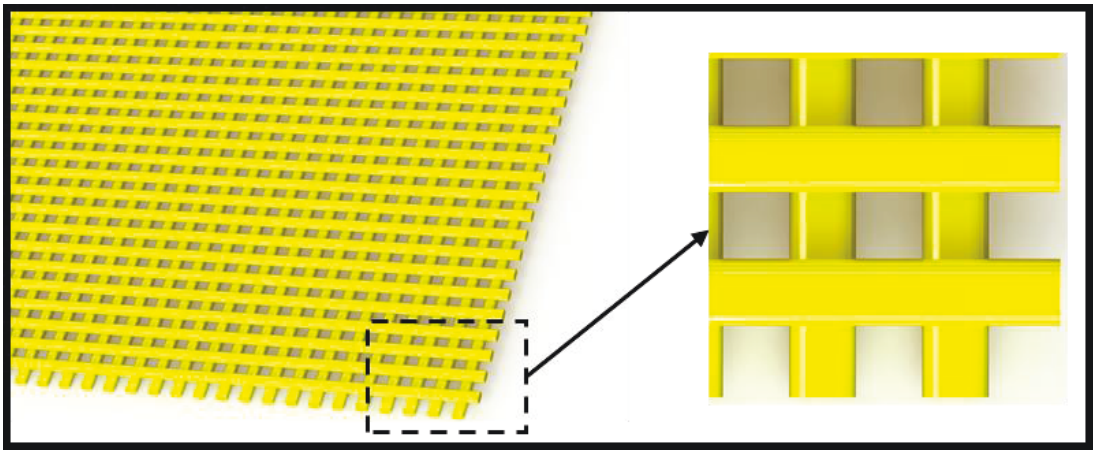

Figure 2-2 Schematic diagram of the structure of the mesh material

Therefore, in this puncture analysis, the mesh structure material is specially designed to consider the effects of anisotropy and inter-yarn contact on the simulation results of puncture resistance. The research results will provide a theoretical reference for the preparation of stab-resistant materials and lay a solid foundation for further research.

2.2.2 Materials

In order to prepare the mesh experiments designed above, aramid fibers and epoxy resins are used to make samples in this experiment. The yarns are made of Kevlar (Teijin Ltd., Tokyo, Japan), and the epoxy resin is obtained from the Nagase ChemteX Corporation (Tokyo, Japan).

2.2.3 Preparation

The grid structure material is designed for puncture analysis. In order to make a sample that conforms to the design, we have carried out the design of many schemes.

After referring to a lot of grid product production processes [16], combined with the characteristics of this experiment, we are constantly adjusting the parameters and processes. Finally, the following preparation process was confirmed. The sample preparation process is shown in the Figure 2-3.

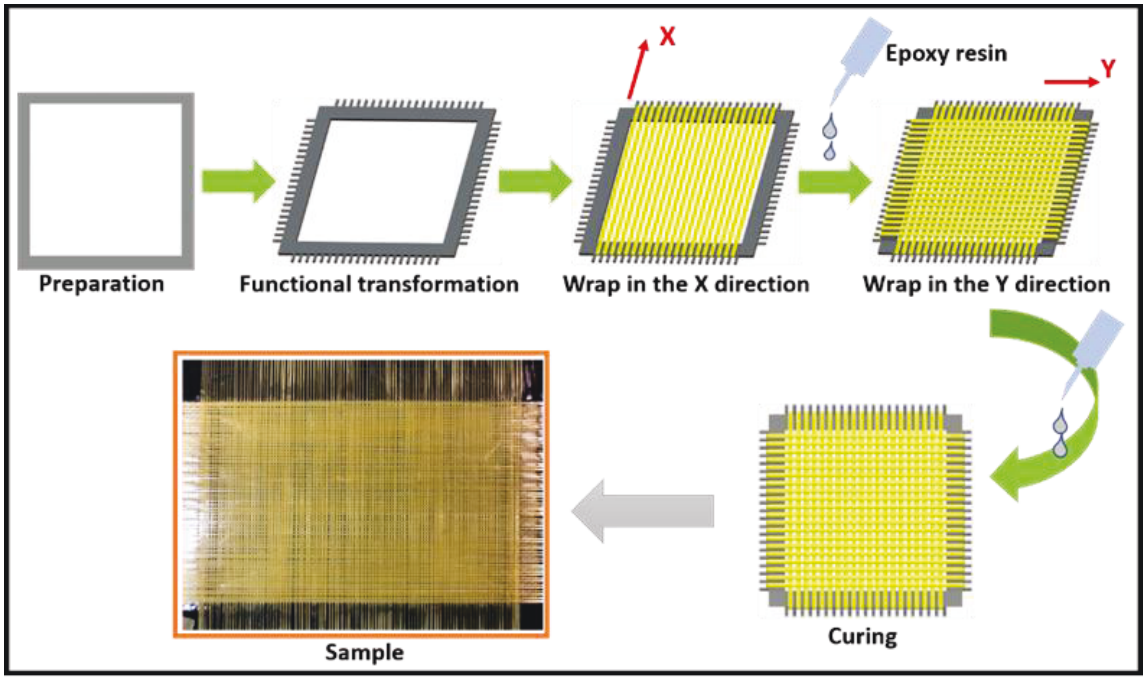

Figure 2-3. Preparation of the composite sample.

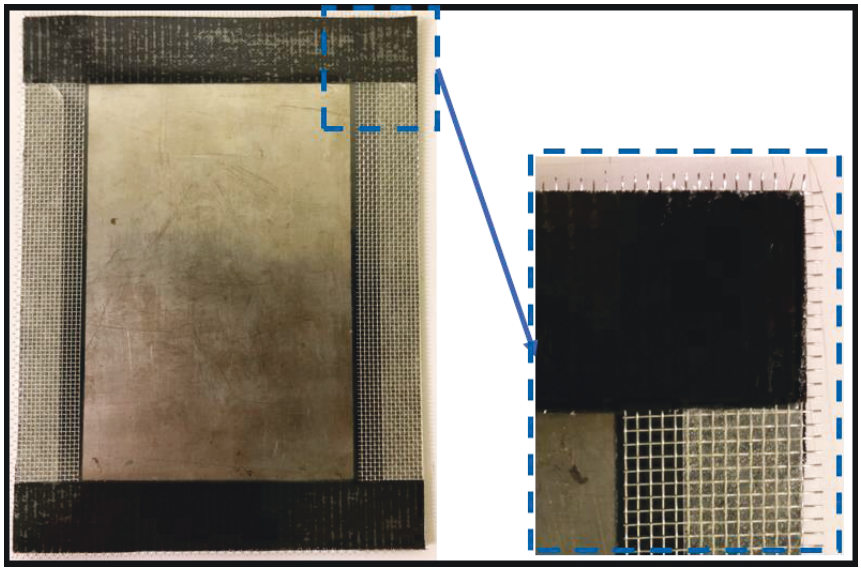

Figure 2-4. Detail drawing of retrofit to metal frame

The preparation of the mesh material requires the laying of double layers of yarns. First, choose a suitable metal frame as the stand. With its surface pretreatment, remove impurities and grease from its surface. Then, the processed frame is transformed according to the spacing of the grid. The zigzag fixing grooves are installed around the metal ore as the fixing base of the yarn. After the transformation, the sawtooth spacing of the metal frame is fixed at 1mm, as shown in the Figure 2-4. The first layer performs the yarn alignment in the X direction. After arranging according to the sawtooth spacing, use epoxy resin to impregnate and cure. Next, the second layer of yarn preparation is made, the yarn is wound in the Y direction and compounded with epoxy resin. The double-layer yarn layup is compounded with the epoxy resin material to form a grid-like composite material.

Figure 2-5 illustrates the partial amplification and the prepared sample. As shown, the yarn and resin composite formed well. Among them, the resin is evenly distributed on the double-layered yarn. At the same time, the X-direction yarns are well combined with the Y-direction yarns.

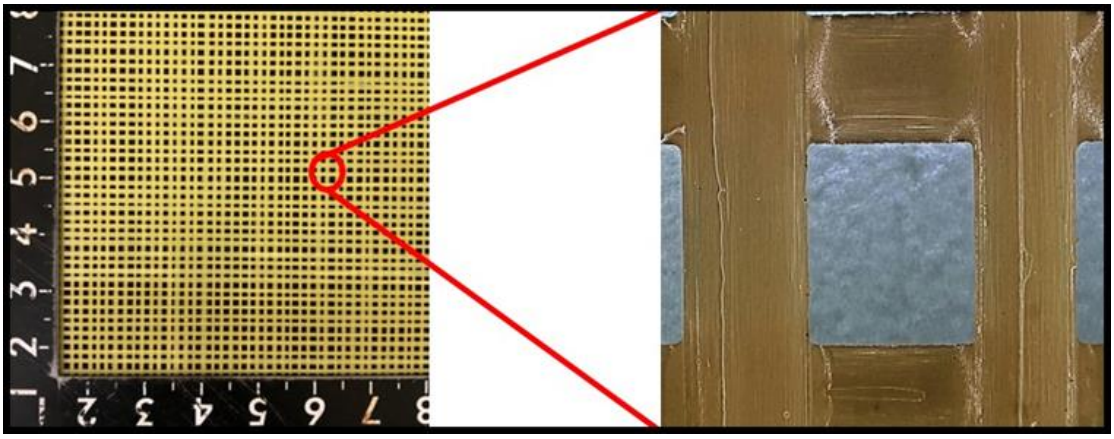

Figure 2-5. Photographs of the composite sample and the partial amplification.

2.2.4 Puncture Tests

The prepared sample is fixed on the puncture mold, as shown in Figure 2-6. The size of the model greatly affects the computation time of the simulation experiments. Therefore, according to the standard of puncture simulation, combined with laboratory equipment, this puncture sample was designed. The test samples were first cut to a size of 50 x 50 mm. Customize the sample holder according to the size of the sample. The sample holder consists of upper and lower halves, in which a puncture hole is reserved in the middle, and the four sides are fixed with screws.

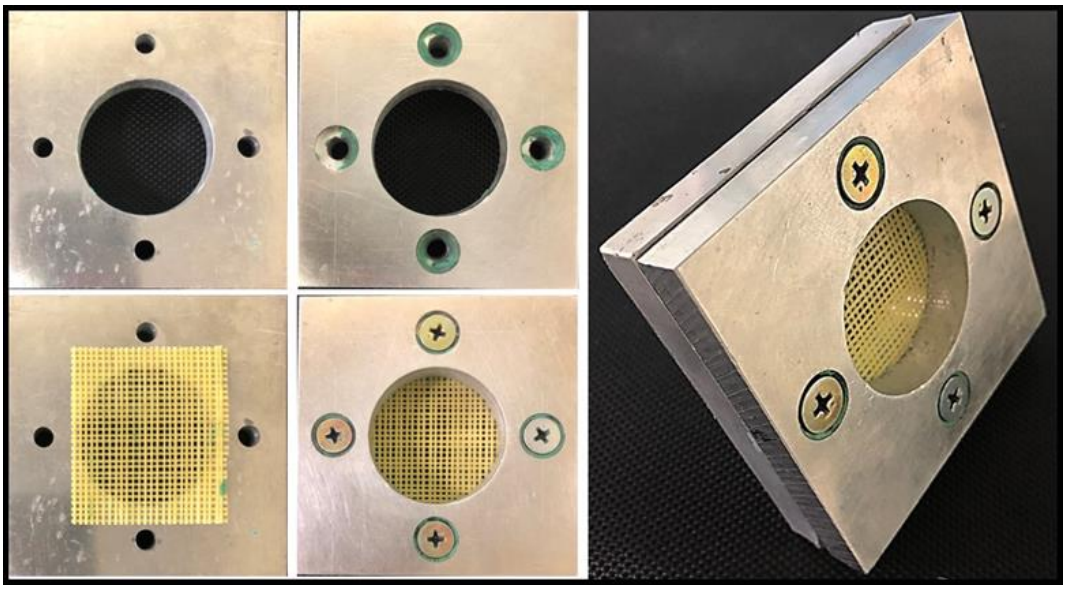

Figure 2-6. Preparation of the puncture sample.

A schematic diagram illustrating the puncture experiment [17] is shown in Figure 2-7. The anti-blade evaluation device is developed by BAO laboratory. In this device, the sample is fixed at the left clay, and the puncture needle is fixed on the air jet device. The puncture speed is controlled by adjusting the air valve. The tail of the needle is connected to a pressure sensor to determine the puncture force. A laser lamp is used to determine the displacement of the needle. From the time the blade comes into contact with the sample

until it penetrates, it is possible to measure the progress of displacement and the change in load. The speed of puncture can also be adjusted from 0.2m/s to 4.8m/s.

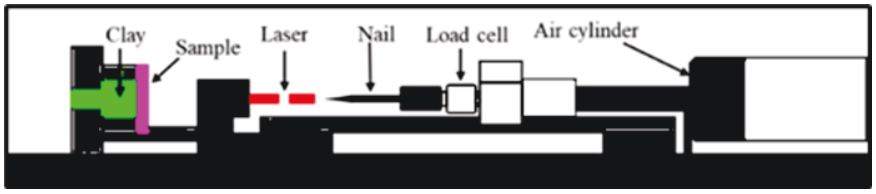

Figure 2-7. Puncture test machine.

Using this device, the puncture experiment of the sample is carried out. In order to observe the failure state of the material during the puncture process, a high-speed camera is used for observation in this experiment [18] as shown in Figure 2-8. The puncture speed used is 2 m/s, and a total of 5 samples are prepared for the test.

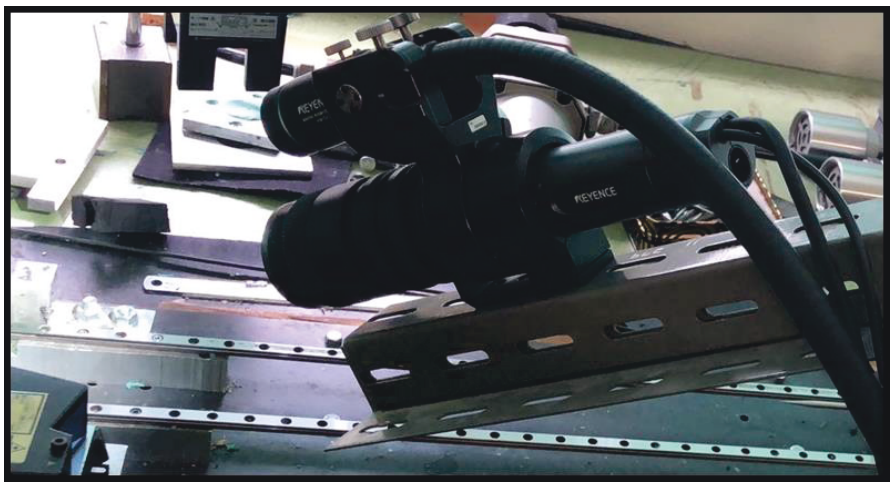

Figure 2-8. High-speed cameras used in puncture experiment

2.3 Results and Discussion

As shown in Figure 2-9, the grid material puncture experiment is divided into five parts (A–E) and the corresponding strain curve is shown in Figure 2-10. In the first stage (part A)—before the puncture needle had touched the material—the curve is relatively

flat; the needle had not yet been subjected to force and the strain is constant. In the second stage (part B), the needle came into contact with the grid structure, the extrusion force on the yarn gradually increased, and the strain began to rise as the needle penetrated deeper. At this time, the yarn began to exhibit slight bending deformation and the square holes gradually expanded into circular holes. The strain reached the first peak and then dropped rapidly when the yarn peeled off at the weakest point of the four crossing points. In the third stage (part C), the needle continued to penetrate the material after the yarn had separated at the intersection of the first ring. As the diameter of the needle continued to expand, the circle of fibers around the needle is subjected to friction and extrusion, and the curve therefore continued in a straight line until the four intersection points of the yarn fell off. The extrusion force on the yarn decreased and the strain also decreased again. In the fourth stage (part D), the needle continued to move forward after it had broken through the first ring. When the diameter of the needle increased, the yarn continued to be squeezed to both sides. At the same time, the cross points between the yarns prevented their expansion again. Therefore, the strain increased again until it reached its maximum. The yarn at the cross point peeled off, the bending degree of the yarn reached the diameter of the needle, the depth of the needle no longer increased the expansion force of the yarn, and the force between the needle and the yarn reached dynamic equilibrium, so the strain decreased and remained constant [19-21].

The analysis provided above indicates that when the needle is inserted, the yarn is mainly subjected to the extrusion and friction forces at the contact point with the needle. The yarn at the intersection is peeled off revealing that the material had been punctured.

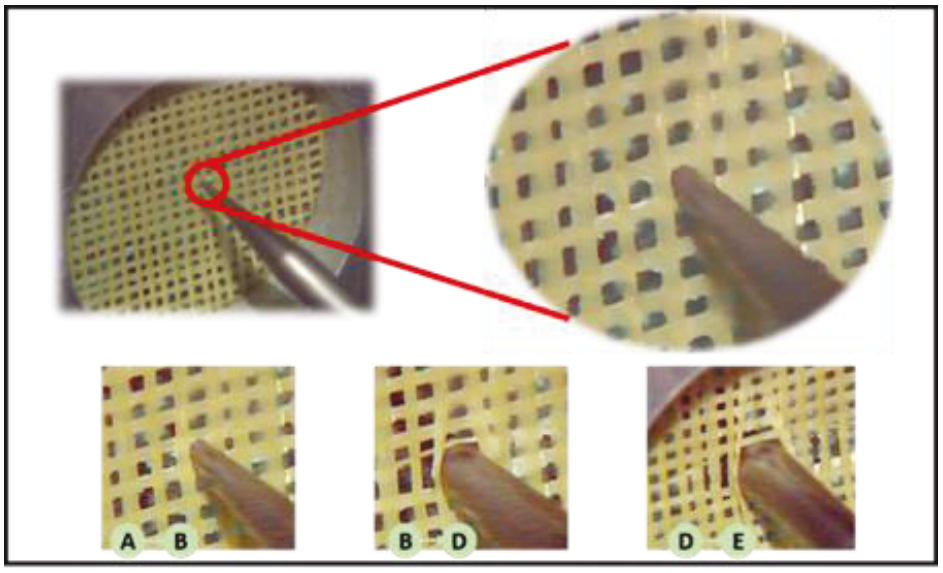

Figure 2-9. The composite puncture experiment.(The three pictures AB, BD, and DE in the figure correspond to the three stages in Figure 2-10)

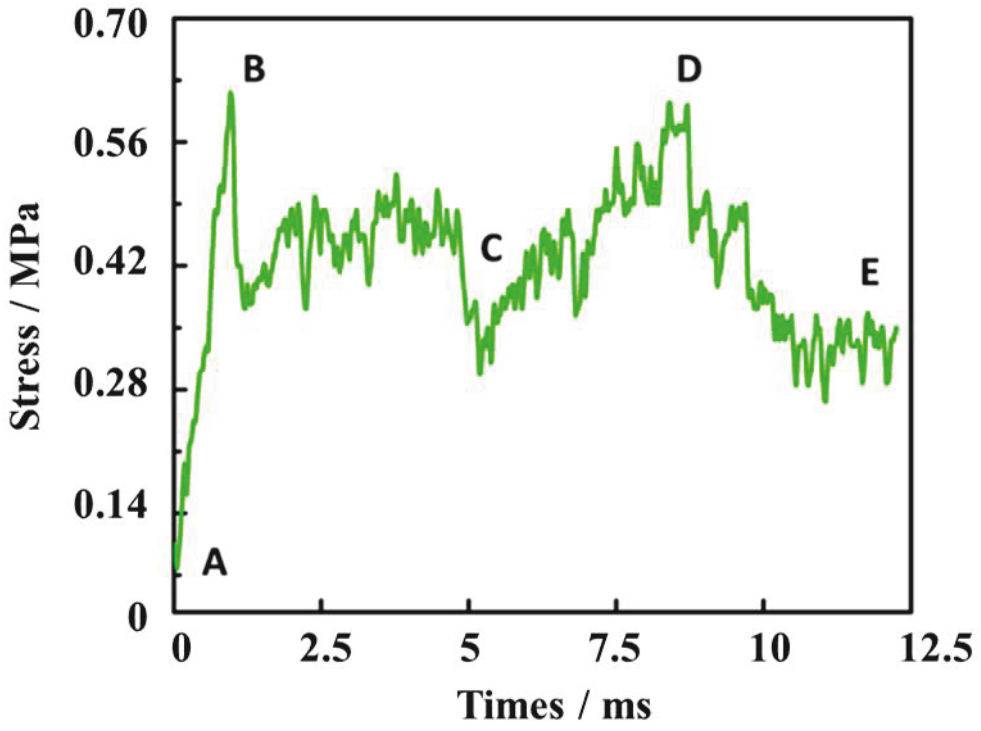

Figure 2-10. Results of the composite puncture experiment.(The curves marked A to E in the figure represent different stages in the puncture process.)

2.4 Conclusions

In this chapter, we design a special structure-mesh material that can be used in the simulation experiments described later. After the mesh material is prepared, the puncture experiment is carried out using the puncture experiment machine developed in our laboratory. At the same time, the analysis of the material puncture failure process is carried out with the help of the high-speed camera. The experimental results show that the main failure modes of the mesh material are resin breakage at the joints, yarn bending deformation, and slippage between the fibers and the resin. This experiment will be used as a benchmark for the subsequent simulation experiments to judge whether the simulation results are accurate.

Using the material structure of this chapter as a basis, we will begin to investigate the effect of the anisotropy of the yarn and the contact between the yarns on the accuracy of the simulation results.

References

[1] Nayak, R.; Crouch, I.; Kanesalingam, S.; Ding, J.; Tan, P.; Lee, B.; Miao, M.; Ganga, D.; Wang, L. Body armor for stab and spike protection, Part 1: Scientific literature review. Text. Res. J. 2018, 88, 812–832. https://doi.org/10.1177/0040517517690623.

[2] Horsfall, I. Stab Resistant Body Armour. Ph.D. Thesis. Engineering Systems Department, College of Defense Technology, Cranfield University, Cranfield, UK, 2000.

[3] Zheng, L.; Zhang, K.; Liu, L.; Xu, F. Biomimetic architectured Kevlar/polyimide composites with ultra-light, superior an-ti-compressive and flame-retardant properties. Compos. Part B Eng. 2022, 230, 109485.

[4] Zhou, J.; Zhang, J.; Sang, M.; Liu, S.; Yuan, F.; Wang, S.; Sun, S.; Gong, X. Advanced

functional Kevlar composite with excellent mechanical properties for thermal management and intelligent safeguarding. Chem. Eng. J. 2022, 428, 131878.

[5] Usman Javaid, M.; Militký, J.; Wiener, J.; Jabbar, A.; Salačová, J.; Umair, M. Effect of surface modification and knife penetration angle on the quasi-static knife penetration resistance of para-aramid fabrics. J. Text. Inst. 2019, 110, 590–599.

[6] Zhang, J.; Wang, Y.; Zhou, J.; Zhao, C.; Wu, Y.; Liu, S.; Gong, X. Intralayer interfacial sliding effect on the anti-impact perfor-mance of STF/Kevlar composite fabric. Compos. Part A Appl. Sci. Manuf. 2021, 145, 106401.

[7] Sy, B.L.; Oguamanam, D.; Bougherara, H. Impact response of a new kevlar/flax/epoxy hybrid composite using infrared thermography and high-speed imaging. Compos. Struct. 2022, 280, 114885.

[8] Eltaher, M.A.; Basha, M.; Wagih, A.; Melaibari, A.; Lubineau, G. On the impact damage resistance and tolerance improvement of hybrid CFRP/Kevlar sandwich composites. Microporous Mesoporous Mater. 2022, 333, 111732.

[9] White, Z.; Vernerey, F. Armours for soft bodies: How far can bioinspiration take us? Bioinspir. Biomim. 2018, 13, 041004.

[10] Guleria, T.; Verma, N.; Zafar, S.; Jain, V. Fabrication of Kevlar-reinforced ultra-high molecular weight polyethylene composite through microwave-assisted compression molding for body armor applications. J. Reinf. Plast. Compos. 2021, 40, 307–320.

[11] Karamooz, M.R.; Rahmani, H.; Khosravi, H. Numerical and experimental investigations on the low-velocity impact proper-ties of hybrid Kevlar fiber/basalt fiber reinforced epoxy composites: Effects of impactor nose shape and fiber stacking se-quences. Polym. Compos. 2021, 42, 6442–6454.

[12] Hetrick, D.R.; Sanei, S.H.R.; Ashour, O.; Bakis, C.E. Charpy impact energy

absorption of 3D printed continuous Kevlar rein-forced composites. J. Compos. Mater. 2021, 55, 1705–1713.

[13] Bao, L.; Wang, Y.; Baba, T.; Fukuda, Y.; Wakatsuki, K.; Morikawa, H. Development of a high-density nonwoven structure to improve the stab resistance of protective clothing material. Ind. Health 2017, 55, 513–520. https://doi.org/10.2486/indhealth.2017-0123.

[14] Bao, L.; Sato, S.; Wang, Y.; Wakatsuki, K.; Morikawa, H. Development of flexible stab-proof textiles impregnated with micro-scopic particles. J. Text. Eng. 2017, 63, 43–48. https://doi.org/10.4188/jte.63.43.

[15] Chuang, Y.-C.; Bao, L.; Lin, M.C.; Lou, C.W.; Lin, T. Mechanical and static stab resistant properties of hybrid-fabric fibrous planks: Manufacturing process of nonwoven fabrics made of recycled fibers. Polymers 2019, 11, 1140.

[16] RITTER, A. Smart coatings for textiles in architecture. In: Active Coatings for Smart Textiles. Woodhead Publishing, 2016. p. 429-453.

[17] Bao, L.; Sato, S.; Morioka, H.; Soma, S. Improving stab-resistant textile materials with a non-woven fabric structure. J. Text. Eng. 2016, 62, 37–42.

[18] ANDERSON, Philip SL; LACOSSE, Jennifer; PANKOW, Mark. Point of impact: the effect of size and speed on puncture mechanics. Interface Focus, 2016, 6.3: 20150111.

[19] ZHANG, Wen; LIU, Shuai; MA, Pibo. Experimental investigation on stab-resistant properties of co-woven-knitted fabric. Journal of Engineered Fibers and Fabrics, 2022, 17: 15589250221090502.

[20] KHUYEN, Nguyen Quang, et al. The Use of Laminates of Commercially Available Fabrics for Anti-Stab Body-Armor. Polymers, 2021, 13.7: 1077.

[21] WEI, Da; WANG, Rui; ZHANG, Shu Jie. The research progress of stab-resistant material. Advanced Materials Research, 2011, 332: 1896-1899.

Chapter 3

Simulation Experiments Considering Yarn Anisotropy

Chapter 3: Simulation Experiments Considering Yarn Anisotropy

3.1 Introduction

In Chapter 2, we specifically design the mesh material required for this experiment. Using aramid fiber and epoxy resin, we carry out the preparation of grid-like material. With reference to the puncture test standard, the puncture experiment is carried out on the puncture machine developed by the laboratory, and the damage process is analyzed and discussed. On this basis, we will continue to conduct puncture simulation experiments to investigate the influence of yarn anisotropy on the simulation results.

It is difficult to observe and analyze the material failure mechanism in the puncture experiment. Therefore, it is necessary to carry out auxiliary analysis with finite element analysis software. Hou et al. [1] established two different finite element models to describe the tensile properties of nonwovens, and macroscopically assessed the influence of thermal bonding points on the deformation mechanism and behavior of the materials. Ridruejo et al. [2] used a combination of experiment and simulation to determine the microscopic mechanism of deformation and damage in a nonwoven glass fiber mat. Zeng et al. [3] used the finite element method to study the effects of yarn inclination, yarn friction, and tensile modulus on yarn properties. Zhou et al. [4] used the finite element method to study the blasting performance of fabric-reinforced rubber composites and found that the rubber improved the breaking strength of the fabric. Sun et al. [5] tested the puncture behavior of various structures using finite element analysis. Puncture damage involves three stages: tensioning of the fabric, slippage of the weft/warp yarn, and breakage of the yarn. Zhu et al. [6] used finite element analysis to study the stab prevention capabilities of fish scales and found that the structure and behavior of natural

fish scales offer effective protection against several types of threat. Lian et al. [7] simulated the dynamic performance of three-dimensional braided composites and found that they offered protection against mild impact. Termonia [8] used models to study the exact mechanism of fabric puncture, which comprise four stages: contact, penetration, friction, and slip.

On the basis of the predecessors, we will use a more precise method to conduct simulation experiments. This chapter focuses on anisotropy in yarns. But why do we focus on this issue? It will be explained in detail next.

3.1.1 Isotropic and Anisotropic Materials

Anisotropy is a common property in materials and media that varies widely in scale. From crystals to various materials in everyday life, to the earth's medium, there is anisotropy. Isotropy and anisotropy are introduced here. [9]

A material is isotropic if its mechanical and thermal properties are the same in all directions. Isotropic materials can have uniform or non-uniform microstructures. A material is orthotropic if its mechanical and thermal properties are single-valued and independent in three mutually perpendicular directions. [10] When the mechanical and thermal properties of a material are different in different directions, the material is anisotropic.

The origin of anisotropic materials is explained from the perspective of microscopic materials science, which is caused by the directional arrangement of atoms in the crystal. The anisotropy of a crystal means that along different directions of the crystal lattice, the periodicity and density of the atomic arrangement are not the same, resulting in different physical and chemical properties of the crystal in different directions. The non-crystal is

in an amorphous state, and the atomic arrangement is disordered, so it is in a long-range disordered state, so there is no obvious difference from the interior of the non-crystal to all directions. Therefore, its physical and chemical properties in different directions are also the same, so it is isotropic[11-13].

Common isotropic materials, including cast iron, glass, concrete, steel, etc. When performing a simulation experiment, the isotropic parameters can be set directly, which will not cause any errors to the simulation results. However, for anisotropic materials, the situation is quite different.

3.1.2 Yarn is Anisotropic Material

Common high-performance yarns, including carbon fiber, aramid, etc., are anisotropic materials, as shown in Figure 3-1. Anisotropic materials have a rich range of applications. People usually use anisotropic materials in a way of "making use of their strengths and circumventing their weaknesses". That is, use the characteristics of the secondary direction in the correct direction to make it play the best performance.

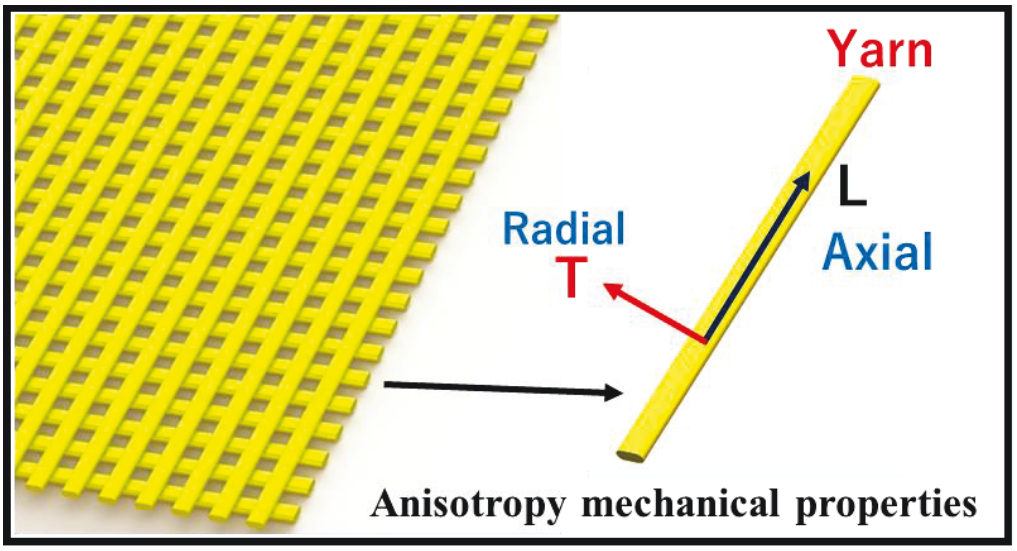

Figure 3-1. Schematic diagram of anisotropy mechanical properties

However, this different performance in different directions will cause great trouble in the process of simulation. As mentioned above, in the simulation, people often perform analysis and calculation with isotropy, and sometimes achieve the effect of simplification. Taking aramid yarn as an example, its performance in the axial direction is much greater than that in the radial direction.[14-16] It is obviously inappropriate to treat it as an isotropic material. However, in the axial tensile simulation experiment, it can achieve a good simplification effect by simplifying it to an isotropic material with tensile properties as the mainstay.

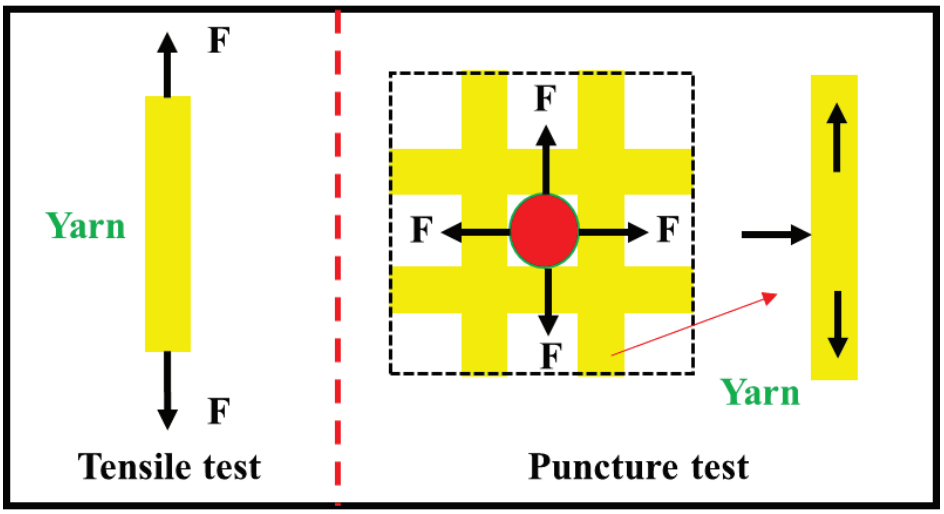

Figure 3-2. Comparison of the force in the tensile test and the puncture test

In the analysis of the puncturing process, when the ice pick pierces, the axial direction of the yarn is stretched and the radial direction of the yarn is compressed. In Figure 3-2, it is clear that the performance in the tensile direction is greater than that in the compression direction. However, when setting the isotropic material parameters in general simulation, the tensile properties parameters that are easy to measure are used. This increases the compressive properties of the material, which can cause large errors in the simulation results. [17-20]

It can be found that different countermeasures need to be considered when conducting different simulation experiments. The simulation of the puncture test must take into account the properties of the yarn in the axial direction and the compression properties of the yarn in the radial direction.

3.2 Experiments

After confirming the importance of yarn anisotropy, we begin to conduct simulation experiments for stab resistance. First and foremost is the establishment of the model.

3.2.1 Model Establishment

With regard to the actual experimental materials, the 1:1 structure model including the composite grid materials, the upper/lower splints, and the piercing needles is established using SolidWorks software (SolidWorks Premium 2016, Dassault Systèmes SolidWorks Corporation ,Concord, Massachusetts, USA).

According to the previous analysis, in order to reduce the amount of calculation, the yarn and resin are prepared into a composite material. So the following assumptions are made about the composition and structure of the composite grid materials:

(1) The yarns are continuous filaments with uniform bars, and the cross section is a runway type.

(2) The composite material has no defects and the resin distribution is uniform [21].

The model explosion diagram and assembly diagram (upper right) shown in Figure 3-3 are based on these assumptions.

In order to save calculation time, the puncture needle in the model adopts the part of the needle tip, as shown in Figure 3-4.

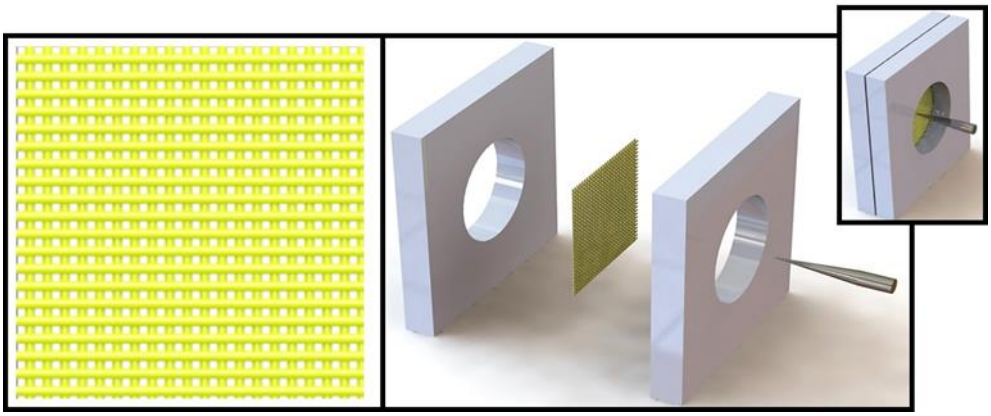

Figure 3-3. Illustration of geometrical puncture simulation model.

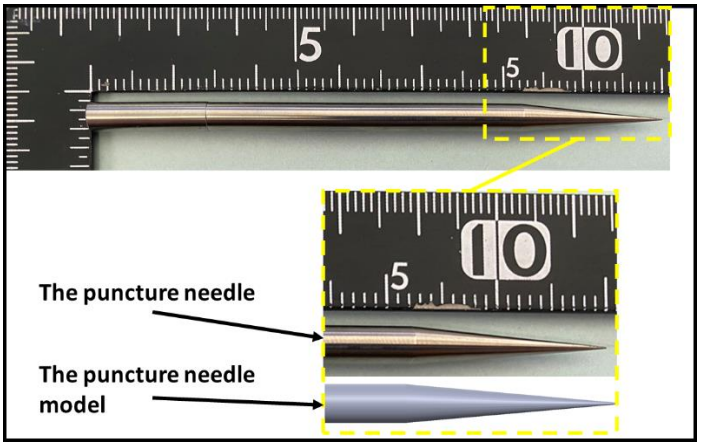

Figure 3-4. Illustration of puncture needle model.

3.2.2 Model Setting

The simulation software used in this experiment is ANSYS. Using the part of explicit dynamics [22], a finite element simulation of the puncture experiment is performed. The model is imported into the finite element software after being established by SolidWorks. There is no Kevlar yarn parameter in the engineering parameter database in the software, so it is necessary to customize the material parameters. We created a new material parameter library and selected the Anisotropic Material option. The warp and weft parameters of the yarn are set according to the values in Table 3-1. Therefore, the

anisotropy of the yarn plays an important role in the numerical simulation.

The model is then meshed. To reduce computation time, the meshes involved in the piercing contact are closely divided, whereas the meshes around the model are relatively sparse [23]. The mesh size of the central area is 0.01 mm, and the surrounding part is 0.05 mm by adopting the type of Hex Dominant. After division, there are 288,301 nodes and 112,468 elements, as shown in Figure 3-5.

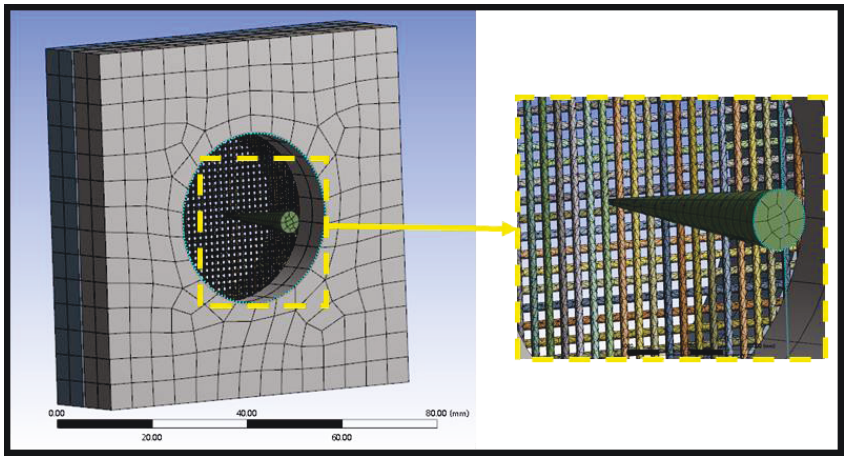

Figure 3-5 Meshing of the model

The model is fixed by referring to the material-fixing method in the actual experiment. The upper and lower clips are set to fixed, and the contact between the yarns and the upper and lower clips are set to bonded. The interfacial contact between the yarns is also set to bonded. At the same time, in order to simulate the failure during puncture, the maximum strain failure criterion is set for the yarns part.

Regarding the setting of the yarn anisotropy parameters in the setup, the next section will introduce the measurement scheme of its parameters in detail.

3.2.3 Measurement of Axial Modulus

The first is the yarn axial performance test. We conduct experiments according to

the standard ASTM D7269 [24] for a description of the determination of the axial modulus of the yarn. The prepared yarn resin composite material is shown in the Figure 3-6. Spacers are installed on both ends of the yarn to prevent the material from slipping and to avoid stress concentration during the pulling process.

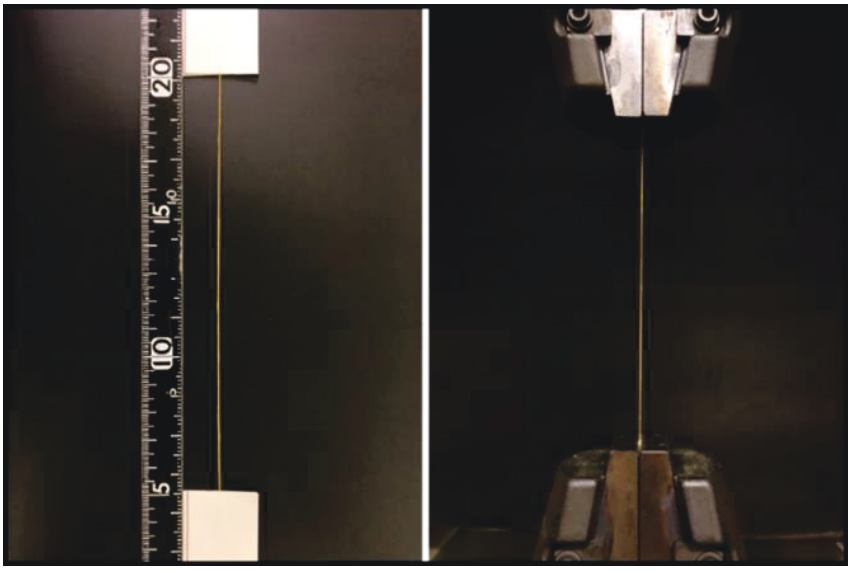

Figure 3-6. Determining the tensile mechanical properties of the Kevlar yarns.

According to Formulae (1)–(4), the yarn stress-strain curve is drawn, and the elastic modulus of the material is calculated. The tensile mechanical properties of the Kevlar yarns are shown in Figure 3-7. (σ: tensile stress, F: tensile strength, A: cross-sectional area of yarn, T: linear density of yarn, D: yarn density, ε: tensile strain, L: length of yarn after stretching, L_0: yarn length, E: tensile elastic modulus)

$$\boldsymbol{\sigma = \frac{F}{A}} \qquad \textbf{(1)}$$

$$\boldsymbol{A = \frac{T}{D}} \qquad \textbf{(2)}$$

$$\boldsymbol{\varepsilon = \frac{L - L_0}{L_0}} \qquad \textbf{(3)}$$

$$\boldsymbol{E = \frac{\sigma_1 - \sigma_2}{\varepsilon_1 - \varepsilon_2}} \qquad \textbf{(4)}$$

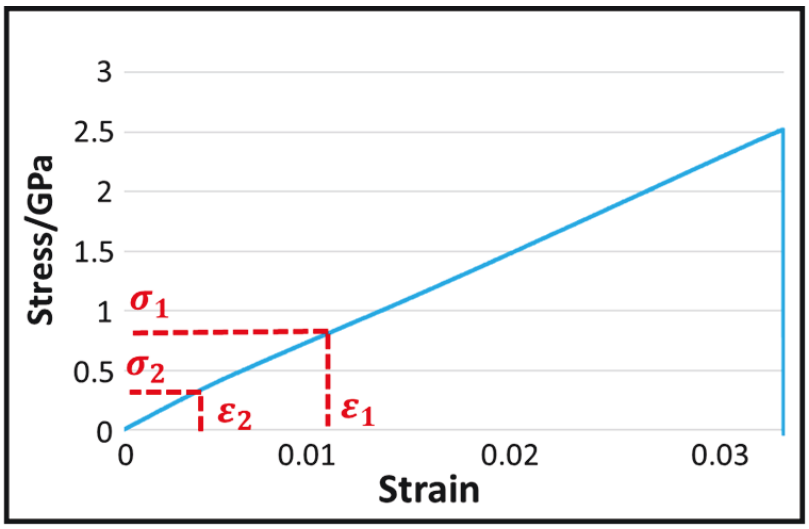

Figure 3-7. Tensile mechanical properties of the Kevlar yarns.

3.2.4 Measurement of Radial Modulus

The next is the yarn radial performance test. Because there is no special test standard for the radial modulus of a yarn, we referred to the test method used for the radial performance of a single fiber. As shown in Formulae (5) and (6), the radial modulus test refers to the method described by Professor Kawabata [25], which can be seen in Figure 3-8.

$$U = (4F / \pi)\left[(1 / E_T) - \left(\nu_{LT}^2 / E_T\right)\right][0.19 + sin\, h^{-1}(R, b)] \quad (5)$$

$$b^2 = (4FR / \pi)\left[(1 / E_T) - \left(\nu_{LT}^2 / E_T\right)\right] \quad (6)$$

where:

U: the change in fiber diameter;

F: the compressive force;

E_T: the transverse modulus of the fiber;

ν_{LT}: the longitudinal Poisson's ratio of the fiber;

R: the radius of the fiber;

b: the contact width of the fiber during compression.

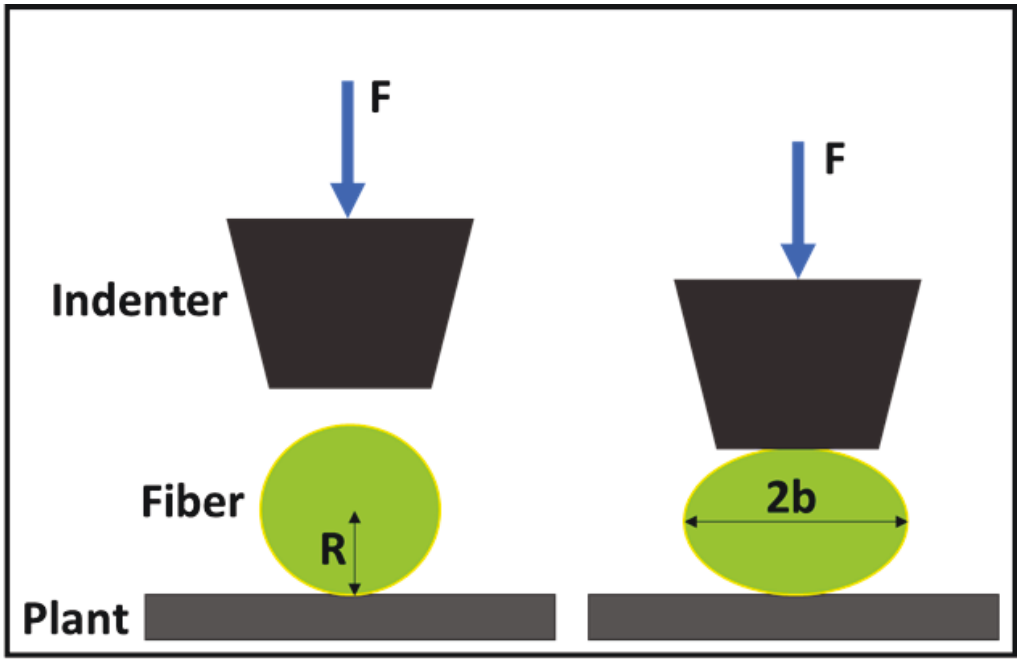

Figure 3-8. Schematic diagram of the transverse tester.

Owing to the limitations of the laboratory equipment, it is impossible to accurately measure all the parameters required in the formulae in the actual test. Therefore, using the results from previous research [26], the formulae described above are further simplified to Formula (7). Yarn compression experiments are carried out according to the parameter requirements of Formula (7). The experimental results are shown in Figure 3-9, and the radial modulus is obtained based on this result (Figure 3-10).

$$E_T = F\pi / 16RL^2\varepsilon^2 \quad (7)$$

where:

E_T: the transverse modulus of the fiber;

F: the compressive force;

R: the radius of the fiber;

L: the length of the fiber during compression; and

ε: the strain of the fiber.

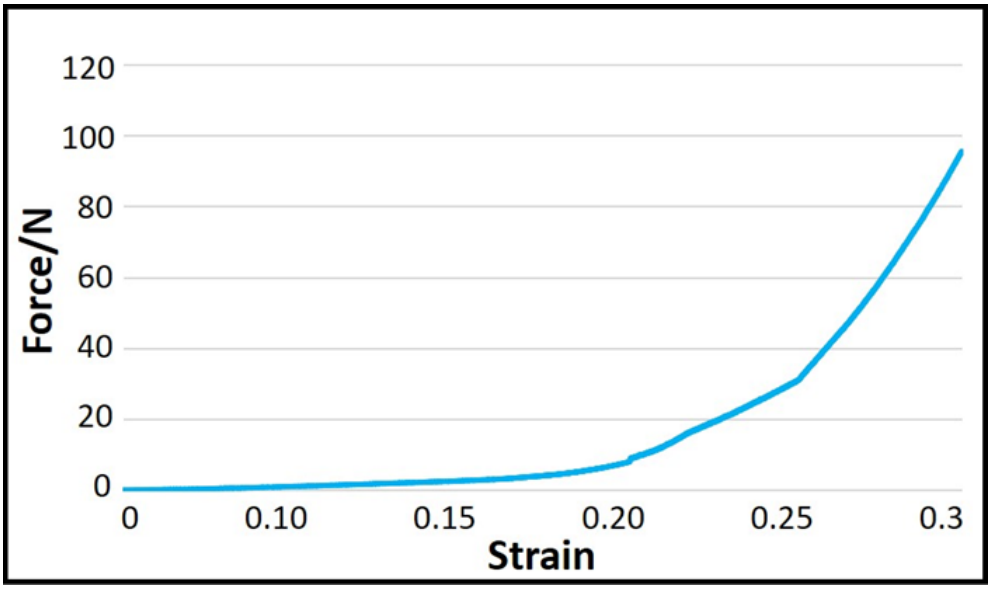

Figure 3-9. Transverse compressive curve of the Kevlar yarns.

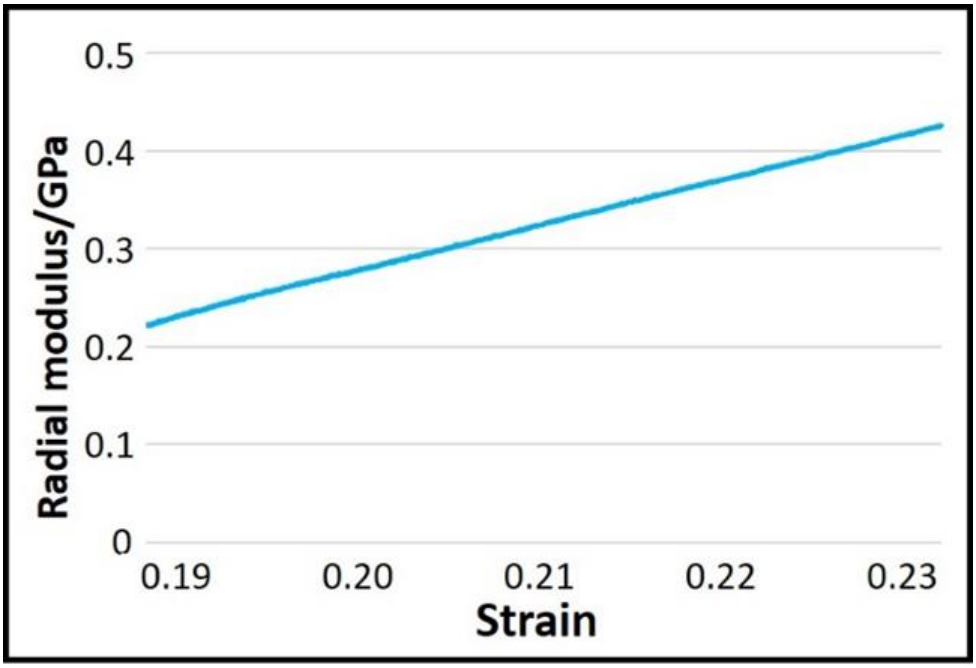

Figure 3-10. Radial modulus of the Kevlar yarns.

According to the above-mentioned test methods for the elastic modulus of the material in the axial and radial directions, the elastic modulus of the material is calculated as shown in Table 3-1 by using Equations (4) and (7).

Table 3-1. Radial and axial parameters of the Kevlar yarns.

	Young's Modulus (GPa)	Tensile/Compression Strength (GPa)	Failure Strain
Axial direction of yarn	78.62 ± 2.54	2.58 ± 0.32	0.032 ± 0.0024
Radial direction of yarn	0.32 ± 0.04	0.23 ± 0.02	0.263 ± 0.031

3.2.5 Puncture Simulation

The puncture speed is set to 2 m/s, and the contact between the blade and the sample is introduced as a general contact with a friction coefficient of 0.2 [27].

For comparative experiments, the parameters are imported without considering material anisotropy and the simulation experiments are carried out under the same conditions. The radial and axial parameters of the yarn in this model are the same and are used to assess how much yarn anisotropy affects the simulation results.

The simulated puncture experiment is carried out after all the settings had been completed.

3.3 Results and Discussion

3.3.1. Comparison of Simulation Results

The results of the puncture simulation experiment are shown in Figure 3-11 and Figure 3-12. The failure morphology between the experiment and simulation is shown in Figure 3-13. As shown in Figure 3-11, the simulation results obtained with the isotropic parameter settings are quite different from the actual results. Although the overall trend of the curve is similar to the actual experimental results, the maximum value is quite different. The strain is generally small between points C and D. This is because when the yarn is regarded as an isotropic material, its radial characteristics are stronger. Therefore, the numerical values shown in the strain curve are quite different from the experimental

values.

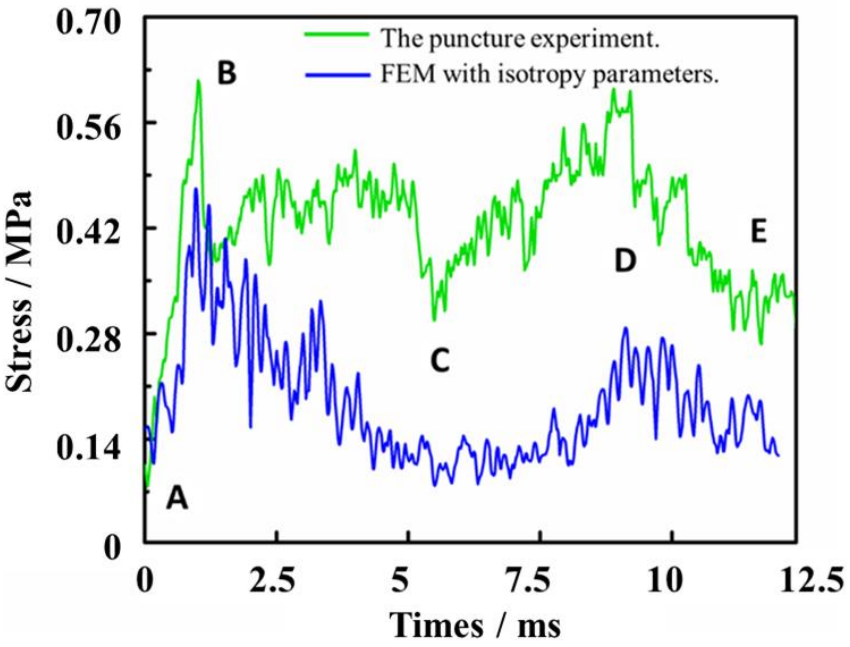

Figure 3-11. Strain results obtained using the finite element method (FEM) with isotropy parameters.

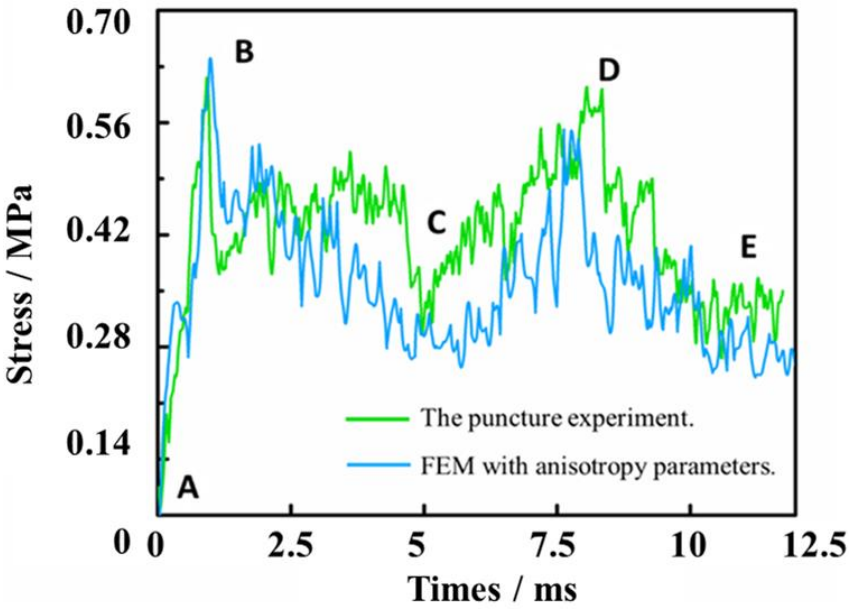

Figure 3-12. Strain results obtained using the finite element method (FEM) with anisotropy parameters.

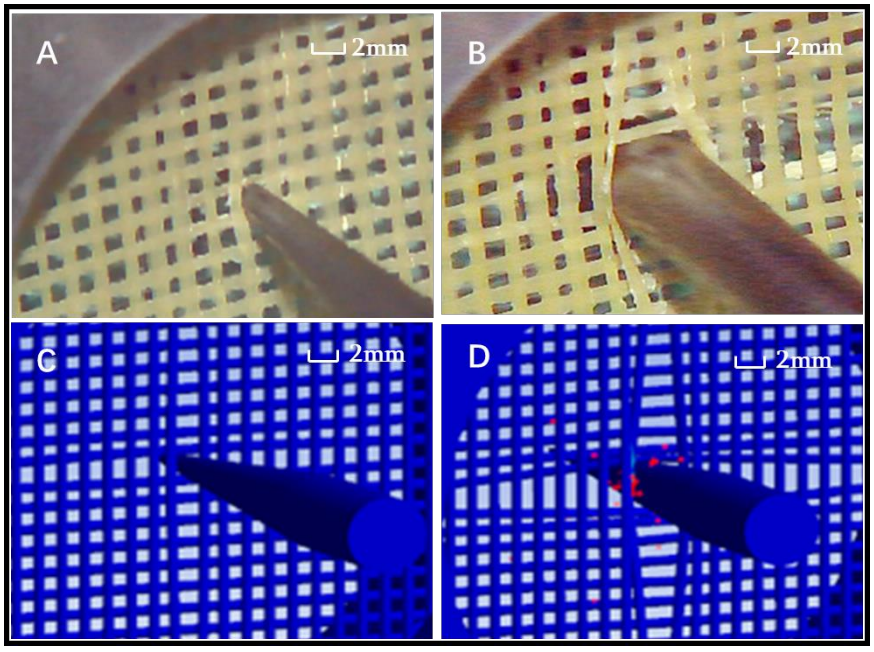

Figure 3-13. Comparisons between the results obtained using the finite element method (FEM) with anisotropy parameters and the experimental results. (A shows the needle contacted material in the experiment, B shows the needle completely penetrated the material in the experiment, C shows the needle contacted material in the simulation experiment, D shows the needle completely penetrated the material in the simulation experiment)

However, compared with the differences between the curves in Figure 3-11 and 3-12, the simulation results using yarn anisotropy parameters are more accurate. The strain curve of the simulation experiment also included five stages, the trend is the same as that in the actual experiment, and the value is within the allowable error range. The difference between the simulation and experimental results occurred in stage B. This is probably due to manual errors in the preparation of the experimental materials. The connection strength of the four crossing points around the grid is not the same, so there is a certain time difference between stripping and shedding. The maximum strain during stage B decreased

and the strain subsequently adopted a straight trend for a period of time. The connection strength of the four crossing points is the same in the simulation experiment, so the strain decreased directly and the fluctuation is more obvious after the maximum strain of the B stage is reached. At the same time, the failure morphology of the simulated experiment under this condition is also consistent with the failure morphology of the actual experiment in the Figure 3-13.

In summary, the simulation results are closer to the actual experiment results after considering yarn anisotropy. Therefore, the simulation results had a certain reference value, so a detailed analysis of the material is carried out.

3.3.2. Microscopic Analysis of the Simulated Puncture Results

(1) Stress analysis of the whole fabric

The upper and lower collets and puncture needles in the model are hidden, and the intermediate material is extracted for analysis. The overall stress nephogram of the grid composite obtained from the puncture load simulation results is shown in Figure 3-14. Different colors in the figure show different stress levels of the material.

The figure reveals that when subjected to puncture load, the yarn stress around the mesh at the puncture site began to increase. As the penetration depth of the needle increased, the yarn began to deform and bend and the stress wave spread rapidly along the transverse and longitudinal directions of the yarn. Under the action of the stress wave, the material absorbed energy through deformation bending, resin fragmentation, and fiber fracture. Until the needle penetrated the material, the yarn deformation bending reached the maximum and the stress value is not increasing.

During the whole process of puncture simulation, the stress values of the yarn are

largest in the longitudinal and transverse directions. This is the main influencing factor of the puncture effect [32] and the yarn around the material is largely unaffected. Therefore, the yarns in the longitudinal and transverse directions are extracted for further refinement analysis.

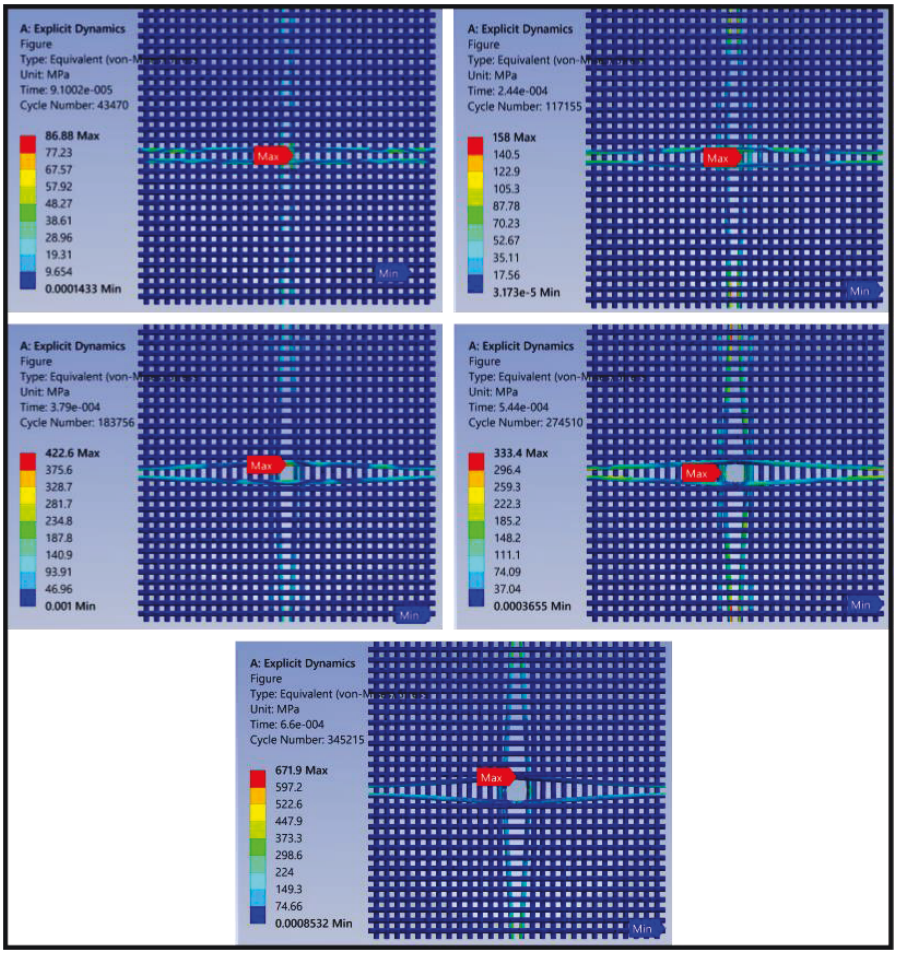

Figure 3-14. Damage morphologies obtained from the finite element method (FEM) results (stress diagram of the overall material).

(2) Stress analysis of central yarns

The yarn stress nephogram at the puncture center is shown in the Figure 3-15. The stress value of the outer yarn in contact with the needle is greatest when the material is subjected to puncture injury, whereas the stress value of the inner yarn is smaller.

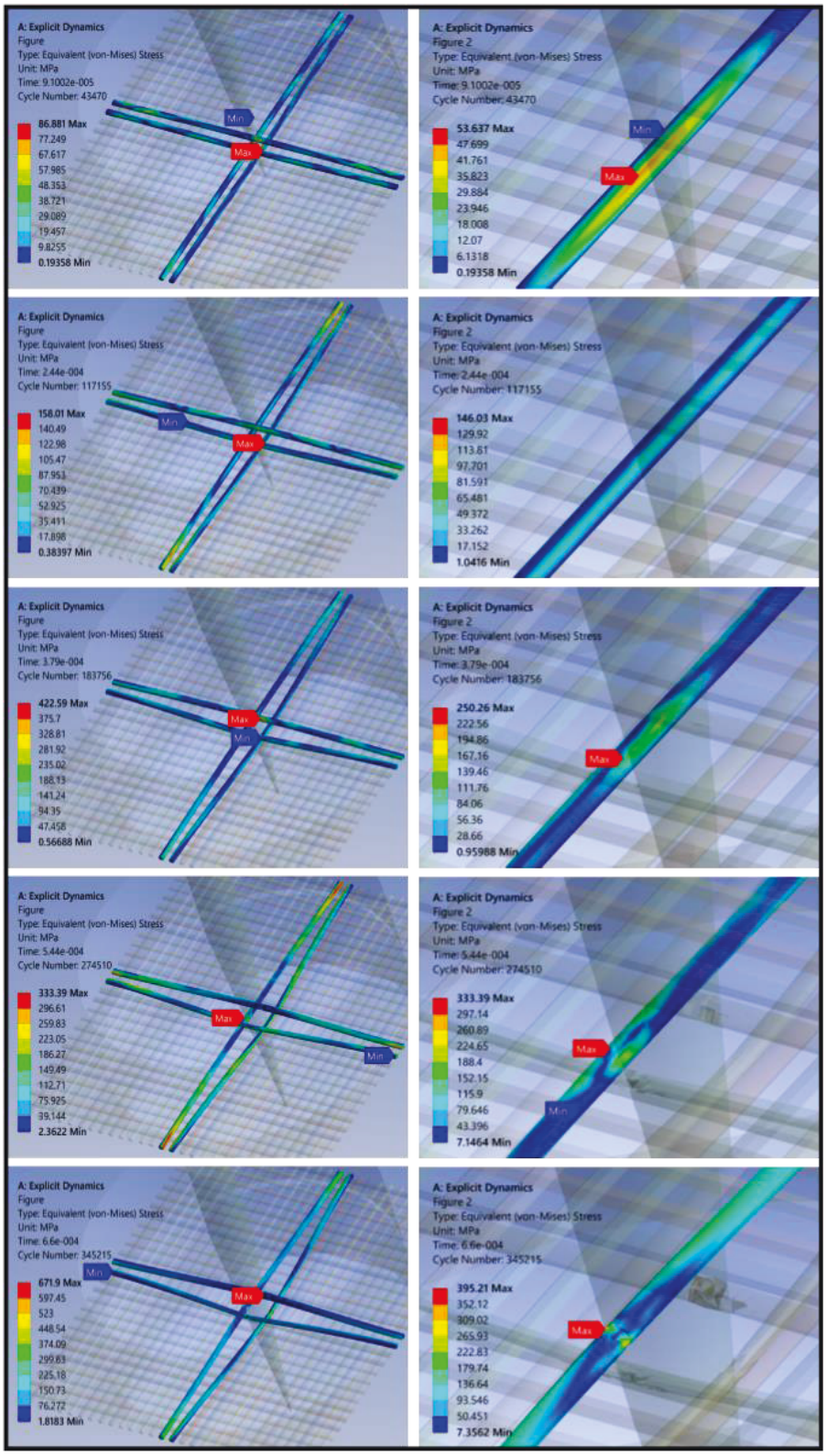

Figure 3-15. Damage morphologies obtained from the finite element method (FEM) results (stress diagram of yarn parts).

As the penetration depth of the needle increased, the stress value of the inner yarn gradually increased. At that time, the yarn began to bend slightly and the maximum value occurred following contact with the needle. The puncture depth increased further and the stress value also increased further. At that time, the maximum stress point is located at the intersection of the two yarns, and the bending degree of the yarns increased further. When the needle is completely inserted, the degree of yarn bending reached a maxi-mum. At that time, the maximum stress point is located at the contact point with the needle and the material at the contact point had a certain degree of damage.

The analysis described above suggests that when subjected to puncture, the yarn at the contact point with the needle and the adjacent yarn intersection are the parts with the largest stress values, and the diffusion stress values along both sides of the yarn axis gradually decreased. The surrounding parts are largely unaffected by the puncture. Yarn deformation and resin peeling are the main modes of damage. When the resin at the intersection peeled off, yarn bending deformation became easier, the needle penetrated completely, and the material is ultimately destroyed.

3.4 Conclusion

In this chapter, details that are easily overlooked in a simulation experiment are explored. In simulation experiments, the anisotropy of the yarn is often neglected owing to various factors. There is a marked difference between the axial and radial properties of a yarn. This may lead to serious research errors. A grid structure composite mate-rial is designed to study the influence of yarn anisotropy on the accuracy of puncture simulation. The results revealed that a simulation that took yarn anisotropy into account is closer to the actual experimental results than a simulation that did not. Numerical simulation can

reveal the stress change inside a material during puncture, and the specific puncture mechanism can be displayed visually. The experimental results demonstrated that the main failure modes of the mesh material are resin fracture at the junction, bending deformation of the yarn, and slippage between the fiber and the resin.

Based on this experimental model, the influence of yarn contact on the simulation results will be investigated and the factors affecting the puncture performance of materials will be investigated further.

References

[1] Hou, X.; Acar, M.; Silberschmidt, V.V. 2D finite element analysis of thermally bonded nonwoven materials: Continuous and discontinuous models. Comput. Mater. Sci. 2009, 46, 700–707. https://doi.org/10.1016/j.commatsci.2009.07.007.

[2] Ridruejo, A.; González, C.; LLorcaab, J. Damage micromechanisms and notch sensitivity of glass-fiber non-woven felts: An experimental and numerical study. J. Mech. Phys. Solids 2010, 58, 1628–1645. https://doi.org/10.1016/j.jmps.2010.07.005.

[3] Zeng, J.; Cao, H.; Hu, H. Finite element simulation of an auxetic plied yarn structure. Text. Res. J. 2018, 89, 3394–3400. https://doi.org/10.1177/0040517518813659.

[4] Zhou, H.; Xiao, X.; Qian, K.; Ma, Q. Numerical simulation and experimental study of the bursting performance of triaxial wo-ven fabric and its reinforced rubber composites. Text. Res. J. 2019, 90, 561–571. https://doi.org/10.1177/0040517519871943.

[5] Sun, B.; Wang, Y.; Wang, P.; Hu, H.; Gu, B. Investigations of puncture behaviors of woven fabrics from finite element analyses and experimental tests. Text. Res. J. 2011, 81, 992–1007. https://doi.org/10.1177/0040517510395999.

[6] Zhu, D.; Szewciw, L.; Vernerey, F.; Barthelat, F. Puncture resistance of the scaled skin

from striped bass: Collective mecha-nisms and inspiration for new flexible armor designs.

[7] Lian, J.; Bohong, G.U. Numerical simulation of dynamic performance of three-dimensional braided composites. J. Text. Res. 2011. 32(1), 41-45.

[8] Termonia, Y. Puncture resistance of fibrous structures. Int. J. Impact Eng. 2006, 32, 1512–1520. https://doi.org/10.1016/j.ijimpeng.2004.11.002.

[9] CZARNECKI, S. Isotropic material design. Computational Methods in Science and Technology, 2015, 21.2: 49-64.

[10] TWETEN, Dennis J., et al. Estimation of material parameters from slow and fast shear waves in an incompressible, transversely isotropic material. Journal of biomechanics, 2015, 48.15: 4002-4009.

[11] VINSON, Jack R. The behavior of sandwich structures of isotropic and composite materials. Routledge, 2018.

[12] VINSON, Jack R. The behavior of shells composed of isotropic and composite materials. Springer Science & Business Media, 2013.

[13] AZZI, V. D.; TSAI, Stephen W. Anisotropic strength of composites. Experimental mechanics, 1965, 5.9: 283-288.

[14] TSAI, Stephen W.; WU, Edward M. A general theory of strength for anisotropic materials. Journal of composite materials, 1971, 5.1: 58-80.

[15] WILLIS, John R. Bounds and self-consistent estimates for the overall properties of anisotropic composites. Journal of the Mechanics and Physics of Solids, 1977, 25.3: 185-202.

[16] GU, Yan, et al. The generalized finite difference method for long-time transient heat conduction in 3D anisotropic composite materials. Applied Mathematical Modelling, 2019, 71: 316-330.

[17] LIU, Zengqian; ZHANG, Zhefeng; RITCHIE, Robert O. Structural orientation and anisotropy in biological materials: functional designs and mechanics. Advanced Functional Materials, 2020, 30.10: 1908121.

[18] FANTUZZI, Nicholas; TROVALUSCI, Patrizia; DHARASURA, Snehith. Mechanical behavior of anisotropic composite materials as micropolar continua. Frontiers in Materials, 2019, 6: 59.

[19] Medeiros, R. J. D., Nóbrega, S. H. S. D., & Aquino, E. M. F. D. Failure theories on carbon/kevlar hybrid fabric based composite laminate: notch and anisotropy effects. Materials Research, 22. 2019.

[20] ALHAZMI, Nahla. Free Vibration Analysis of Anisotropic Composite Materials of a Fixed-Wing. In: Materials Science Forum. Trans Tech Publications Ltd, 2022. p. 57-62.

[21] Ju, W.; Dai, W.W. Application of ANSYS Workbench in structural transient dynamic analysis. Inner Mong. Coal Econ. 2014, 8, 110–113.

[22] Stolarski, T.; Nakasone, Y.; Yoshimoto, S. Engineering Analysis with ANSYS Software; Butterworth-Heinemann: Oxford, UK, 2018.

[23] Zhu, L.; Liu, W.; Fang, H.; Qian, Z.; ZHUANG, Y. et al. Experiment and finite element analysis of lattice reinforced composite sandwich panels subjected to low-velocity impact. J. Nanjing Univ. Technol. Nat. Sci. Ed. 2017, 39, 126–132.

[24] Carrillo, J.G.; Castellanos, R.G.; Flores-Johnson, E.A.; Gonzalez-Chi, P.I. Ballistic performance of thermoplastic composite laminates made from aramid woven fabric and polypropylene matrix. Polym. Test. 2012, 31, 512–519.

[25] Kawabata, S. Measurement of the transverse mechanical properties of high-performance fibres. J. Text. Inst. 1990, 81, 432–447.

[26] Ruan, F.; Bao, L. Mechanical enhancement of UHMWPE fibers by coating with

carbon nanoparticles. Fibers Polym. 2014, 15, 723–728.

[27] Gzaiel, M.; Triki, E.; Barkaoui, A. Finite element modeling of the puncture-cutting response of soft material by a pointed blade. Mech. Mater. 2019, 136, 103082.

Chapter 4

Simulation Experiments Considering the Contact Between Yarns

Chapter 4: Simulation Experiments Considering the Contact Between Yarns

4.1 Introduction

In the chapter 3, we conduct puncture simulation experiments. In the simulation experiments, we fully consider the anisotropy of the yarn. The axial performance parameters and radial performance parameters of the yarn are measured by the tensile test and the compression test of the yarn respectively. The stab-resistant simulation found that after considering the yarn anisotropy, the simulation results are closer to the actual experimental results. However, the simulation results without considering the yarn anisotropy are far from the actual experimental results. This can confirm that the idea of this experiment is correct.

On this basis, we will carry out the study of the second condition. This chapter mainly focuses on the simulation experiments after considering the contact between the yarns.

Let us first summarize the research progress of predecessors on stab-resistant materials. Li et al. [1] prepared a recyclable and puncture-resistant soft composite material by combining fibers with a gel matrix. Sheng et al. [2] found that the stab-proof performance of a composite material is significantly improved when they manufactured it from Aramid fabric and a shear-thickening fluid (STF). LU et al. [3] also found that the addition of an STF enhanced the friction between yarns and thus improved the puncture performance of a composite material. Wang et al. [4] used an STF modified with nanocellulose and Aramid fabric to prepare composite materials with improved stab-proof performance. Das et al. [5] prepared mixed stab-proof materials, which had excellent

performance but high production costs, by combining hard parts with soft parts. Yuhazri et al. [6] combined softness and stab-proof performance by adding two different reinforcers to the matrix. Starting with two different fibers, Tian et al. [7] prepared a composite material with improved stab-proof performance. The results showed that the performance of the coated yarn is better than that of a single yarn. DU et al. [8] combined Aramid and stainless-steel fibers in a coated yarn to investigate the influence of twist and layer number on puncture performance. Xing et al. [9] investigated the mechanism underlying the stab-proof performance of a fabric from the perspective of mechanics. The theory of tool impact force and kinetic energy conversion can be verified by experiments. Varte et al. [10] improved the fit of protective materials from the perspective of the human body to combine comfort and stab-proof performance. To save production costs, Khuyen et al. [11] prepared laminate materials using ordinary fabrics and adhesives. They found that the adhesives had a considerable influence on the anti-stab performances of the materials. Porwal et al. [12] analyzed the impact performance of multi-layer flexible materials. They comprehensively investigated the effects of layer spacing, isotropy, and elastic mechanical properties on impact properties.

As can be seen, research has mainly focused on the design and material modification of stab-proof structures, and there have been few investigations of the specific influencing factors and underlying mechanism of stab-proof structures. Among them, the contact part between the yarns is very important for the mechanism analysis and the research on the influencing factors.

4.1.1 Type of Contact

The mathematical description of the contact includes the choice of the method of

applying the interface constraints, the definition of the master and slave surfaces of the contact surface, and the description of the sliding. With the development of computers, it has become possible for us to simulate the contact problem. [13-14]

At present, the contact between materials is mainly divided into the following six types in the simulation software. [15]

(1) Bonded

This contact type constrains the normal and tangential motion of the contact surface and the target surface and realizes the function of connecting different bodies together.

(2) No Separation

This contact type constrains the normal direction of the contact surface and the target surface. The tangential direction of the contact surface and the target surface can move with degrees of freedom, which is equivalent to the tangential direction of free sliding without friction.

(3) Frictionless

This contact type is not constrained on the normal and tangential directions of the contact surface and the target surface. The tangential direction is free movement, and the movement of the normal direction depends on the external load.

(4) Rough

This contact type constrains the tangential motion between the contact surface and the target surface, and the normal motion of the contact surface and the target surface depends on the external load. Once there is a gap between the contact surface and the target surface, the tangential direction of the contact surface and the target surface is also free.

(5) Frictional

This contact type satisfies Coulomb's friction law in the tangential motion of the contact surface and the target surface, that is, once the calculated friction exceeds the maximum friction force that can be provided between the contact surface and the target surface, the contact surface and the target surface begin to slide, and vice versa , the adhesive contact between the contact surface and the target surface is maintained.

(6) Forced Frictional Sliding.

This option is only available for rigid body dynamics, it is similar to the friction type, but without the static friction stage.

4.1.2 Contact Between Yarns

From the above description it has been found that the most appropriate contact with the yarns is frictional contact. [16-17]

However, during the actual operation, it is found that the thousands of filaments in the yarn could not be reproduced in the simulation software. At the same time, due to the continuous penetration of the ice pick during the puncturing process, the pressure on the yarn is increasing, and the friction is also increasing. Simple frictional contact does not present a complex puncture process. The idealized simulation experiment will lose the real failure process of many materials, which has a very serious impact on the mechanism research of stab-resistant materials.

Therefore, the new contact program is imminent. In this experiment, as seen in Chapter 2, the yarn and resin form a composite material. Thus, the yarn becomes a whole without the friction of the inner filaments. At the same time, the yarns are also connected by the resin, so here we focus on how to define the contact of the yarn composite connected by the resin.

4.2 Experiments

The simulation experiments in Chapter 3 only consider the anisotropy of the yarns in the model. This chapter builds on that and continues to optimize the contact between yarns in the model. In order to be as accurate as possible, it is first necessary to analyze the contact of the yarns in the actual experiment.

4.2.1 Analysis of Failure Parts

Figure 4-1a shows an enlarged view of the contact points of the material. The figure shows the structure of the material, which comprises a pair of yarn-reinforced epoxy composites (YRECs) connected by resin. The fracture interface morphology of the material after puncture damage is shown in Figure 4-1b、c、d.

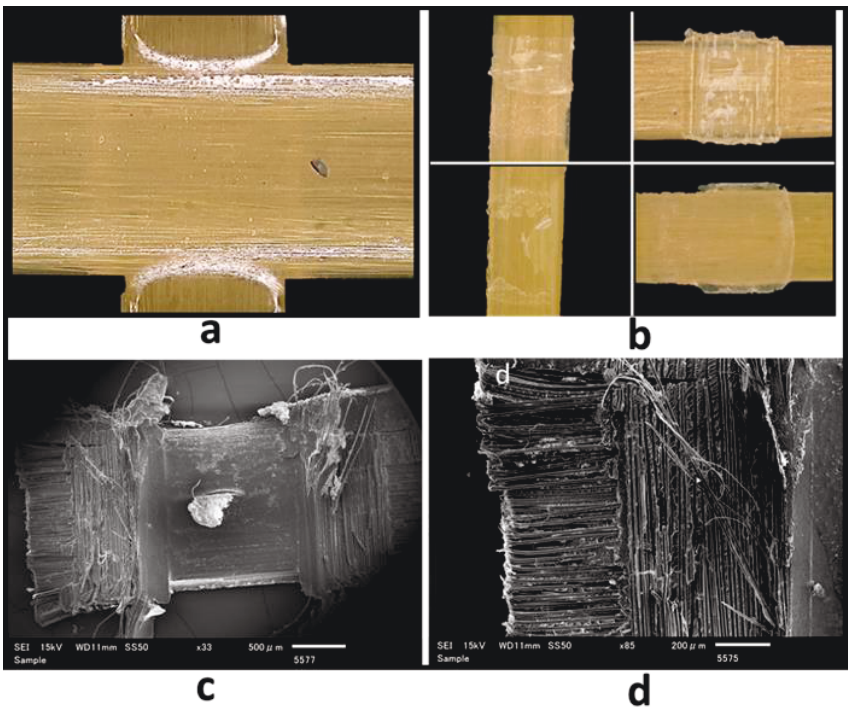

Figure 4-1. (a) Contact point between yarn-reinforced epoxy composites (YRECs), (b) Damage morphology of the materials, (c) Damage morphology of the materials in SEM, (d) Partial magnification in c

In general, since the puncture needle did not directly act on the YREC part, the damage to this part is very small. Figure 4-1 shows that the failure mode of the material is mainly the cracking of the resin at the joint. Analysis has revealed that the resin damage takes two forms, as shown in Figure 4-2. In the first case, the resin breaks evenly along the middle so that approximately equal amounts of resin remain attached to the individual YRECs. In the second case, the resin breaks unevenly along the middle. In both forms, the fragmentation occurs within the resin itself mainly.

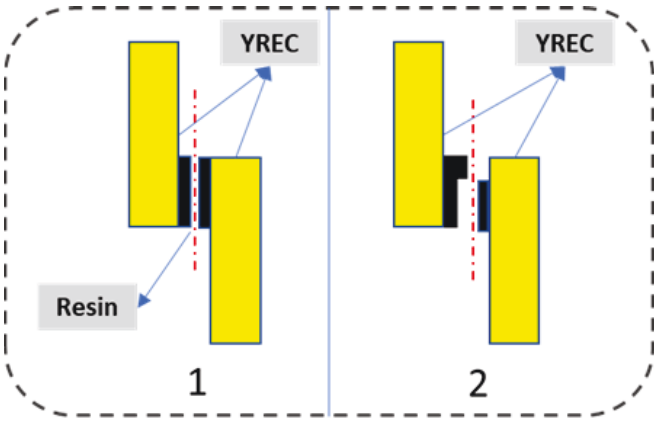

Figure 4-2. Schematic showing the two forms of material destruction

4.2.2 Model Preparation

The 1:1 model is drawn using FEM software according to detailed analysis of the experimental samples described above. As shown in Figure 4-3, the model includes upper and lower splints, composite materials, and puncture needles. Each part is drawn separately and then assembled to form the complete model. The YREC part is regarded as a whole, and its cross section is idealized as the runway type [18].

The model is rigorously optimized to further improve the accuracy of the simulation results. The axial and radial moduli of the YREC are defined in previous experiments. The other major issue is the interface contact. The bonding together of the two YRECs

has a large effect on the accuracy of the simulation results. Therefore, the main optimization of this part focuses on the interface contact between the YRECs. Damage analysis of the puncture experiments described above revealed that, in general, the resin itself is broken during puncture, whereas the portion connecting the resin and the YRECs remained almost intact. Therefore, resin blocks are added, and their upper and lower surfaces are bound to the YRECs [19], as shown in Figure 4-4.

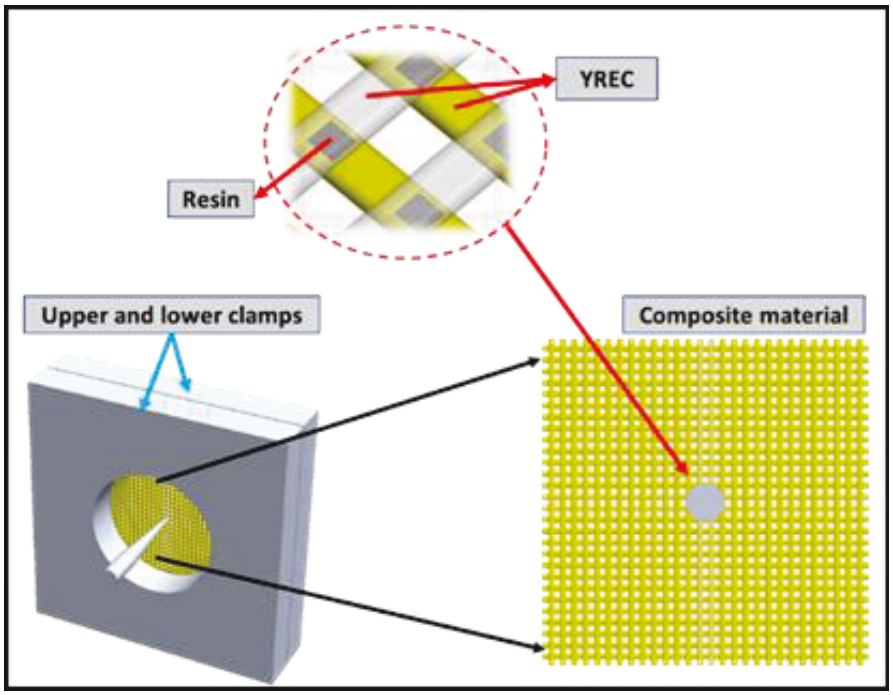

Figure 4-3. Puncture model and contact details

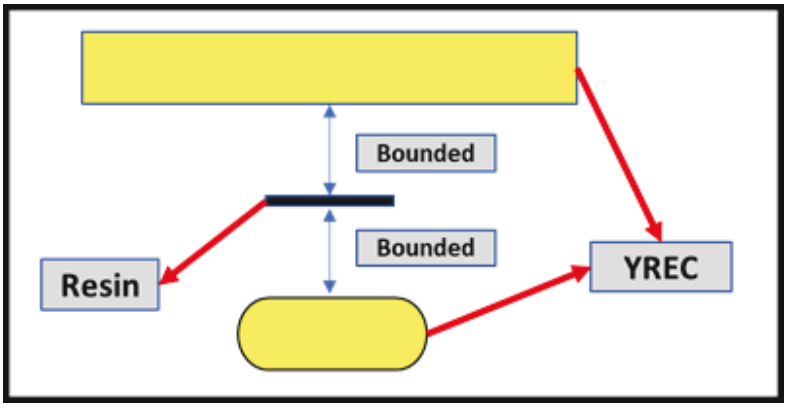

Figure 4-4. Schematic showing the contact between the YRECs and the resin

4.2.3 Puncture Tests

In the simulation software, we use the maximum principal stress failure theory to define the failure of the resin part. Through this optimization, the failure mode of the material in the simulation can be made consistent with that in the actual experiment. This avoids the error caused by ignoring the interface problem. The parameters used in the model are shown in Table 3-1. After dividing the mesh [20-21], the needle is set to a speed of 2 m/s for the puncture experiment.

4.3 Results and Discussion

As can be seen from Chapter 3, Figure 3-11 shows that the process of puncture is divided into 5 steps. In the case of only considering the anisotropy of the yarn, the simulation results are consistent with the actual experimental results. But there are some differences in the details. Particularly at A-B, this is the stage where the contact portion between the innermost yarns is broken. Therefore, this chapter focuses on observing the data changes in segments A-B.

The simulation results without and considering the inter-yarn contact are shown in the Figure 4-5, 4-6. The first is the result of not setting the yarn-to-yarn contact. It can be seen from the figure that the simulation results are close to the actual experimental values. But the gap is still huge. Mainly because only the friction contact is set in the simulation experiment, the specific force situation when it is subjected to puncture is not the same as the actual one. This makes it possible to find that not setting the contact between the yarns correctly can lead to errors in the simulation results, which can lead to problems in analyzing the failure mechanism.

Figure 4-6 shows the stress–time curves of simulation experiment by considering

contact. Within the error range, the simulation results are in good agreement with the actual results. Especially compared to the results without considering the yarn contact, the simulated values tend to be closer to the real experiments. This shows that it is important to set the correct type of contact between the yarns.

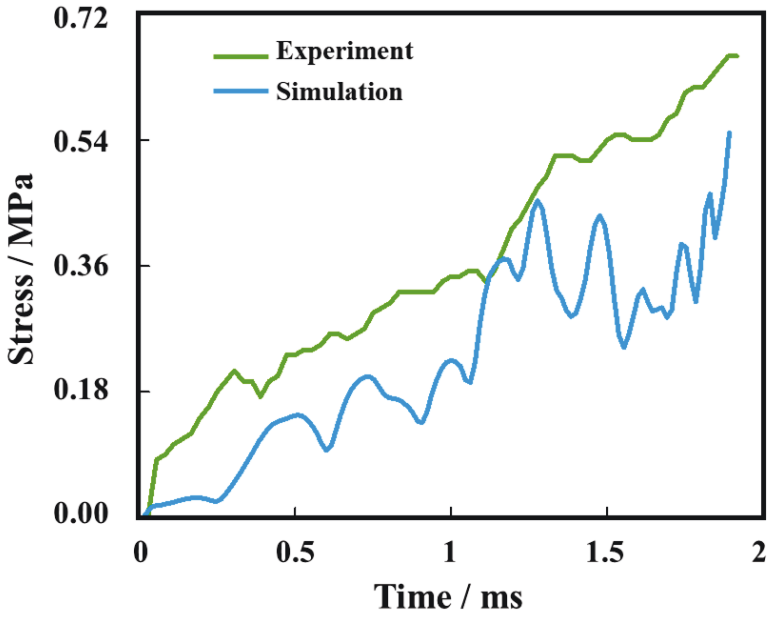

Figure 4-5. Stress-time curves of simulation experiment without contact

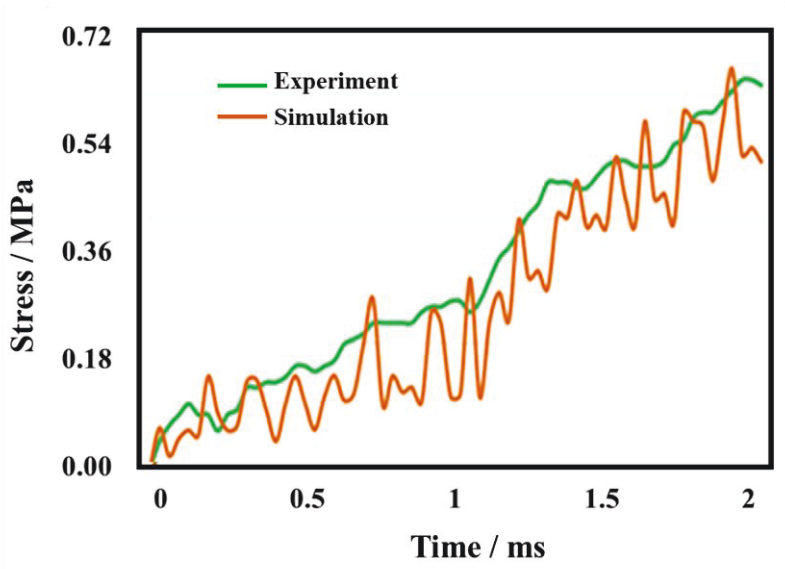

Figure 4-6. Stress-time curves of simulation experiment by considering contact

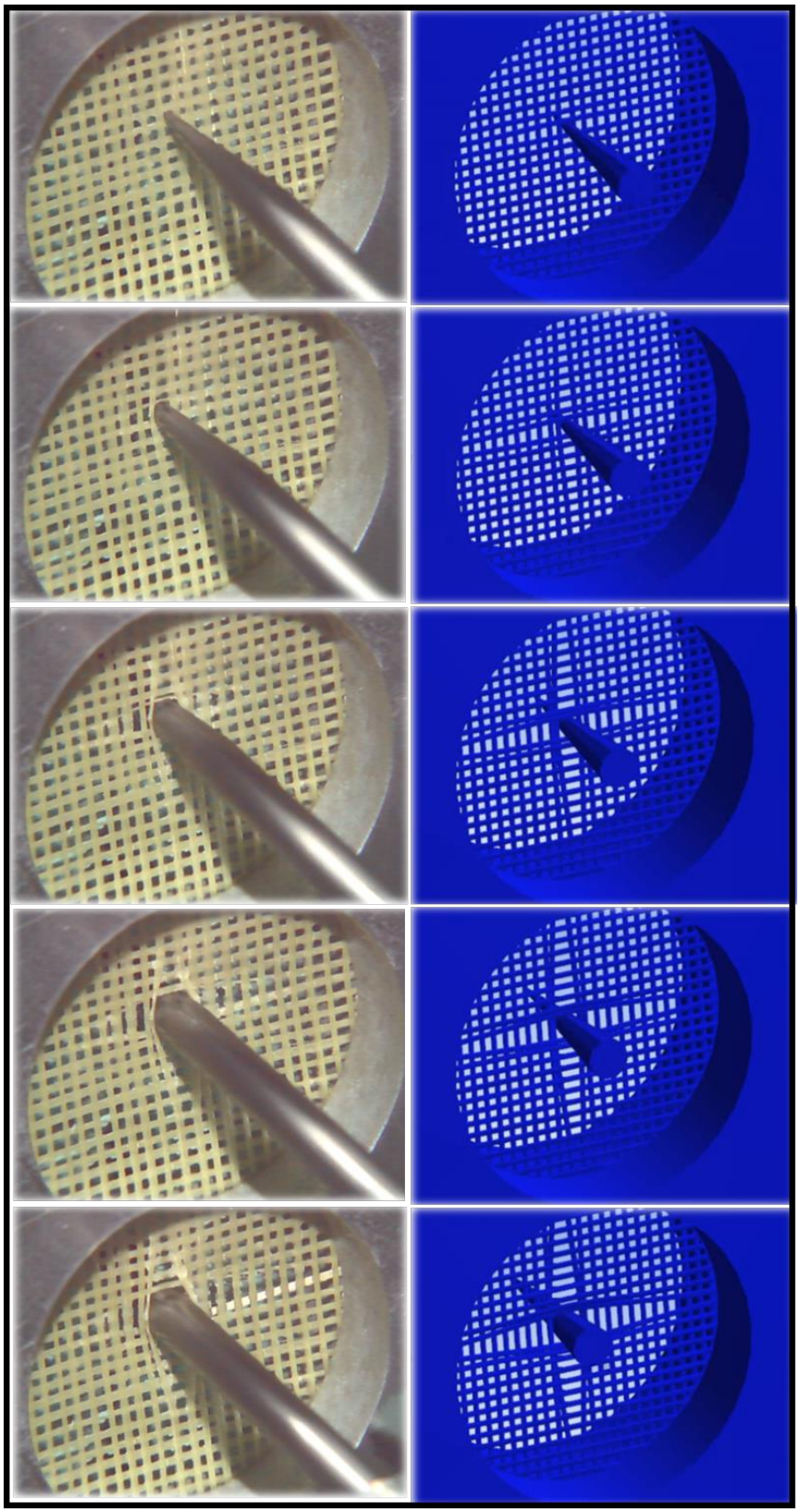

Figure 4-7. Comparison between the actual and simulated puncture processes

At the same time, we find that the stress–time curve of the simulation results fluctuates considerably. This is because in the finite element calculation, the model is divided into tiny element units. Therefore, during damage and failure there are fluctuations in the curve. However, the overall trend is consistent with that of the actual experiment. The puncture process diagram reveals that as the puncture needle advanced, the grid gradually expanded and the YREC gradually deformed. The changes in the simulated puncture process are also consistent with those in the actual experiment. As A. Shahkarami et al. [22] conducted the impact simulation of woven fabrics experiment, the simulation results are in better agreement with the experimental results after considering the warp and weft properties of the yarn. Therefore, the model is valuable for both reference and using.

Figure 4-7 shows the comparison between the simulation results and the actual experimental failure modes. The damage details such as the bending deformation of the yarn and the damage of the contact part between the yarns are perfectly displayed. This lays the foundation for the analysis of the failure mechanism of the subsequent materials and the study of the influencing factors.

4.4 Conclusion

In this chapter, we use a combination of actual experiments and simulations to study the influence of the yarn-to-yarn contact problem on the simulation results. The results show that considering the contact between the yarns has a great influence on the accuracy of the simulation values.

Accurate simulation results are very important for simulation experiments. Only analysis based on the correct model is valid. After the detailed analysis in Sections 3-4, it

is important to consider the anisotropy of the yarn and the contact of the yarn for the simulation results. Through this model, we can correctly analyze the mechanism of stab prevention and the research on the influencing factors.

References

[1] TT Li, Xing M, Gao B,et al. Multiscale synergistic toughened pluronic/PMEA/ hydroxyapatite hydrogel laminated aramid soft composites: Puncture resistance and self-healing properties[J]. Composites Part B Engineering, 2021, 216(78):108856.

[2] Sheng X, Qin J, Wang T, et al. Properties of Kevlar fabric composites reinforced by STF composed of monodisperse polystyrene microspheres[J]. Thin-Walled Structures, 2021, 167: 108238.

[3] Zhenqian LU , Yue XU . Study on stab-resistant performance of shear thickening fluids impregnated ultra-high-molecular-weight polyethylene fabric[J]. Journal of Textile Research, 2018, 39(10): 58-62.

[4] Wang F, An C, Jia Q. Effect of multi-phase STF on the high-speed impact performance of shear-thickening fluid (STF)-impregnated Kevlar Composite Fabrics[C]//Journal of Physics: Conference Series. IOP Publishing, 2021, 1759(1): 012015.

[5] Das P P , Chaudhary V , Singh R K , et al. Advancement in hybrid materials, its applications and future challenges: A review[J]. Materials Today: Proceedings, 2021(1): 3794-3801.

[6] Yuhazri M Y, Nadia N HCMH, Sihombing H, et al. A review on flexible thermoplastic composite laminate for anti-stab applications[J]. Journal of Advanced Manufacturing Technology (JAMT), 2015, 9(1): 28-40.

[7] Tian L , Shi J , Chen H , et al. Cut-resistant performance of Kevlar and UHMWPE

covered yarn fabrics with different structures[J]. Journal of the Textile Institute, 2021(8):1-7.

[8] Lingling D U , Tingting L I , Pan J , et al. Preparation and stab-resistance performance of aramid/stainless-steel fiber core-spun fabrics[J]. Journal of Textile Research, 2017. 38(6): 33-39.

[9] Xing J, Qian X. Stab-resistant mechanism of fabrics and influence of cutter shape on stab resistance[J]. Journal of Textile Research, 2017 , 38(08): 55-61.

[10] Varte L R, Kakkar D, Rawat S, et al. Data Mining Anthropometric Parameters for the design and Sizing of Female Full Body Protector[J]. Defence Life Science Journal 2021,6(4) : 275-283.

[11] Khuyen N Q, Han P V D, Nguyen N T, et al. The Use of Laminates of Commercially Available Fabrics for Anti-Stab Body-Armor[J]. Polymers, 2021, 13(7): 1077.

[12] Porwal P K, Phoenix S L. Modeling system effects in ballistic impact into multi-layered fibrous materials for soft body armor[J]. International journal of fracture, 2005, 135(1): 217-249.

[13] ZHANG, Zhibing, et al. Numerical Simulation Method for Hydroforming of Tube. China Mechanical Engineering, 2008, 19.16: 0.

[14] ZHAOPING, Tang; JIANPING, Sun. The contact analysis for deep groove ball bearing based on ANSYS. Procedia Engineering, 2011, 23: 423-428.

[15] LEE, Huei-Huang. Finite element simulations with ANSYS Workbench 18. SDC publications, 2018.

[16] KHAWAJA, H.; PARVEZ, K. Validation of normal and frictional contact models of spherical bodies by FEM analysis. The International Journal of Multiphysics, 2010, 4.2: 175-185.

[17] BELHOCINE, Ali; ABDULLAH, Oday Ibraheem. Finite element analysis (FEA) of frictional contact phenomenon on vehicle braking system. Mechanics based design of structures and machines, 2022, 50.9: 2961-2996.

[18] JU W, DAI W. Application of ANSYS Workbench in the transient dynamic analysis of structure[J]. Inner Mongolia Coal Economy, 2014. (8):110-113.

[19] Ai P, Feng P, Lin H, et al. Novel self-anchored CFRP cable system: Concept and anchorage behavior[J]. Composite Structures, 2021, 263: 113736.

[20] Lee H H. Finite Element Simulations with ANSYS Workbench 2021: Theory, Applications, Case Studies[M]. SDC publications, 2021.

[21] CAI, C., et al. Modeling of material damping properties in ANSYS. In: CADFEM users' meeting & ANSYS conference. 2002. p. 9-11.

[22] SHAHKARAMI, Ali; VAZIRI, Reza. A continuum shell finite element model for impact simulation of woven fabrics. International Journal of Impact Engineering, 2007, 34.1: 104-119.

Chapter 5:

Discussion on Influencing Factors of Puncture Performance

Chapter 5: Discussion on Influencing Factors of Puncture Performance

5.1 Introduction

In previous chapters, we delved into the accuracy of simulation experiments. The content of the discussion mainly includes two parts, the first is to study the influence of yarn anisotropy on the simulation results. The second is to study the influence of the contact between the yarns on the simulation results. It is found that the accuracy of the simulation results is greatly improved after setting the yarn anisotropy and the yarn-to-yarn contact. This proves that the idea of this experiment is very important. By using this accurate model, this chapter will analyze the mechanism of stab resistance and the factors affecting the stab resistance performance.

A puncture experiment is a transient process, and it is difficult to comprehensively analyze the destruction of materials. Finite element software provides a satisfactory solution to this problem. Shetty et al. [1] verified the effectiveness of the finite element method (FEM) by using it to study delamination failure during the drilling of a composite material. Gzaiel et al. [2] accurately predicted the puncture resistance of materials using the FEM and an energy-based method. Jirawattanasomkul et al. [3] used a 2D FEM to conduct simulation analysis on the tensile properties and stab resistance of a composite mat by optimizing its stiffness parameters. Brooker [4] used ABAQUS software to conduct a parameterized study of pipeline puncture performance, and the predicted simulation results are consistent with those from the actual experiment. Raimondo et al. [5] applied a 3D material damage model to study the low-speed impact response of unidirectional laminates. This method not only improves the accuracy of the simulation results, but greatly reduces the cost of calculation. Liao and Liu [6] investigated the

dynamic mechanical responses and damage mechanisms of materials subjected to low-speed impact using the finite element model. Gama and Gillespie [7] used the FEM to study the damage process of materials at various impact speeds. The simulation results can be optimized so that they closely resemble the actual results by adjusting the material parameters. Chen et al. [8] used the adaptive finite element material point (AFEMP) method to better simulate the impact experiment, which is suitable for dealing with the problem of extreme deformation. Catalanotti et al. [9] proposed a new three-dimensional failure theory based on the FEM. The theory takes into account the influence of the thickness direction on material emphasis. Naik et al. [10] studied the impact of woven fabrics, refined the impact process, and proposed an analysis formula in combination with the FEM. The predicted results correlate well with the experimental results. Wicklein et al. [11] predicted and verified the dynamic behavior of carbon fiber-reinforced plastic (CFRP) under impact by deducing the experimental orthogonal anisotropy model data set using the FEM. Ji et al. [12] studied the damage of 3D orthogonal braided composites under transverse impact, and established a single cell model with the help of the FEM to investigate the damage mechanism. Minak and Ghelli [13] conducted low-speed impact experiments on CFRP laminates. The influence of sample size and boundary condition on damage is studied using the FEM. Within the error range, the main failure characteristics can be predicted correctly by numerical analysis. Rao et al. [14] studied the impact resistance of Aramid fabric using the FEM; they investigated the influence of material properties and friction force on the performance. Xiao et al. [15] studied the punching and shearing properties of glass fiber composite laminates. The FEM can be used to simulate and analyze the damage mechanism of materials with different layers; the simulated results are in good agreement with the actual experimental results.

As can be seen, our predecessors have mainly focused on material modification and structural design when studying stab-proof materials and have adjusted and optimized continuously. However, there has been little research on the puncture mechanism. Furthermore, most models and their parameters are idealized in finite element analysis, and consequently the results do not have strong reference value. In the actual experiments, the type of yarn and its parameters are fixed. Therefore, it is difficult to test the anti-puncture performance by adjusting the parameters of the yarn, and the factors that affect that performance are also difficult to investigate.

To achieve this goal, in the present study we used Aramid yarns and the epoxy resin to prepare a composite grid material and combined actual experiments with simulation analysis. In the simulation experiment, the parameter settings of the model are refined, and the interface between the resin and the yarn is defined [16-18] to ensure that the simulation results are consistent with the experimental results. In this work, we focused on mechanical properties of composites at initial damage. Using the optimized model, the variation rule of the anti-stab performance of the material is studied by adjusting its parameters. The variation parameters comprised the ratio of the axial and radial elastic modulus of the yarn (E_L/E_T), the ratio of the tensile strength of the yarn to the shear strength of the resin ($\sigma F/\sigma R$), and the diameter of the yarn (R_F).

5.2 Setting of Influencing Factors

5.2.1 E_L/E_T

First, we discussed the influence on the puncture performance of the ratio of the elastic modulus of the YREC in the axial direction to that in the radial direction (E_L/E_T). With the help of the model described above, we kept the other parameters the same and

altered the E_L/E_T ratio, as shown in Table 5-1. We changed the ratio by keeping E_L constant and adjusting the magnitude of E_T; the ratio ranged from 1:1 to 200:1.

Table 5-1. E_L/E_T parameter setting

E_L / E_T	1:1	5:1	10:1	15:1	20:1	25:1	50:1	100:1	200:1
E_L/GPa	78.62	78.62	78.62	78.62	78.62	78.62	78.62	78.62	78.62
E_T/GPa	78.62	15.72	7.86	5.24	3.93	3.14	1.57	0.79	0.39

5.2.2 E_{LC}

After analyzing the E_L/E_T ratio, we found that the axial parameters also have a considerable impact on anti-stab performance. Therefore, the influence of the change in the axial elastic modulus of the YREC (E_{LC}) on puncture performance would be discussed separately.

We kept the other parameters constant and changed E_{LC}, as shown in Table 5-2 .

Table 5-2. E_{LC}/E_L parameter setting

E_{LC} / E_L	10:1	5:1	1:1	1:5	1:10
E_{LC}/GPa	786.20	393.10	78.62	15.72	7.86
E_L /GPa	78.62	78.62	78.62	78.62	78.62

5.2.3 σ_F / σ_R

The analysis described above shows that the failure of the material is mainly due to the fragmentation of the resin. Therefore, the strength of the resin is also very important. The main form of failure of the resin is shear failure. Therefore, we discussed the impact of the resin shear strength (σ_R) and the tensile strength of the yarn in the YREC (σ_F) on puncture performance. We kept the other parameters constant and changed the σ_F / σ_R, as

shown in Table 5-3 .

Table 5-3. σ_F/σ_R parameter setting

σ_F / σ_R	200:1	100:1	50:1	1:1
σ_F / GPa	2.56	2.56	2.56	2.56
σ_R / GPa	0.013	0.026	0.051	2.56

5.2.4 R_F

Finally, we discussed the influence of the yarn diameter on puncture performance. If the diameter of the yarn is simply increased without changing the warp and weft density of the material, the results will not be convincing because the stab resistance will obviously increase. Therefore, we kept the total content of the yarn in the material constant, and reduced the warp and weft densities of the yarn while increasing the yarn diameter. We kept the other parameters constant, and changed the yarn diameter, as shown in Figure 5-1. (S_F is the spacing distance between two YRECs.)

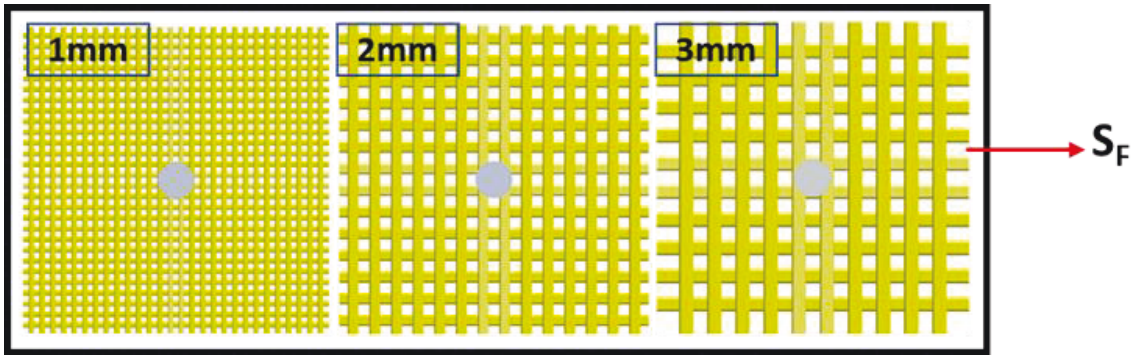

Figure 5-1. Composite material model with various yarn diameters

5.3 Analysis of Influencing Factors

5.3.1 Puncture Mechanism Analysis

The analysis described above reveals that, when subjected to puncture, the mesh is stretched and the YREC is deformed. However, it is impossible to see how the material is destroyed. With the aid of simulation experiments, the YREC components inside the composite material are extracted for meso-analysis. We investigated the destruction mechanism of the materials during the puncture process.

As shown in Figure 5-2 A, when the material is punctured, the portion that first contacts the needle is squeezed. At this time, the stress at the contact point is greatest under the action of the squeezing force. As the needle continues to move forward, the squeezing force at the contact area increases, and the YREC gradually begins to deform and bend. At this time, owing to the bending of the YREC, the outside is stretched and the inside is compressed, and the stress at the stretching point reaches a maximum, as shown in Figure 5-2 B. In Figure 5-2 C, the needle continues to move forward. At this time, two stress concentration areas appear in the YREC. That is, the force reaches a maximum here. As shown in Figure 5-2 D, when the YREC is deformed to a certain extent, the resin at the joint is stressed more and more until it breaks. At this time, the resin stress at the intersection reaches a maximum. When the resin at the YREC contact is damaged, as the needle continues to move forward, the YREC repeats the processes shown in Figure 5-2 B and C, as shown in Figure 5-2 E and F.

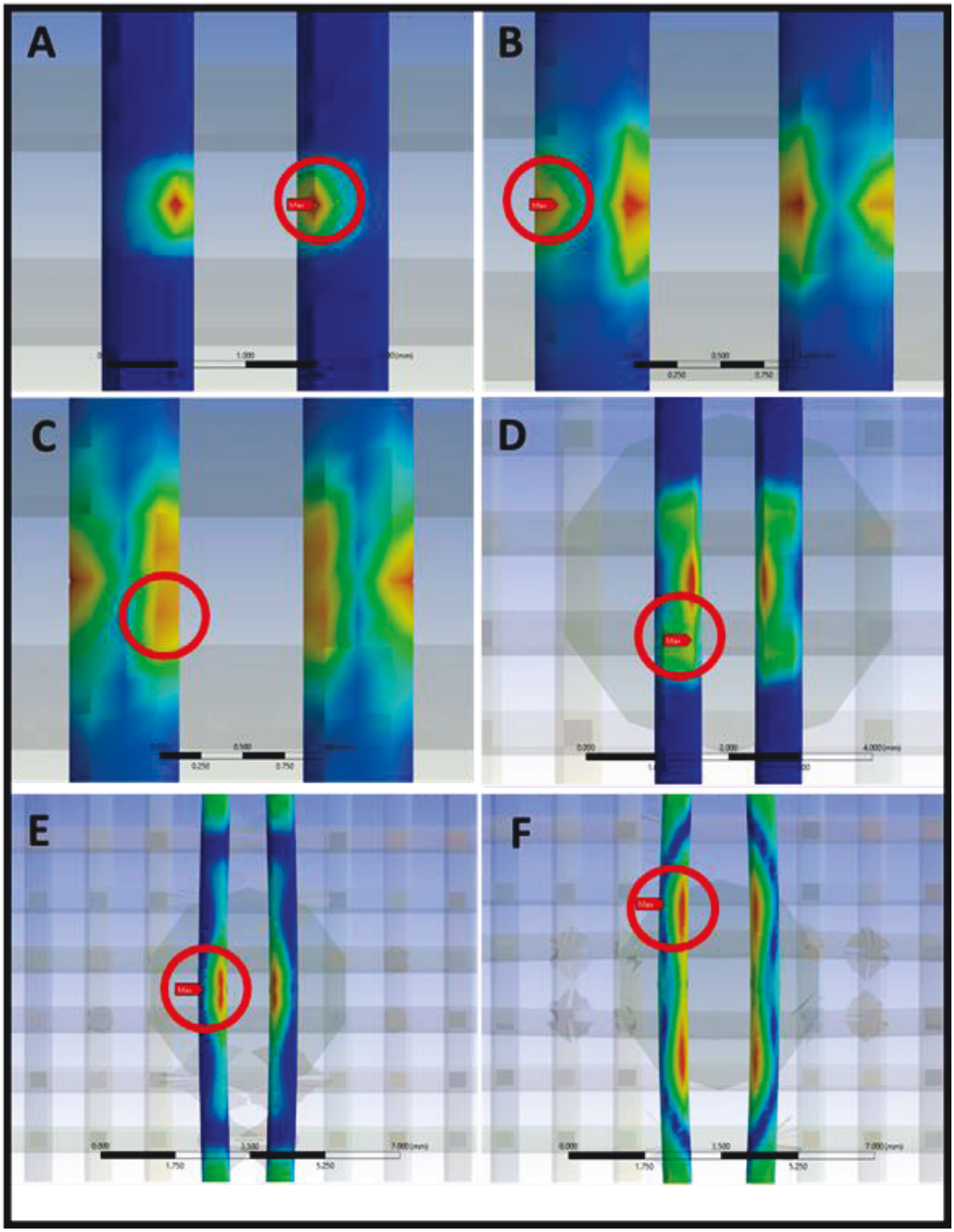

Figure 5-2. Stress diagram of yarn-reinforced epoxy composite (YREC) in the simulation experiment

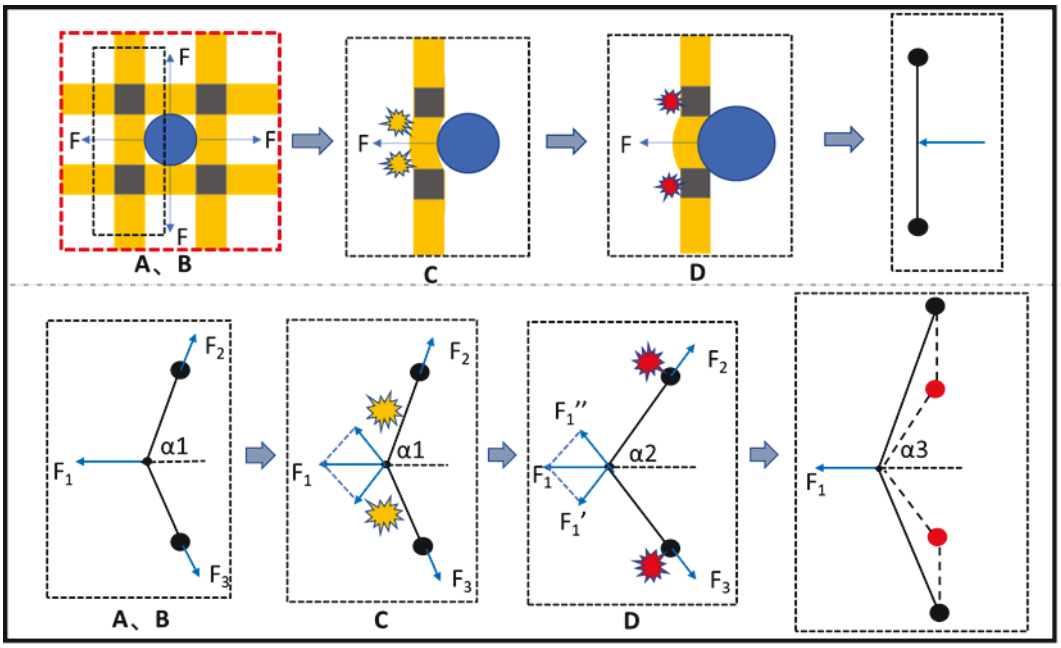

Figure 5-3. Simplified diagram showing the stress experienced by the yarn-reinforced epoxy composite (YREC)

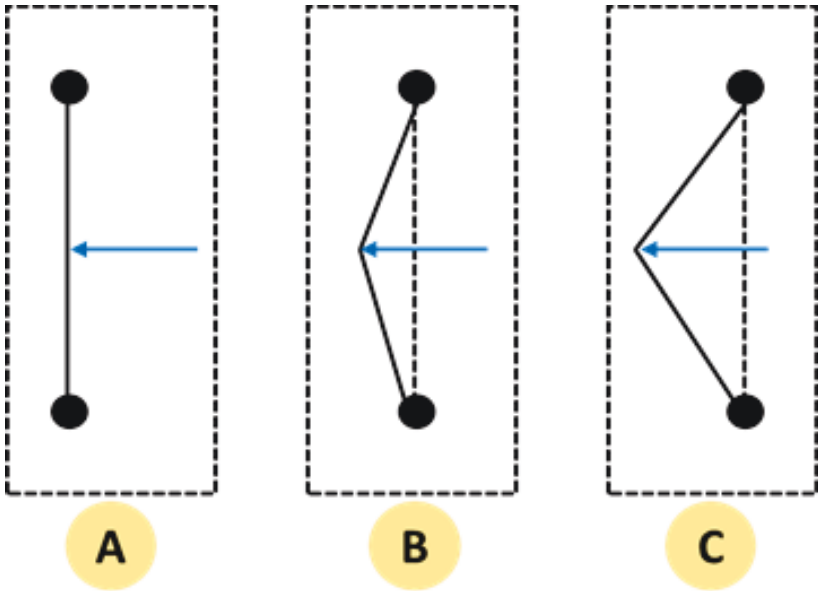

Figure 5-4. Simplified diagram showing the material failure

When analyzing the force of the material, a method similar to M.J.King [19] is used. In response to the observations reported above, we created a simplified model diagram for mechanical analysis (Figure 5-3). We extracted one of the YRECs and further simplified it to a line segment model. The resin at the YREC contact is simplified to black dots at both ends of the line segment.

After puncture, the YREC is subjected to force from three directions. The first is the extrusion force F1, which is followed by tensile forces F2 and F3 generated by the resin at both ends of the YREC. Therefore, Figure 5-3 A and B showed that the stress at the contact is relatively large. The stress values of YREC during stretching and extrusion are shown. As the puncture needle advanced, the value of F1 increased. Simultaneously, the values of F2 and F3 also increased before reaching step 2. In the example shown, the YREC is divided into upper and lower parts along F1. As shown in Figure 5-3 C, F1 can be decomposed into two directions of force: F1′ and F1″. The upper part of the YREC is subjected to forces F1′ and F2, so the stress in the middle part increased. In the same way, the lower part of the YREC is subjected to F1″ and F3. This explains why two areas with larger stress values appear in Figure 5-3 C. When the resin at the contact is broken, the bending angle of the YREC decreased and the length of deformation increased. The resin in the second area then started to work, so the process described above is repeated.

The analysis described above indicates that the steps in the destruction of the material are contact extrusion, YREC bending, and resin destruction, as shown in Figure 5-4. The main factor in puncture prevention is the absorption of puncture energy. Based on the steps described above, the puncture energy absorption of the material mainly comprises two components: the energy absorbed when the YREC is deformed, and the energy absorbed when the resin is broken.

5.3.2 E_L/E_T

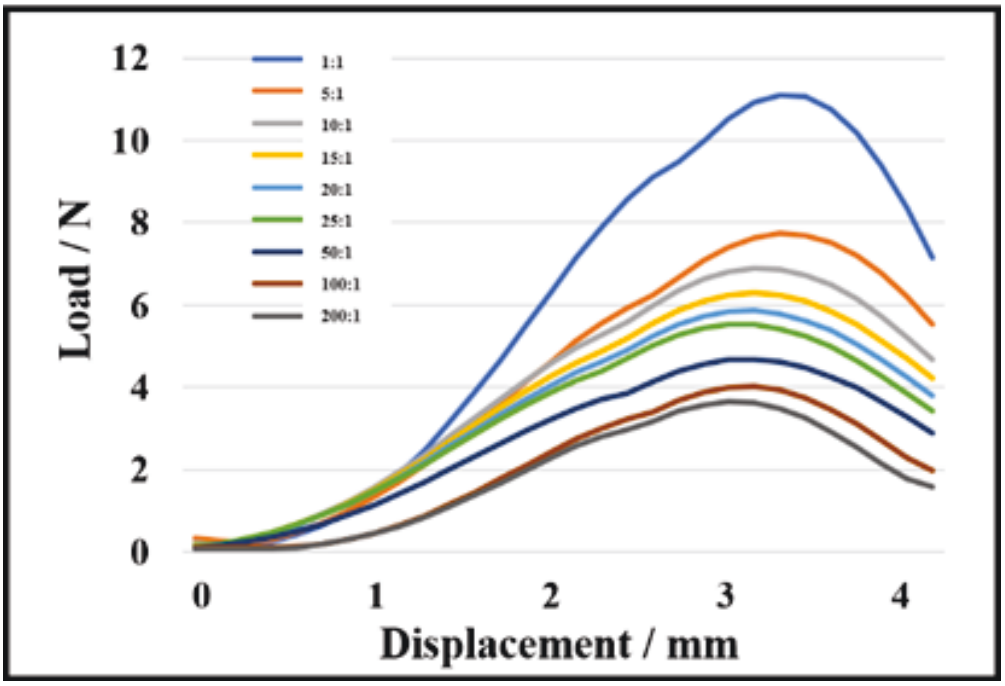

Figure 5-5. Puncture energy at various EL/ET ratios the puncture needle

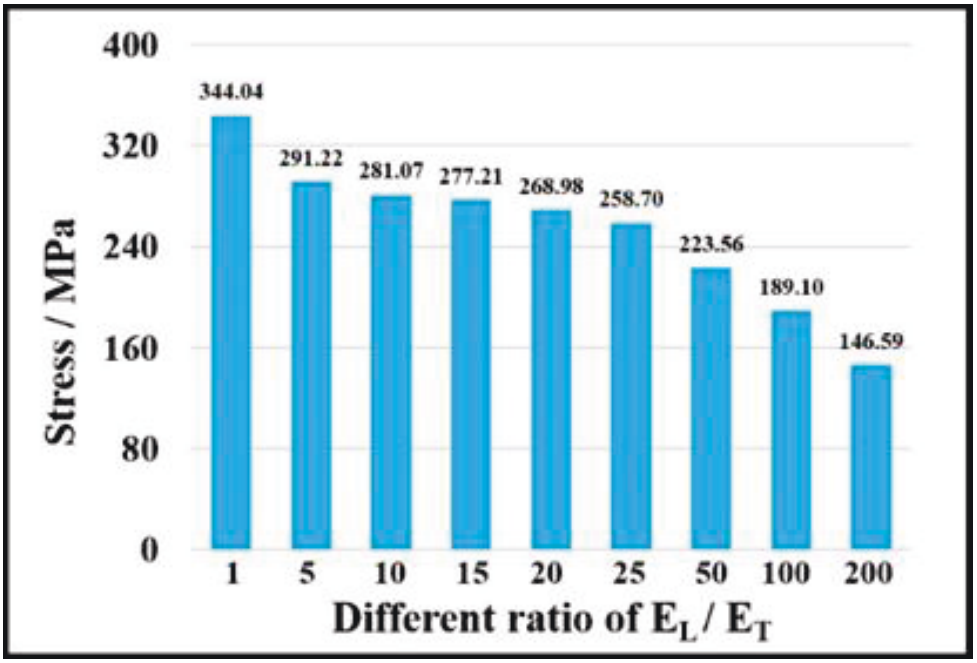

Figure 5-6. Stress values of the YREC as the puncture needle moves 3 mm.

As demonstrated by the puncture energy curve, the smaller the E_L/E_T ratio, the higher the puncture resistance in the Figure 5-5. In this model, the only variable is the E_L/E_T ratio of the YREC. There are no changes in the other parameters of the resin. Therefore, the difference in the energy absorbed by YREC deformation accounts for the difference in puncture energy.

As shown in Figure 5-6, the larger the E_L/E_T ratio, the smaller the maximum stress of the YREC. During puncture, when the displacement of the puncture needle is kept constant, the smaller the radial modulus, the smaller the maximum stress of the YREC. When the structure designed in the present study is punctured, the YREC is first squeezed and bent, and then shear force is applied to the resin at the joint, which eventually ruptures the resin and the material to be penetrated. When the radial modulus of the YREC increases, the deformation of the material under extrusion decreases, which reduces the shear force on the resin at the joint. Compared with a scenario in which the YREC has a relatively small radial modulus, when the YREC has a large radial modulus the piercing needle requires more energy to squeeze the YREC, thereby preventing the needle from penetrating the material. When the radial modulus increases, the material is more easily deformed when squeezed, so the internal stress decreases. M. N. Krivosheina [20] also found that the strength properties of anisotropic materials are lowest in the in-plane direction compared to isotropic materials. In this scenario, the material is more likely to be destroyed. Therefore, the smaller the E_L/E_T ratio, the higher the puncture resistance of the material.

5.3.3 E_{LC}

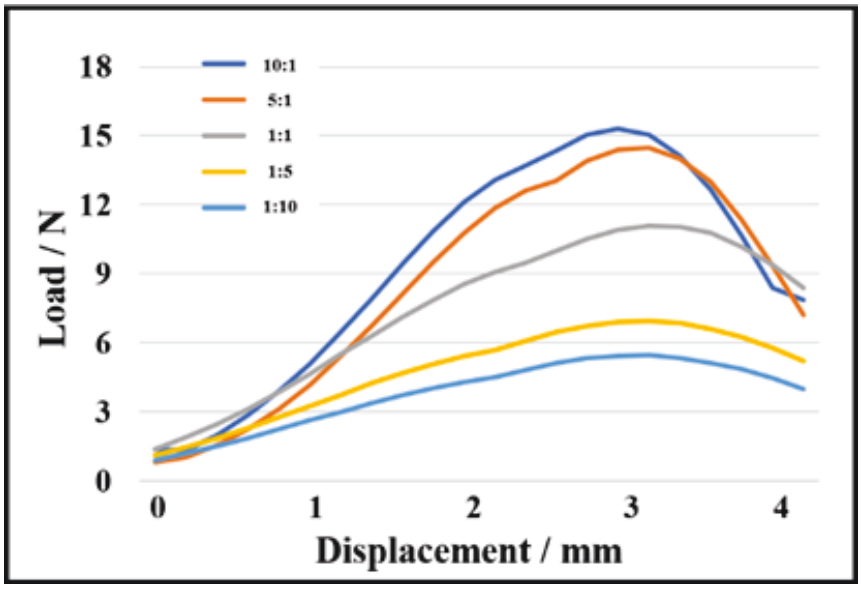

Figure 5-7. Puncture energy at various E_{LC}/E_L ratios

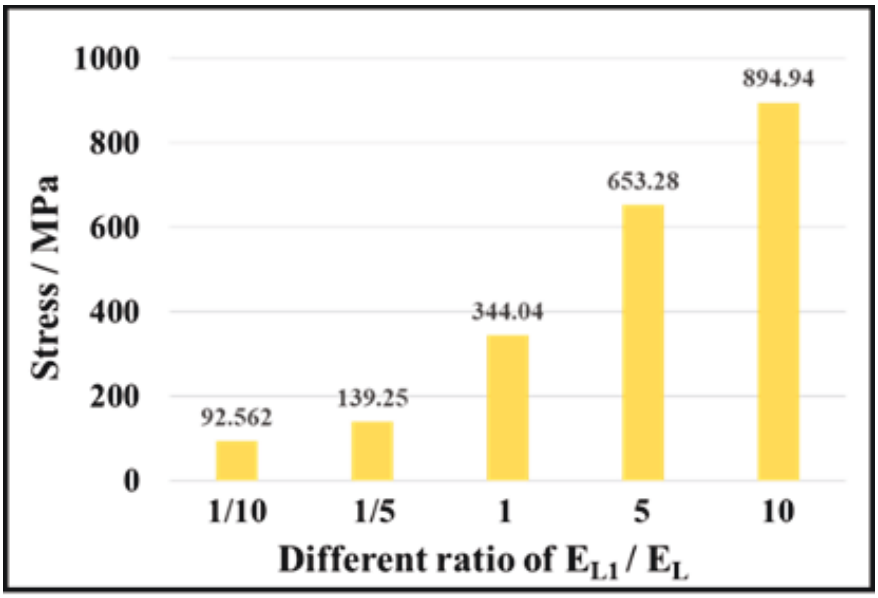

Figure 5-8. Stress value of the YREC as the puncture needle moves 3 mm.

The larger the E_{LC}, the greater the stab resistance of the material. As shown in Figure 5-7, as the E_{LC} increased, the energy required for puncture increased—i.e., the puncture resistance of the material increased. Similarly, because the parameters of the resin are

kept constant, the results for the YREC in the model are extracted for analysis. Figure 5-8 shows that as the E_{LC} increased the stress value of the YREC increased. According to the analysis described above, the larger the E_{LC}/E_L ratio, the less likely the YREC is to deform, and the less likely the resin between the YRECs will be damaged. As the needle penetrates deeper, it takes more energy to squeeze the YREC and force it to bend, damaging the material. In the study of other scholars, such as TT Li [21], when studying the effect of aramid fiber content on the stab resistance of the material, it is found that because of its large modulus, with the increase of the content of aramid yarn, the stab resistance of the material also increased. Therefore, the higher the ratio, the less likely the material is to be damaged.

5.3.4 σ_F / σ_R

The smaller the σ_F/σ_R ratio, the greater the stab resistance of the material in the Figure 5-9. When the σ_F/σ_R is small, the energy required for puncture gradually increased—i.e., the puncture performance of the material gradually increased. Unlike in the scenario described above, this time the parameters of the resin are changed, but the parameters of the YREC are not. Therefore, the values for the resin component are extracted for analysis.

As shown in the Figure 5-10, the smaller the σ_F/σ_R ratio, the greater the stress value. When the YREC strength is constant, the main factor affecting material damage is the energy absorbed during resin damage. As the ratio decreases, the strength of the resin gradually increases, and the puncture needle requires more energy to rupture the resin. Therefore, the stronger the resin, the greater the puncture resistance of the material.

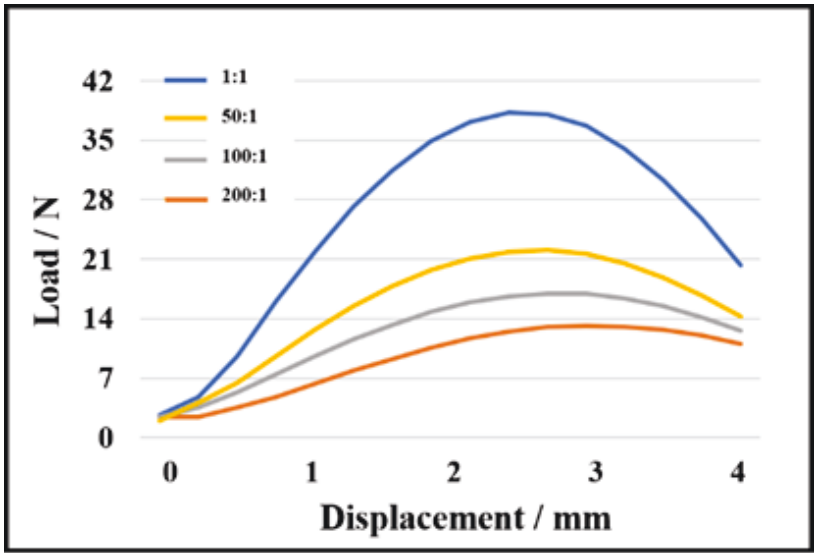

Figure 5-9. Puncture energy at various σ_F/σ_R ratios puncture needle

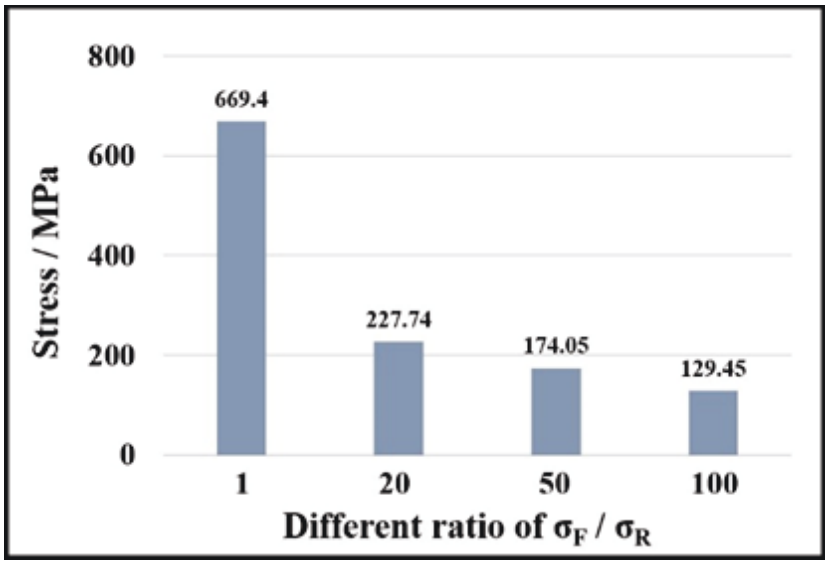

Figure 5-10. Stress value of the resin as the puncture needle moves 3 mm.

5.3.5 R_F

The larger the diameter of YREC, the better the stab resistance of the material in the Figure 5-11. As the diameter of the YREC increases, the force consumed by the puncture is greater, and more energy needs to be consumed when the puncture distance is the same.

Therefore, the material penetration performance is improved. The key observation part here is the YREC part because its parameters are the most important changes. As shown in the Figure 5-12, the stress value of yarn increases with the increase of yarn diameter. As the diameter of yarn increases, its deformation resistance is enhanced, and it is less likely to bend when extruded. As the needle gets deeper, it needs more energy to squeeze the yarn and force it to bend. At the same time, as the diameter increases, the amount of resin used in the contact area also increases, and the energy consumed by resin crushing also increases. Therefore, as RF increases, the puncture performance of the material increases.

Based on the above analysis, we can find that the change of different parameters had more or less influence on the stab resistance of the material. In practical experiments, although the parameters of the material cannot be directly changed, we can increase its stab-proof performance through different combinations of materials. In this simulation experiment, the parameters of the best puncture simulation performance of the material are shown in Table 5-4.

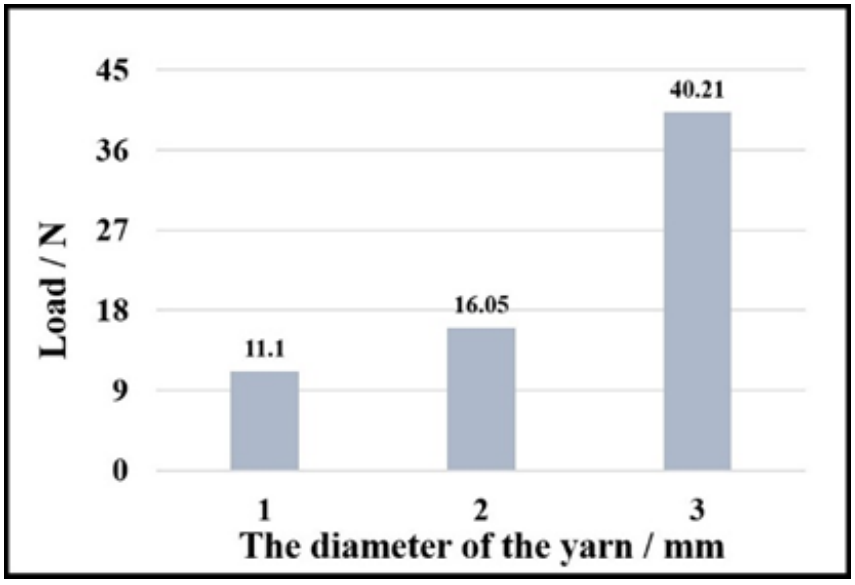

Figure 5-11. Puncture strength with yarns of various diameters

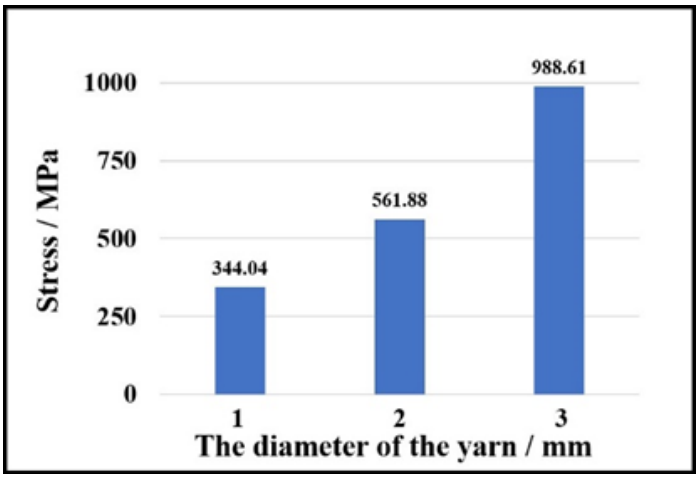

Figure 5-12. Stress value of the yarn as the puncture needle moves 3 mm.

Table 5-4. Optimum parameter setting

	E_L / E_T	E_{LC} / E_L	σ_F / σ_R	R_F / R_1
Ratio	1:1	10:1	1:1	3:1

5.4 Conclusion

In the present study, we used a combination of actual experimentation and simulation to investigate the factors affecting the anti-stab performance of composite materials. We used an optimized finite element model to adjust the parameters for analysis. These parameters comprised the ratio of the axial and radial elastic moduli of the YREC (E_L/E_T), the ratio of the tensile strength of the YREC to the shear strength of the resin (σ_F/σ_R), and the diameter of the YREC (R_F). The experimental results showed that as the E_L/E_T ratio increased, the puncture performance of the material deteriorated; as the E_{LC}/E_L ratio increased, the puncture performance of the material increased; and as the σ_F/σ_R ratio increased, the puncture performance of the material decreased. As the RF increased, the puncture performance of the material increased.

The results of this experiment could provide a reference for the design of similar

products. At the same time, the experimental method could be extended to different fields for analysis and prediction. Based on this experiment, we will continue to conduct in-depth analyses of the anti-stab performance of materials with different structures.

References

[1] Shetty N, Shahabaz S M, Sharma S S, et al. A review on finite element method for machining of composite materials[J]. Composite Structures, 2017, 176: 790-802.

[2] Gzaiel M, Triki E, Barkaoui A. Finite element modeling of the puncture-cutting response of soft material by a pointed blade[J]. Mechanics of Materials, 2019, 136: 103082.

[3] Jirawattanasomkul T, Kongwang N, Jongvivatsakul P, et al. Finite element analysis of tensile and puncture behaviours of geosynthetic cementitious composite mat (GCCM)[J]. Composites Part B: Engineering, 2019, 165: 702-711.

[4] Brooker D C. Numerical modelling of pipeline puncture under excavator loading. Part II: parametric study[J]. International journal of pressure vessels and piping, 2003, 80(10): 727-735.

[5] Raimondo L, Iannucci L, Robinson P, et al. A progressive failure model for mesh-size-independent FE analysis of composite laminates subject to low-velocity impact damage[J]. Composites Science and Technology, 2012, 72(5): 624-632.

[6] Liao B B, Liu P F. Finite element analysis of dynamic progressive failure of plastic composite laminates under low velocity impact[J]. Composite Structures, 2017, 159: 567-578.

[7] Gama B A, Gillespie Jr J W. Finite element modeling of impact, damage evolution and penetration of thick-section composites[J]. International Journal of Impact

Engineering, 2011, 38(4): 181-197.

[8] Chen F, Chen R, Jiang B. The adaptive finite element material point method for simulation of projectiles penetrating into ballistic gelatin at high velocities[J]. Engineering Analysis with Boundary Elements, 2020, 117: 143-156.

[9] Catalanotti G, Camanho P P, Marques A T. Three-dimensional failure criteria for fiber-reinforced laminates[J]. Composite Structures, 2013, 95: 63-79.

[10] Naik N K, Shrirao P, Reddy B C K. Ballistic impact behaviour of woven fabric composites: Formulation[J]. International journal of impact engineering, 2006, 32(9): 1521-1552.

[11] Wicklein M, Ryan S, White D M, et al. Hypervelocity impact on CFRP: testing, material modelling, and numerical simulation[J]. International Journal of Impact Engineering, 2008, 35(12): 1861-1869.

[12] Ji C, Sun B, Qiu Y, et al. Impact damage of 3D orthogonal woven composite circular plates[J]. Applied Composite Materials, 2007, 14(5): 343-362.

[13] Minak G, Ghelli D. Influence of diameter and boundary conditions on low velocity impact response of CFRP circular laminated plates[J]. Composites Part B: Engineering, 2008, 39(6): 962-972.

[14] Rao M P, Duan Y, Keefe M, et al. Modeling the effects of yarn material properties and friction on the ballistic impact of a plain-weave fabric[J]. Composite Structures, 2009, 89(4): 556-566.

[15] Xiao J R, Gama B A, Gillespie Jr J W. Progressive damage and delamination in plain weave S-2 glass/SC-15 composites under quasi-static punch-shear loading[J]. Composite structures, 2007, 78(2): 182-196.

[16] Spahn J, Andrä H, Kabel M, et al. A multiscale approach for modeling progressive

damage of composite materials using fast Fourier transforms[J]. Computer Methods in Applied Mechanics and Engineering, 2014, 268: 871-883.

[17] ROTERS, Franz, et al. DAMASK–The Düsseldorf Advanced Material Simulation Kit for modeling multi-physics crystal plasticity, thermal, and damage phenomena from the single crystal up to the component scale. Computational Materials Science, 2019, 158: 420-478.

[18] SLISERIS, Janis; YAN, Libo; KASAL, Bohumil. Numerical modelling of flax short fibre reinforced and flax fibre fabric reinforced polymer composites. Composites part B: engineering, 2016, 89: 143-154.

[19] King M J, Jearanaisilawong P, Socrate S. A continuum constitutive model for the mechanical behavior of woven fabrics[J]. International journal of solids and structures, 2005, 42(13): 3867-3896.

[20] Krivosheina M N, Kobenko S V, Tuch E V, et al. Fracture features of anisotropic materials at different impact velocities[J]. European Journal of Computational Mechanics, 2017, 26(5-6): 609-621.

[21] Li T T, Wang Z, Zhang X, et al. Dynamic cushion, quasi-static stab resistance, and acoustic absorption analyses of flexible multifunctional inter-/intra-bonded sandwich-structured composites[J]. The Journal of The Textile Institute, 2021, 112(1): 47-55.

Chapter 6

Conclusions

Chapter 6: Conclusions

In this dissertation, we focus on the effect of considering anisotropy and contact of yarn on the accuracy of stab-resistance simulation results. On this basis, the influencing factors of material stab resistance are predicted. The study finds that the addition of the radial properties of the yarn and the optimization of the contact part of the yarn will greatly improve the accuracy of the simulation results. After obtaining accurate simulations, we conduct an in-depth analysis of the stab-proof mechanism and the factors affecting the stab-proof performance. With the help of the optimized model, the simulation results have great reference value.

In Chapter 2, in order to better achieve the goal of this experiment, we carefully designed the material structure of the experiment. After studying the influence of fabric interweaving structure on this experiment, we design a composite with a mesh structure for puncture analysis, using Kevlar/epoxy to prepare mesh composites with the mesh spacing of 1 mm. Using the prepared new material structure, the puncture resistance of the material is tested by the puncture machine developed by our laboratory. The puncture failure morphology is analyzed with the help of a high-speed camera, and the puncture energy is analyzed using the force-displacement curve. The results of this analysis will serve as a benchmark against which to simulate the experimental results.

In Chapter 3, we focus on yarn anisotropy. The influence of the anisotropy of the yarn on the accurate value of the simulation results is mainly studied. On the basis of the above experiments, we conduct stab-proof simulation experiments. Firstly, a 1:1 simulation model of mesh composite material is established by CAD software. Then, a simulated puncture experiment is carried out according to the actual experimental conditions and material parameters. When setting the material parameters, the problem

of yarn anisotropy is mainly considered. The tensile properties of the yarn in the axial direction are tested, and then the compressive properties of the yarn in the radial direction are tested by the method developed by Professor KAWAMURA after optimization. The test finds that the radial modulus of the yarn is much smaller than the axial modulus of the yarn. Using the measured data, the model parameters are set according to the material anisotropy. After accounting for the yarn anisotropy, the results of the stab-resistance simulation are closer to the actual results. The simulation results without considering the yarn anisotropy are quite different from the actual results. Therefore, the anisotropy of the yarn has a great influence on the accuracy of the simulation results.

In Chapter 4, we focus on the issue of contact part of yarn. The influence of the contact between the yarns on the precise value of the simulation results is mainly studied. In order to ensure the accuracy of the interface optimization in the model, we have carried out a detailed analysis of the real object. The interface is then observed by electron microscope, and the damage morphology of the interface failure is analyzed by SEM. Comparing the types of subsequent destruction of the classic interface, the most accurate optimization solution is finally confirmed. In the model, a resin layer is added to the part where the yarn is in contact with the yarn, and the contact between the yarns is optimized by setting the contact surface of the resin layer and the setting of the failure criterion. By optimizing the contact conditions between the yarns, the details of the stab-resistant simulation results are more in line with the actual results. However, the details of the simulation results without serious consideration of the contact between the yarns are quite different from the actual results. It is found that after considering the anisotropy of the yarn and the contact between the yarns, the accurate value of the simulation results is greatly improved, and it is closer to the actual experimental results. That is, it is

meaningful to consider the yarn anisotropy and the yarn-to-yarn contact in the simulation experiments.

In chapters 5, using the optimized model, we deeply analyze the puncture mechanism of this material and the influencing factors of its puncture resistance. The simulation results show that the main failure modes of the mesh material are resin fracture and flexural deformation of the yarns at the splices, while the surrounding area of the material is hardly affected. Based on this optimized model, by adjusting the parameters of the material, the influencing factors of the stab resistance of the material are studied. The influencing factors include the ratio of the axial and radial elastic moduli of the yarn (E_L/E_T), the ratio of the tensile strength of the yarn to the shear strength of the resin (σ_F/σ_R), and the diameter of the yarn (R). Experiments show that as the E_L/E_T ratio increases, the stab resistance of the material decreases. The stab resistance performance of the material improves with increasing E_L or yarn diameter but deteriorates with increasing σ_F/σ_R ratio.

In the puncture simulation experiment, the ignored details can greatly deviate the simulation results. Under the material structure designed in this paper, considering the anisotropy of the yarn and the contact with the yarn will greatly improve the accuracy of the simulation results. The method of this experiment has very important guiding significance for the subsequent simulation of other structures.

List of Publications

[1] Luo C, Bao L, Sun Y, et al. Initial damage and influence of material properties on the puncture response of the Aramid yarn-reinforced epoxy composite[J]. Composites Science and Technology, 2022, 225: 109481.

[2] Luo, C., Sun, Y., Wakatsuki, K., Morikawa, H., & Bao, L. (2022). Consideration of Yarn Anisotropy in the Investigation of the Puncture Resistance of Fibrous Materials. *Polymers*, *14*(5), 883.

Oral Presentations

1. Luo C, Sun Y, Wakatsuki K, Morikawa, H, Bao, L, Research on the influencing factors and mechanism of the puncture resistance of fibrous materials. 2022 Japan-Taiwan Textile & Composite Research Forum. January 7th, 2022, Online, Japan.
2. Luo C, Sun Y, Wakatsuki K, Morikawa, H, Bao, L, Research on the Influencing Factors and Mechanism of the Puncture Resistance of Fibrous Materials. The 49th Textile Research Symposium (2022), Kyoto Institute of Technology, Japan. October 9th, 2022

Acknowledgements

This doctoral dissertation is completed under the supervision of Professor Limin Bao. I would like to thank Professor Bao for his sincere teachings. With his guidance and support, I am able to solve all the difficulties step by step and finally complete this very meaningful doctoral research.

Secondly, I would like to thank Shinshu University and Bao Lab. It is a very important opportunity for me to successfully enter Shinshu University and join Bao's laboratory. The platform provided by the school and the research laboratory allows me to complete all the research during the doctoral period with sufficient conditions. At the same time, thanks to the scholarship from the Japanese government, I can have sufficient living security.

In addition, I would like to thank the members of the Bao Lab for their assistance during the experimentation and writing. Especially during the period of COVID-19, everyone helps and encourages each other to avoid the harm of the epidemic.

Finally, I would like to thank my favorite parents and wife for their patience and support during this time. I am also grateful to my close friends for their concern.